DYNAMIC BEHAVIOR OF ELASTO-INELASTIC BEAMS SUBJECTED TO MOVING LOADS

Thesis for the Degree of Ph. D.

MICHIGAN STATE UNIVERSITY

Teoktistos Toridis

1964

This is to certify that the

thesis entitled

DYNAMIC BEHAVIOR OF ELASTO-INELASTIC BEAMS SUBJECTED TO MOVING LOADS

presented by

Teoktistos Toridis

has been accepted towards fulfillment
of the requirements for

Ph. D. degree in Civil Engineering

Robert K. L. Wen
Major professor

Date Sept. 25, 1964

O-169

ABSTRACT

DYNAMIC BEHAVIOR OF ELASTO-INELASTIC
BEAMS SUBJECTED TO MOVING LOADS

by Teoktistos Toridis

An analytical study is made of the elasto-inelastic behavior of beams subjected to moving loads. The structure analyzed consists of a slender beam resting on rigid supports. The types of moving loads used in this study are a single unsprung mass, a sprung mass, and a combination of a sprung and unsprung mass connected by an elastic spring and a viscous damper.

Although the method of analysis can be applied conveniently to continuous beams, only simply supported beams have been considered in obtaining the numerical results for this investigation. The analysis is based on a discrete beam model consisting of massless rigid panels connected by flexible joints with point masses. The flexibility and mass of the joints are obtained by lumping the corresponding continuous properties of the actual beam. This model facilitates considerations of the nonlinear deformation characteristics of the beam and possible non-uniform distribution of the beam mass.

The solution of the problem is carried out by numerical techniques. The results were obtained by the use of a high speed digital

computer with the objective of gaining an insight into the physical problem, illustrating certain features in the workings of the mathematical model, and assessing the influences of certain parameters on the beam response.

For an elastic perfectly plastic beam, it is found that the beam could suffer permanent damage due to the passage of a load, whose weight is less than the static yield load. On the other hand, loads much heavier than the static yield load can cross the beam, if large deformations are allowed. However, in general, the inelastic deformations increase at a rapid rate when the load is increased beyond the static yield load. For unsprung loads, an increase in the load speed generally results in an increase in the permanent deflection. The opposite is true for sprung loads.

In the case of beams having an "inelastic stiffness," it is found that even a small positive inelastic stiffness reduces the permanent displacement significantly. For such beams, an increase in load speed decreases the amount of permanent displacement.

DYNAMIC BEHAVIOR OF ELASTO-INELASTIC BEAMS SUBJECTED TO MOVING LOADS

By

Teoktistos Toridis

A THESIS

Submitted to
Michigan State University
in partial fulfillment of the requirements
for the degree of

DOCTOR OF PHILOSOPHY

Department of Civil and Sanitary Engineering

1964

ACKNOWLEDGEMENTS

The study reported herein was made as part of a research project on the elasto-inelastic behavior of beams subjected to moving loads conducted in the Department of Civil Engineering of Michigan State University under the direction of Dr. R. K. Wen. The work is supported by the National Science Foundation under Grant No. G.12143 administered by the Division of Engineering Research.

This report also constitutes the author's doctoral dissertation. It has been written under the direction of Dr. R. K. Wen, the author's advisor, to whom gratitude is extended for his valuable guidance during the course of this study.

The author also wishes to express his thanks and appreciation to the members of his guidance committee, to Dr. C. E. Cutts, for his encouragement during the course of the author's graduate studies, to Dr. L. E. Malvern, Dr. W. A. Bradley, and Dr. C. S. Duris, for their valuable advice.

Thanks are also due the staff of the Computer Laboratory of the University for their help and cooperation.

TABLE OF CONTENTS

LIST OF FIGURES

I. INTRODUCTION

1.1. General

In recent years the elasto-inelastic analysis of structures subjected to dynamic loads has received much attention. Due to the nonlinear nature of the deformation characteristics of the structure, rigorous mathematical solutions of problems of this type are usually hard to obtain. In order to arrive at workable methods of solution, researchers have been forced to make major or even drastic simplifying assumptions regarding the physical characteristics of the structure and/or the loading, thus often significantly limiting the applicability of such analyses.

Past work in this field has mainly been concentrated on elastic perfectly plastic structures. The only work known to the author dealing with a more general moment-curvature relation is that of Bohnenblust[1] who developed a method for calculating the response of a semi-infinite elasto-inelastic beam to an impact at one end of the beam. However, it does not seem feasible to extend this method to beams either with a finite length or with a lateral loading. Bleich and Salvadori[2] presented a variation of the normal mode approach for the analysis of elasto-plastic structures. This method, although theoretically sound, is unwieldy to apply to practical problems,

except the simplest ones.

A relatively simple solution for large plastic deformations by the "rigid-plastic" theory for the dynamic analysis of beams was presented by Lee and Symonds.[3] This solution can be applied only to the particular case of very large plastic deformations as compared to the elastic ones. The work was followed by a number of applications and extensions of the theory. For example, the influence of strain rate was considered by Ting and Symonds.[4]

In all of the above studies the continuum nature of the structure was maintained; namely, a continuous distribution of both flexibility and mass was considered. A different direction during the more recent research efforts in this area has been the use of a discrete model representing the actual structure. Thus, Berg and DaDeppo[5] developed a method for the analysis of multi-story elastic perfectly plastic structures responding to lateral dynamic forces by lumping the mass of the actual structure at the floor levels. This method was based on a "predictor-corrector" approach which had previously been proposed by Bleich.[6] The "predictor" is, in essence, an elastic solution that satisfies dynamics but generally violates the material property at some parts of the structure by requiring resisting moments larger than the yield moment. The "corrector" consists of also an elastic solution with hinges inserted at certain appropriate points; at these hinges, equal and opposite moments having the same magnitude

as the yield moment of the section are applied. If the "predictor" and "corrector" solutions are superposed, the result is a system which satisfies both the laws of dynamics and the material properties (including the effects of past history of deformation such as the direction of plastic yielding).

A finite difference approach based on the "predictor-corrector" procedure was presented by Baron, Bleich, and Weidlinger.[7] The method is easy to use. However, again, it deals with elastic perfectly plastic structures only. All of the above mentioned methods of analysis, dealing with systems of finite dimensions, are limited to structures with specialized moment-curvature relations: either the elastic perfectly plastic, or the rigid plastic type. A method applicable to structures having a more general type of non-linear moment-curvature relation was proposed by Wen and Toridis.[8] Several discrete models, based on the lumping of the mass and/or the flexibility of the structure have been considered. Extensive numerical results were presented to demonstrate the credibility of the approach.

The methods of analysis mentioned above, in general, have been developed to handle dynamic problems involving stationary loading in the sense that the position of the load does not change with time. The problem of a beam subjected to a moving load has attracted a great deal of attention through the years, mainly because of its

practical importance in bridge engineering. In fact, the first fundamental paper by Stokes[15] was published as early as 1849. A great amount of work has since been done on this general problem. A bibliography on this subject can be found in Reference 9. However, all the papers listed in that bibliography have dealt with the elastic behavior of beams subjected to moving loads.

Since the end of the Second World War, the concept of ultimate strength, as applied to the design of structures, has gained increasing attention. For an application of this concept to the analysis and design of bridges, the study of the inelastic behavior of beams subjected to moving loads seems to be of basic importance. It is of interest to note that although the earliest work on the elastic behavior of beams under moving loads was reported in 1849, the first paper on the inelastic behavior under a similar loading did not appear until 1958.[10] Then, Parkes analyzed the inelastic behavior of a beam traversed by a single unsprung mass. The beam is assumed to be massless, and to possess a rigid-plastic moment-curvature relation. One of his major findings was that there is an upper limit to the load that can cross the beam, irrespective of the magnitude of the speed. The limit given is 1.228 times the static yield load.

Symonds and Neal,[11] in 1960, reported a similar study in which the effect of the mass is taken into consideration, but the beam is again assumed to be rigid-plastic. The analysis showed that

there is no upper limit to the magnitude of the load that can cross the beam provided the load moves at a sufficiently high speed.

In passing, it may be mentioned that more recently, Heidebrecht, Fleming and Lee[12] have described a procedure that is applicable to the analysis of elastic perfectly plastic beams subjected to a moving force of constant magnitude. However, it seems that an extension of their approach to problems involving moving masses would give rise to insurmountable difficulties.

The work presented herein may be regarded as an extension of that reported in Reference 8. However, whereas the work in Reference 8 was confined to problems of prescribed dynamic loading, the moving load problem treated here involves certain major difficulties in the analysis because of the interactions between the mechanical system of the load and that of the beam. In relation to the work of Parkes, and Symonds and Neal mentioned earlier, the present analysis considers more realistic moment-curvature relations and load characteristics, such as a load unit consisting of a combination of a sprung and an unsprung mass. As in Reference 8, in this study the continuous beam is also replaced by a discrete model, and solutions are obtained by using numerical techniques.

In Chapter II, the physical system considered is first specified. Also, in the same chapter, the general method of analysis including the derivation of the equations of motion is presented. In

Chapter III, the method of analysis is specialized to the case of a simply supported beam subjected to a single axle load unit; the variables are made dimensionless, and the parameters of the problems defined. The detailed steps of the numerical solution are discussed therein also. In Chapter IV are presented typical numerical solutions obtained by using a computer program developed for this investigation; the results are examined and interpreted. In the same chapter, a discussion of the results in the light of previous works is given. The final chapter comprises a summary and conclusion of the present study.

1.2. Notation

The symbols used in this report are defined in the text where they first appear. For convenience, they are listed here in alphabetical order, with English letters preceding Greek letters.

Dots appearing over certain variables represent differentiations with respect to time. Similarly a bar above a letter is used to refer to the dimensionless version of the variable in question.

c_j = damping constant of spring connecting the j-th sprung mass to the j-th unsprung mass;

E = modulus of elasticity;

g = gravitational acceleration;

h = L/N;

h_i = i-th panel length;

i, j = subscripts;

I = moment of inertia;

k = curvature of beam, or spring constant;

k_j = spring constant of spring connecting the j-th sprung mass to the j-th unsprung mass;

k_1, k_2 = elastic and inelastic slopes of a bilinear moment-curvature relation, respectively; see Figure 5a;

k'_1, k'_2 = elastic and inelastic slopes of a bilinear moment-rotation relation, respectively; see Figure 5b;

$k(x)$ = flexibility distribution of beam;

L = span length of beam;

m = mass per unit length of a uniform beam;

m_i = lumped mass at joint (i);

$m(x)$ = mass distribution of beam;

M = bending moment;

M_e = elastic limit moment; see Figure 5a;

M_i = moment at joint (i);

n = ratio of modulus of elasticity of steel to that of concrete;

N = number of rigid panels into which a beam is divided;

N_i^+, N_i^- = positive and negative transition moments, respectively; see Figure 5b;

$p(x, t)$ = distributed external load on beam;

$P_i(t)$ = lumped external load at joint (i);

$P_j(t)$ = interacting force between the j-th unsprung mass and the beam;

P_y = the magnitude of the concentrated static force causing a yield moment at mid-span when applied at mid-span;

Q_b = total mass of beam;

Q_s = the sprung mass of a moving load;

Q_u = the unsprung mass of a moving load;

$(Q_u)_j$ = the j-th unsprung mass of a moving load;

Q_v = total mass of moving load;

R = stiffness ratio = k_2/k_1;

t = time coordinate;

T_1 = fundamental elastic period of vibration;

v = constant horizontal velocity of moving load;

V_i, V_i' = resultant shear force to the left and to the right of m_i, respectively;

w = absolute vertical displacement of Q_s;

W_v = total weight of moving load;

x = length coordinate of beam;

$\bar{x}$ = x/L;

x_i = length coordinate of joint (i);

y = vertical deflection of beam;

y_i = deflection of joint (i);

y_ζ = deflection of unsprung mass, or beam point in contact with moving load;

z_i = distance of moving load from left end of rigid panel between joints (i-1) and (i);

z_i' = $(h_i - z_i)$ = complement of z_i;

$\bar{z}_i$ = z_i/h

$\alpha = \frac{T_1 v}{L}$

$\beta = W_v / P_y$;

$\gamma = Q_v / Q_b$;

$\delta = P_y L^3 / 48 EI$;

δ_{st} = shortening in the spring connected to a sprung mass at its static equilibrium position;

Δ = prefix indicating increment;

θ_i = angle of rotation of joint (i);

$\lambda = Q_u / Q_v$;

ζ = position of moving load from near support of beam; and

$\tau = tv/L$.

II. METHOD OF ANALYSIS

In this chapter, the characteristics of the physical problem considered are described first, followed by a presentation of the method of analysis.

2.1. System Considered

The structure considered is shown in Figure 1. It consists of a slender beam, resting on rigid supports. Both the mass and flexibility of the beam are continuously distributed along the beam.

For beams considered herein, the relation between the bending moment, M, and curvature k is, in general, nonlinear and depends on the history of deformation. Such a relation is a rather complex one, particularly when loading and unloading are involved. A general shape of a moment-curvature diagram is illustrated in Figure 2. Starting from the origin, for some of the most common structural materials, the correspondence between moment and curvature is linear between the points (k_e, M_e) and $(-k_e, -M_e)$, where k_e and M_e refer to the elastic limit curvature and bending moment, respectively. The relation beyond these points, however, depends on the history of the deformation and usually exhibits hysteretic behavior. For all the numerical results obtained in this

study, the moment-curvature relation has been taken to be of the bilinear type discussed in detail in Chapter III.

The beam shown in Figure 1 is subjected to load units that traverse at a constant horizontal speed, v. The types of moving loads considered in this study are: a "single-axle load unit," a "sprung mass," and an "unsprung mass." A single-axle load unit consists of a sprung mass connected to a single unsprung mass through a linear spring and a viscous damper. Shown in Figure 1 are also special cases of a single-axle load such as a single sprung mass and a single unsprung mass. In addition to the moving loads, of course, the beam may be subjected to other prescribed time dependent loads.

2.2. Analysis of System

2.2.1. Discretization of Beam. In order to effect an analysis of the system described above, the continuous properties of the beam are lumped or discretized. The manner of discretization corresponds to "Model B" discussed in Reference 8, but for the sake of completeness, is given below.

This model, as illustrated in Figure 3a, replaces a beam of continuum by a series of rigid and massless panels connected by joints. At these joints both the flexibility and the mass of the beam are lumped. It is not necessary for the panels to be of equal length;

the symbol h_{i+1} is used to denote the length of the panel between the joints (i) and (i+1), as shown in the figure.

The relation between the flexibility of the continuum and that of the discrete model may be illustrated by considering joint (i) at x_i, in Figure 3a. At this joint the rotation represents all the curvature changes in the actual beam over a length tributary to this joint; i.e., from $x_i' = x_i - \frac{h_i}{2}$ to $x_i'' = x_i + \frac{h_{i+1}}{2}$, as shown in the figure. Let θ_i denote the rotation at joint (i). Assuming $k(x) = k(x_i)$ within the tributary interval, one obtains:

$$\theta_i = \int_{x_i'}^{x_i''} k(x)\,dx = (1/2)(h_i + h_{i+1})\, k(x_i) \qquad (1)$$

The above shows that the moment-rotation diagram for joint (i) may be obtained directly from the moment-curvature diagram for the cross-section at x_i. Thus, the abscissas of the moment-rotation diagram are equal to the abscissas of the moment-curvature diagram multiplied by $(1/2)(h_i + h_{i+1})$.

Assuming that the angle of rotation is small, the relation between the vertical deflections y_{i-1}, y_i, y_{i+1} and θ_i may be derived from Figure 3b as:

$$\theta_i = -\frac{1}{h_i}\, y_{i-1} + \left(\frac{1}{h_i} + \frac{1}{h_{i+1}}\right) y_i - \frac{1}{h_{i+1}}\, y_{i+1} \qquad (2)$$

The deflections are taken as positive downward, while the rotations

are

sho

dis

bit

con

cas

are considered positive if the joint in question is concave upward as shown in the figure.

The lumped mass m_i at joint (i) for the model is related to the distributed mass $m(x)$ of the continuum by the equation

$$m_i = \int_{x'_i}^{x''_i} m(x)\, dx \qquad (3)$$

2.2.2. Assumptions. The assumptions made in the derivation of the differential equations governing the motion of the system in consideration are outlined below.

(1) The deformation of the beam is assumed to be due to bending only; the effects of shear, strain rate and geometry changes on the beam deformation are not considered.

(2) The unsprung mass of a moving load is assumed to be in contact with the beam at all times.

(3) The horizontal component of the load velocity is assumed to remain constant during the passage of the load over the beam, even at relatively large deformations of the beam. Also, the interaction force between the moving load and the beam is supposed to act vertically.

2.2.3. Derivation of Equations of Motion. Consider the general case of a number of single-axle load units moving across a beam. The

position of the j-th unsprung mass in contact with the beam, at any time, is denoted by the variable ζ_j (see Figure 3a), where ζ is a function of time, t. Assume that at a certain time the unsprung mass in question is on the panel between the joints (i-1) and (i). Considering the fact that each beam panel between two flexible joints (or a support and a flexible joint) is rigid, the vertical deflection $(y_\zeta)_j$, of the j-th unsprung mass in contact with the beam can be expressed as:

$$(y_\zeta)_j = y_{i-1} + \frac{z_i}{h_i}(y_i - y_{i-1}),\ x_{i-1} \leq (\zeta_j) \leq x_i \tag{4}$$

in which z_i denotes the distance of the unsprung mass from the left end of the rigid panel between the joints (i-1) and (i).

The velocity and acceleration of the unsprung mass are:

$$(\dot{y}_\zeta)_j = \dot{y}_{i-1} + \frac{\dot{z}_i}{h_i}(y_i - y_{i-1}) + \frac{z_i}{h_i}(\dot{y}_i - \dot{y}_{i-1}) \tag{5a}$$

$$(\ddot{y}_\zeta)_j = \ddot{y}_{i-1} + \frac{2\dot{z}_i}{h_i}(\dot{y}_i - \dot{y}_{i-1}) + \frac{z_i}{h_i}(\ddot{y}_i - \ddot{y}_{i-1}) \tag{5b}$$

where each dot represents a differentiation with respect to time.

Let w_j denote the absolute vertical displacement of the j-th sprung mass, $(Q_s)_j$, from its original static equilibrium position. The equation of motion of $(Q_s)_j$ in the vertical direction is:

$$(Q_s)_j \ddot{w}_j = -k_j(w_j - (y_\zeta)_j) - c_j \frac{d}{dt}(w_j - (y_\zeta)_j) \tag{6}$$

where k_j and c_j represent the spring constant and damping constant,

respectively, of the system connecting the j-th sprung mass to the j-th unsprung mass.

To facilitate the use of the equations for other cases of loading (e.g. a number of unsprung masses, time-dependent distributed pressure, etc.), the reaction between the j-th unsprung mass and the beam will be denoted by $P_j(t)$, a time dependent force (see Figure 3a).

Considering the free body of a joint (i), as shown in Figure 4a, one obtains the equation:

$$-m_i \ddot{y}_i + V_i' - V_i = 0 \tag{7}$$

in which $\ddot{y}_i$ represents the acceleration of the mass at joint (i), and V_i and V_i' the resultant shear force to the left and to the right of joint (i), respectively.

Additional equations may be obtained by a consideration of the equilibrium of moment. Referring to the free body of the panel (i-1) - (i) in Figure 4b, the requirement for equilibrium of moments around the left end of the panel yields:

$$M_{i-1} - M_i + V_i h_i + P_j(t)\, z_i = 0 \tag{8}$$

where M_{i-1} and M_i are the bending moments at the joints (i-1) and (i), respectively. In deriving the preceding equation the rotational inertia of the panel is neglected.

Similarly, considering the free body of Panel (i) - (i+1) shown

in Figure 4c, and summing moments around the right end of the panel one obtains:

$$M_i - M_{i+1} + V'_i h_{i+1} - P_{j+1}(t)\, z'_{i+1} = 0 \qquad (9)$$

in which z'_{i+1} is the complement of the distance z_{i+1} as shown in the figure.

Assuming that $h_i = h_{i+1} = h$, or equal panel length throughout the beam, and subtracting Equation (9) from Equation (8) the following equation is obtained:

$$M_{i-1} - 2M_i + M_{i+1} + (V_i - V'_i)h + P_j(t)\, z_i + P_{j+1}(t)\, z'_{i+1} = 0 \qquad (10)$$

Finally, substitution of Equation (7) into Equation (10) and solution of the resulting equation for $\ddot{y}_i$ yields:

$$\ddot{y}_i = \frac{1}{hm_i}\left[(M_{i-1} - 2M_i + M_{i+1}) + P_j(t)\, z_i + P_{j+1}(t)\, z'_{i+1}\right] \qquad (11)$$

in which,

$$P_j(t) = (Q_v)_j g - (Q_u)_j (\ddot{y}_\zeta)_j + k_j(w_j - (y_\zeta)_j) + c_j \frac{d}{dt}\left[w_j - (y_\zeta)_j\right] \qquad (12)$$

where $(Q_v)_j$ denotes the total mass of the j-th single-axle load unit, $(Q_u)_j$ represents the j-th unsprung mass, and g the gravitational acceleration. The expression for $P_{j+1}(t)$ may be obtained from Equation (12) by replacing j by j+1.

An equation of the form of Equation (11) can be written for each joint, resulting in a set of equations which are coupled in the $\ddot{y}_i$'s. The fact that the equations are coupled may be seen by an

examina

for P_{j-1}

In

right of

y

T

subject

easily

externa

forces

tional

(11) r

ing to

one u

either

joint

examination of Equations (5b), (11), and (12), and the expression for $P_{j+1}(t)$.

If no load unit is located on the panel either to the left or to the right of joint (i), Equation (11) reduces to:

$$\ddot{y}_i = \frac{1}{hm_i} (M_{i-1} - 2M_i + M_{i+1}) \tag{13}$$

The differential equation for a beam having equal panels and subjected to a time-dependent distributed pressure can be derived easily by use of Equation (13). Let $p(x,t)$ denote the distributed external load on the beam to be lumped in the form of concentrated forces, $P_i(t)$, acting at each joint (i). Thus:

$$P_i(t) = \int_{x'_i}^{x''_i} p(x,t)\,dx \tag{14}$$

It is obvious that $P_i(t)$ enters into Equation (7) as an additional term and this in turn changes Equation (13) to

$$\ddot{y}_i = \frac{1}{hm_i} [(M_{i-1} - 2M_i + M_{i+1}) + P_i(t)] \tag{15}$$

Returning to the case of a beam traversed by a load, Equation (11) may be used to derive certain differential equations corresponding to particular conditions. Due to practical considerations, only one unsprung mass at most is assumed to be located at any time either on the rigid panel immediately to the left or to the right of any joint (i). (The case of an unsprung mass exactly over a joint is

treated in Art. 2.2.4.) This assumption may be justified by the fact that for the case of a multiple-axle load unit the above condition can usually be met by choosing a panel length that is small enough. Thus, if the j-th unsprung mass is on the panel immediately to the left of joint (i), Equation (11) becomes:

$$\ddot{y}_i = \frac{1}{hm_i}\left[(M_{i-1} - 2M_i + M_{i+1}) + P_j(t)z_i\right] \tag{16}$$

Similarly, if the j-th unsprung mass is on the panel immediately to the right of joint (i), Equation (11) reduces to:

$$\ddot{y}_i = \frac{1}{hm_i}\left[(M_{i-1} - 2M_i + M_{i+1}) + P_j(t)z'_{i+1}\right] \tag{17}$$

where $P_j(t)$ is given by Equation (12). Of course, $(y_\zeta)_j$ and its time derivatives appearing in Equation (12) are to be found from Equations (4), (5a) and (5b), in each case with due consideration given to the location of the unsprung mass. For example, if the j-th unsprung mass is to the right of joint (i), Equations (4), (5a) and (5b) take the form of:

$$(y_\zeta)_j = y_i + \frac{z_{i+1}}{h_{i+1}}(y_{i+1} - y_i) \tag{18}$$

$$(\dot{y}_\zeta)_j = \dot{y}_i + (\dot{z}_{i+1}/h_{i+1})(y_{i+1} - y_i) + (z_{i+1}/h_{i+1})(\dot{y}_{i+1} - \dot{y}_i) \tag{19}$$

$$(\ddot{y}_\zeta)_j = \ddot{y}_i + (2\dot{z}_{i+1}/h_{i+1})(\dot{y}_{i+1} - \dot{y}_i) + (z_{i+1}/h_{i+1})(\ddot{y}_{i+1} - \ddot{y}_i) \tag{20}$$

where h_{i+1} can be replaced by h.

The differential equation for each joint is obtained from one

of the three Equations (13), (16) or (17) depending on the location of each unsprung mass and the joint in consideration.

It should be noted that, using Equation (16) and (17) for the joints immediately to the left and to the right of the point where an unsprung mass is located causes the resulting equations to be coupled in the accelerations of the two joints in question. However, this coupling is of local nature, and if a single-axle load unit alone is considered to cross the beam, only two of the equations are coupled, while the remaining ones are uncoupled and can be solved independently.

Equations (16) and (17) apply also the case of a beam traversed by a single sprung mass. For this purpose $(Q_u)_j$ in Equation (12) should be set equal to zero. The solution for this case is substantially easier to obtain since the accelerations are not coupled.

In passing, it may be noted that the above analysis may be easily adapted to the case of a multiple-axle load unit. A major change involved would be the consideration of the rotatory properties of the sprung mass.

2.2.4. Discontinuities in the Velocity and Acceleration Functions. If a mass moves on a beam with a continuous distribution of flexibility, so long as it is in contact with the surface of the beam, its vertical velocity and acceleration are continuous functions of time. Such is not the case for the discrete beam model used in the

present analysis. On account of the discontinuity in the slope at, say the i-th joint, jump discontinuities in the vertical velocities and accelerations of the lumped mass at joint (i) and the moving mass occur when the latter passes over the joint. The magnitudes of these jumps may be computed by using previously derived equations for $\dot{y}_\zeta$ and $\ddot{y}_\zeta$ when an unsprung mass is to the left or to the right of joint (i). Denote by t_i the time corresponding to the j-th unsprung mass being exactly over joint (i), and by t_i^- and t_i^+ the times an infinitesimal amount before and after t_i, respectively. For t_i^-, application of Equations (5a) and (5b) with $z_i = h_i = h$ gives:

$$[(\dot{y}_\zeta)_j]_{t=t_i^-} = \dot{y}_i^- + \frac{\dot{z}_i}{h}(y_i - y_{i-1}) \tag{21a}$$

$$[(\ddot{y}_\zeta)_j]_{t=t_i^-} = \ddot{y}_i^- + \frac{2\dot{z}_i}{h}(\dot{y}_i^- - \dot{y}_{i-1}) \tag{21b}$$

Similarly, for t_i^+ use of Equations (5a) and (5b) with $z_{i+1} = 0$ and $h_{i+1} = h$ yields:

$$[(\dot{y}_\zeta)_j]_{t=t_i^+} = \dot{y}_i^+ + \frac{\dot{z}_{i+1}}{h}(y_{i+1} - y_i^+) \tag{22a}$$

$$[(\ddot{y}_\zeta)_j]_{t=t_i^+} = \ddot{y}_i^+ + \frac{2\dot{z}_{i+1}}{h}(\dot{y}_{i+1}^+ - \dot{y}_i^+) \tag{22b}$$

Note that when $t = t_i$ (or $\zeta = x_i$), $\dot{z}_i = \dot{z}_{i+1} = v$, where v is the velocity of the moving load. Therefore, the magnitudes of the jumps in the $(\dot{y}_\zeta)_j$ and $(\ddot{y}_\zeta)_j$ functions in the neighborhood of joint (i) are

found to be:

$$(\Delta\dot{y}_\zeta)_j = [(\dot{y}_\zeta)_j]_{t=t_i^+} - [(\dot{y}_\zeta)_j]_{t=t_i^-}$$

$$= (\dot{y}_i^+ - \dot{y}_i^-) + \frac{v}{h}(y_{i+1} - 2y_i + y_{i-1})$$

$$= \Delta\dot{y}_i + \frac{v}{h}(y_{i+1} - 2y_i + y_{i-1}) \qquad (23a)$$

$$(\Delta\ddot{y}_\zeta)_j = [(\ddot{y}_\zeta)_j]_{t=t_i^+} - [(\ddot{y}_\zeta)_j]_{t=t_i^-}$$

$$= (\ddot{y}_i^+ - \ddot{y}_i^-) + \frac{2v}{h}(\dot{y}_{i+1} - 2\dot{y}_i^- + \dot{y}_{i-1} - \Delta\dot{y}_i)$$

$$= \Delta\ddot{y}_i + \frac{2v}{h}(\dot{y}_{i+1} - 2\dot{y}_i^- + \dot{y}_{i-1} - \Delta\dot{y}_i) \qquad (23b)$$

in which $(\Delta\dot{y}_\zeta)_j$ and $(\Delta\ddot{y}_\zeta)_j$ represent the jumps in the $(\dot{y}_\zeta)_j$ and $(\ddot{y}_\zeta)_j$ functions, respectively; $\Delta\dot{y}_i$ and $\Delta\ddot{y}_i$ represent the jumps in the $\dot{y}_i$ and $\ddot{y}_i$ functions, respectively.

The conservation of the linear momentum in the vertical direction furnishes an additional expression for the determination of $(\Delta\dot{y}_\zeta)_j$ and $\Delta\dot{y}_i$:

$$(Q_u)_j(\Delta\dot{y}_\zeta)_j + m_i\Delta\dot{y}_i = 0 \qquad (24)$$

Solving Equations (23a) and (24) simultaneously one obtains:

$$(\Delta\dot{y}_\zeta)_j = \frac{v}{h}\left[\frac{1}{1 + \frac{(Q_u)_j}{m_i}}\right](y_{i+1} - 2y_i + y_{i-1}) \qquad (25a)$$

$$(\Delta\dot{y}_i) = -\frac{v}{h}\left[\frac{1}{1 + \frac{m_i}{(Q_u)_j}}\right](y_{i+1} - 2y_i + y_{i-1}) \qquad (25b)$$

Similarly, use of Equations (16) and (17) at t_i^- and t_i^+, respectively, with $z_i = z'_{i+1} = h$, yields:

$$(Q_u)_j (\Delta\ddot{y}_\zeta)_j + m_i \Delta\ddot{y}_i + c_j (\Delta\dot{y}_\zeta)_j = 0 \tag{26}$$

After a substitution of Equation (25) into Equation (26) the resulting equation may be solved simultaneously with Equation (23b) to determine $(\Delta\ddot{y}_\zeta)_j$ and $\Delta\ddot{y}_i$. Considering the simple case of $c_j = 0$, one obtains:

$$(\Delta\ddot{y}_\zeta)_j = \frac{2v}{h} \left[\frac{1}{1 + \frac{(Q_u)_j}{m_i}}\right] (\dot{y}_{i+1} - 2\dot{y}_i + \dot{y}_{i-1} - \Delta\dot{y}_i) \tag{27a}$$

$$(\Delta\ddot{y}_i) = -\frac{2v}{h} \left[\frac{1}{1 + \frac{m_i}{(Q_u)_j}}\right] (\dot{y}_{i+1} - 2\dot{y}_i + \dot{y}_{i-1} - \Delta\dot{y}_i) \tag{27b}$$

When using Equations (6) and (16) or (17) the above jumps should be applied to the values of $\dot{y}_i$, $\ddot{y}_i$, $\dot{y}_\zeta$, and $\ddot{y}_\zeta$, each time an unsprung mass moves over a flexible joint.

2.2.5. Boundary Conditions. The boundary conditions for the model used in this analysis can be handled in a very simple manner. Thus, at a simple support both the deflection, y, and the bending moment, M, are equated to zero. At an interior support of a continuous beam the deflection is zero; however, in general, at such a support neither the moment nor the rotation is zero.

III. SIMPLY SUPPORTED BEAMS SUBJECTED TO A SINGLE MOVING LOAD

3.1. General

The equations of motion derived in the previous chapter are applied here to the special case of a simply supported beam subjected to a single moving load unit. Thus, Equations (6), (12), and one of the Equations (13), (16), or (17) can be used to determine the dynamic response of the system. To consider simpler types of moving loads, the above equations need only be simplified accordingly. For example, when the moving load consists of a single sprung mass, Q_u appearing in Equation (12) is simply set equal to zero. On the other hand, if the moving load is a single unsprung mass, the spring constant k and damping constant c appearing in Equation (12) are equated to zero. Of course, in this case Equation (6) does not apply.

3.2. Dimensionless Form of Equations

In what follows, the differential equations for a simply supported beam of uniform cross-section are rendered dimensionless. A list of the physical quantities used for this purpose and not defined so far, is given below:

L = span length of beam;

P_y = concentrated load which if applied statically at mid-span causes a yield moment at mid-span;

m = mass per unit length of a uniform beam;

EI = elastic stiffness of cross-section of a uniform beam;

W_v, Q_v = weight and mass of moving load, respectively; and

Q_b = total mass of beam ($= mL$).

In addition, to render the equations dimensionless, the following notation is introduced:

$$\delta = P_y L^3 / 48 EI;$$

$$M_e = P_y L / 4$$

T_1 = fundamental period of elastic vibration $= \frac{2L^2}{\pi}\sqrt{\frac{m}{EI}}$;

$$\tau = tv/L$$

$$\bar{y}_i = \frac{y_i}{\delta}; \quad \frac{d\bar{y}_i}{d\tau} = \frac{L}{v\delta}\frac{dy_i}{dt}; \quad \frac{d^2\bar{y}_i}{d\tau} = \frac{L^2}{v^2\delta}\frac{d^2y_i}{dt^2}$$

$$\bar{w} = \frac{w}{\delta}; \quad \frac{d\bar{w}}{d\tau} = \frac{L}{v\delta}\frac{dw}{dt}; \quad \frac{d^2\bar{w}}{d\tau^2} = \frac{L^2}{v^2\delta}\frac{d^2w}{dt^2}$$

$$\bar{x} = x/L$$

$$\bar{M}_i = \frac{M_i}{M_e} = \frac{M_i}{P_y L/4}$$

$$\bar{P} = \frac{P}{P_y}$$

$$\alpha = \frac{T_1 v}{L}$$

$$\beta = \frac{W_v}{P_y} = \frac{Q_v g}{P_y}, \qquad \gamma = Q_v/Q_b$$

$$\lambda = \frac{Q_u}{Q_v}$$

$$\bar{k} = \frac{k(T_1)^2}{Q_b}$$

$$\bar{c} = \frac{c(T_1)}{Q_b} \tag{28}$$

Substituting Equation (12) into Equations (16) and (17), and using the above defined quantities, Equations (6), (13), (16), and (17) are reduced to the dimensionless form shown below:

$$\frac{d^2\bar{w}}{d\tau^2} = -\frac{1}{a(1-\lambda)\gamma}\left[\frac{1}{a}\bar{k}\left(\bar{w} - (\bar{y}_\zeta)_{i \text{ or } i+1}\right) + \bar{c}\left(\frac{d\bar{w}}{d\tau} - \left(\frac{d\bar{y}_\zeta}{d\tau}\right)_{i \text{ or } i+1}\right)\right] \tag{29}$$

(The subscript "i" or "i+1" should be used according as the load is to the left or to the right of joint (i).)

$$\frac{d^2\bar{y}_i}{d\tau^2} = \frac{48N^2}{\pi^2 a^2}\left(\bar{M}_{i-1} - 2\bar{M}_i + \bar{M}_{i+1}\right) \tag{30}$$

$$\frac{d^2\bar{y}_i}{d\tau^2} = \frac{48N}{\pi^2 a^2}\left[N\left(\bar{M}_{i-1} - 2\bar{M}_i + \bar{M}_{i+1}\right) + 4\beta\bar{z}_i\right] +$$

$$N\left[-\gamma\lambda\left(\frac{d^2\bar{y}_\zeta}{d\tau^2}\right)_i + \frac{1}{a^2}\bar{k}\left(\bar{w} - (\bar{y}_\zeta)_i\right) + \frac{1}{a}\bar{c}\left(\frac{d\bar{w}}{dt} - \left(\frac{d\bar{y}_\zeta}{d\tau}\right)_i\right)\bar{z}_i\right] \tag{31}$$

$$\frac{d^2\bar{y}_i}{d\tau^2} = \frac{48N}{\pi^2 a^2}\left[N(\bar{M}_{i-1} - 2\bar{M}_i + \bar{M}_{i+1}) + 4\beta\bar{z}'_{i+1}\right] +$$

$$N\left[-\gamma\lambda\left(\frac{d^2\bar{y}_\zeta}{d\tau^2}\right)_{i+1} + \frac{1}{a^2}\bar{k}\left(\bar{w} - (\bar{y}_\zeta)_{i+1}\right) + \frac{1}{a}\bar{c}\left(\frac{d\bar{w}}{d\tau} - \left(\frac{d\bar{y}_\zeta}{d\tau}\right)_{i+1}\right)\bar{z}'_{i+1}\right] \quad (32)$$

where

$$(\bar{y}_\zeta)_i = \bar{y}_{i-1} + \bar{z}_i(\bar{y}_i - \bar{y}_{i-1}) \quad (33a)$$

$$\frac{d(\bar{y}_\zeta)_i}{d\tau} = \frac{d\bar{y}_{i-1}}{d\tau} + N(\bar{y}_i - \bar{y}_{i-1}) + \bar{z}_i\left(\frac{d\bar{y}_i}{d\tau} - \frac{d\bar{y}_{i-1}}{d\tau}\right) \quad (33b)$$

$$\frac{d^2(\bar{y}_\zeta)_i}{d\tau^2} = \frac{d^2\bar{y}_{i-1}}{d\tau^2} + 2N\left(\frac{d\bar{y}_i}{d\tau} - \frac{d\bar{y}_{i-1}}{d\tau}\right) + \bar{z}_i\left(\frac{d^2\bar{y}_i}{d\tau^2} - \frac{d^2\bar{y}_{i-1}}{d\tau^2}\right) \quad (33c)$$

and $(\bar{y}_\zeta)_{i+1}$ and its derivatives are obtained from Equations (33a)-(33c) by replacing (i) by (i+1). Again, in the case of a single sprung mass, λ appearing in Equations (29), (31), and (32) is set equal to zero. Similarly, for a single unsprung mass, $\bar{k}$ and $\bar{c}$ in Equations (29), (31), and (32) are equated to zero; Equation (29) is not applicable in this case.

3.3. Bilinear Moment-Curvature Relation

Although the mathematical model used in this analysis is adaptable for use with a large class of nonlinear, history-dependent moment-curvature relations, for simplicity, a bilinear bending moment-curvature relation has been used for the numerical solutions

to be presented. This relation is illustrated in Figure 5a, in which k_1 and k_2 represent the elastic and inelastic stiffnesses, respectively. The appropriateness of such a bilinear relation obviously depends on the actual shape of the bending moment-curvature diagram of the beam cross section for which this relation is used. In Reference (8) it was shown that for two particular problems the numerical solutions obtained by using both an actual curvilinear moment-curvature relation and a bilinear moment-curvature relation are in good agreement.

As was mentioned in the preceding chapter, the moment-rotation diagram of joint (i) at x_i may be obtained directly from the corresponding moment-curvature diagram which is known. In the numerical solution of a problem, the moment-rotation diagram is used to find the change in one of the variables due to a change in the other. Specifically, given a change, $\Delta\theta_i$, in the rotation θ_i of joint (i), the corresponding change ΔM_i in the bending moment, M_i, is found as follows.

Referring to Figure 5b, to facilitate the determination of the incremental moment, ΔM_i, it is convenient to introduce the term "transition moment." Thus, associated with each joint (i) of the beam, in each phase of external loading there is a positive transition moment, N_i^+, and a negative transition moment, N_i^-. They play the following role in determining the moment-rotation relation of joint (i):

For $\Delta\theta_i \geq 0$:

$$\Delta M_i = k'_1 \Delta\theta_i, \qquad \text{if } N_i^+ \geq k'_1 \Delta\theta_i \tag{34a}$$

$$\Delta M_i = N_i^+ + \frac{k'_2}{k'_1}(k'_1 \Delta\theta_i - N_i^+), \qquad \text{if } N_i^+ \leq k'_1 \Delta\theta_i \tag{34b}$$

For $\Delta\theta_i \leq 0$:

$$\Delta M_i = k'_1 \Delta\theta_i, \qquad \text{if } N_i^- \leq k'_1 \Delta\theta_i \tag{35a}$$

$$\Delta M_i = N_i^- + \frac{k'_2}{k'_1}(k'_1 \Delta\theta_i - N_i^-), \qquad \text{if } N_i^- \geq k'_1 \Delta\theta_i \tag{35b}$$

where

$$k'_1 = \frac{1}{2}(h_i + h_{i+1})k_1; \qquad k'_2 = \frac{1}{2}(h_i + h_{i+1})k_2 \tag{36}$$

It may be noted that the transition moments are essentially the elastic limit moments at a particular stage of deformation history. For example, for a section at its virgin state (no prior history of bending), represented by the origin in Figure 5b, the positive and negative transition moments are equal to M_e and $-M_e$, respectively. However, during the various stages of loading the magnitudes of the positive and negative transition moments are not, in general, equal to each other. Nevertheless, the transition moments for the j-th phase of loading can always be determined from the transition moments and the change in bending moment of the preceding (j-1)-th phase. It is seen from Figure 5b that:

$$(N_i^+)_j = (N_i^+ - \Delta M_i)_{j-1}, \quad \text{if } 0 \leq (N_i^+ - \Delta M_i)_{j-1} \leq 2M_e$$

$$(N_i^+)_j = 0, \quad \text{if } (N_i^+ - \Delta M_i)_{j-1} \leq 0 \qquad (37a)$$

$$(N_i^+)_j = 2M_e, \quad \text{if } (N_i^+ - \Delta M_i)_{j-1} \geq 2M_e$$

and,

$$(N_i^-)_j = (N_i^- - \Delta M_i)_{j-1}, \quad \text{if } 0 \geq (N_i^- - \Delta M_i)_{j-1} \geq -2M_e$$

$$(N_i^-)_j = 0, \quad \text{if } (N_i^- - \Delta M_i)_{j-1} \geq 0 \qquad (37b)$$

$$(N_i^-)_j = -2M_e, \quad \text{if } (N_i^- - \Delta M_i)_{j-1} \leq -2M_e$$

Obviously, at any phase of the loading, the sum of the absolute values of N_i^+ and N_i^- is equal to $2M_e$. Therefore, if either one is known, the other can be determined easily as the complement to $2M_e$. These relations are, of course, defined for $j > 1$. For a given problem $(N_i^+)_1$ and $(N_i^-)_1$ should be specified.

In conclusion, the above procedure allows one to determine for each joint (i) the change in bending moment, when the corresponding change in the rotation of the joint is known. The history of loading and deformation is taken into account by using the transition moments described above.

3.4. Properties of Actual Bridges and Parameters of Problem

To determine a relatively realistic range of parameters, a study of seven simply-supported bridges considered in Reference 13 was made. A typical cross-section and its properties are shown in

Figure 6. In this particular case, the ratio, n, of the modulus of elasticity of steel to that of concrete was taken as 10.

The speed parameter, $\alpha (= T_1 v/L)$, incorporates in it the effect of the stiffness of the beam and its span length. However, for a given beam, the only variable in the expression of α is the horizontal component of the velocity, v, of the moving load. In the case of the typical bridges under consideration, a speed range of 10 to 80 mph corresponds approximately to a range of values of α from 0.042 to 0.333. However, if the properties of standard bridges given in Table 1 of Reference 9 are used, the above range of α corresponds to approximately 7 to 55 mph.

The load parameter, $\beta \left(= \frac{W_v}{P_y}\right)$, is a measure of the weight of the moving load with respect to the static mid-span yield load, P_y. A value of $\beta = 1.00$ corresponds to a moving load the weight of which is equal to that of the static mid-span yield load for the beam.

The weight parameter, γ, represents the ratio of the weight of the moving load to that of the beam. In the case of a load consisting of both an unsprung and a sprung mass, the parameter λ denotes the ratio of the unsprung mass to the total mass of the weight of the load, and $\bar{k}$ and $\bar{c}$ are the dimensionless versions of the spring and damping constants, respectively.

The stiffness ratio, R, is the ratio of the inelastic stiffness to the elastic stiffness of the beam. (See Figure 5a.) If R = 0, the

beam is elastic perfectly plastic; R = 1.0 corresponds to the perfectly elastic case.

3.5. Procedure of Numerical Solution

For simplicity, in what follows, the method of numerical solution for a beam traversed by a single unsprung mass is outlined.

Let the time when the moving unsprung mass is exactly over the entry support be denoted by t_o. For all numerical solutions obtained, at $t = t_o$ both the moving load and the beam have been assumed to be in static equilibrium. With given initial conditions, it is possible to compute the dynamic response of the beam when the unsprung mass has moved a short distance on the beam, provided the time elapsed is small enough. Proceeding in a similar manner one can determine the response of the beam at any time t, where $t > t_o$.

For the numerical solution, the problem may be stated as follows: Given at time $t = t_1$ the values of the variables $y_i(t_1)$, $\dot{y}_i(t_1)$, $\ddot{y}_i(t_1)$, $\theta_i(t_1)$ and $M_i(t_1)$ it is required to determine the values of these variables at $t = t_2 = t_1 + \Delta t$, where Δt is a small increment of time.

It may be said that, the numerical solution hinges on the numerical integration of the differential equations. In this study, the numerical integration has been carried out by using the following expressions:[14]

$$y_i(t_2) = y_1(t_i) + (\Delta t)\dot{y}(t_1) + \frac{1}{2}(\Delta t)^2 \ddot{y}(t_1) \qquad (38a)$$

$$\dot{y}(t_2) = \dot{y}(t_1) + \frac{1}{2}\Delta t\,[\ddot{y}_i(t_1) + \ddot{y}_i(t_2)] \qquad (38b)$$

The procedure of solution is outlined below:

1) Obtain the value of $y_i(t_2)$ for each joint (i) by using Equation (38a), and form:

$$\Delta y_i = y_i(t_2) - y_i(t_1)$$

2) From Equation (2) obtain $\Delta\theta_i$ by substituting therein Δy_i for y_i and $\Delta\theta_i$ for θ_i.

3) Compute ΔM_i using the value of $\Delta\theta_i$ according to the bending moment-rotation relation of the individual joints (see Art. 3.3). Having ΔM_i, form the quantity:

$$M_i(t_2) = M_i(t_1) + \Delta M_i$$

4) Write out the expressions for y_ζ, $\dot{y}_\zeta$, $\ddot{y}_\zeta$ using Equations (4)-(5b). Note that these expressions cannot be written out explicitly, since some of the variables involved are still unknown.

5) With the quantities found in steps 1, 3 and 4, obtain a set of equations in the $\ddot{y}(t_2)$, by using one of the Equations (13), (16), or (17) depending on the joint in consideration and the location of the moving load. Solve the above set of equations simultaneously for the unknown $\ddot{y}(t_2)$'s.

6) Obtain $\dot{y}_i(t_2)$ from Equation (38b).

7) Repeat the previous steps to extend the solution of the problem from t_2 to $t_2 + \Delta t$, etc.

For the numerical integration method used in the present study, the time increment, Δt, should be small enough to satisfy the criteria of stability and convergence. In Reference 15, the upper bound of the time increment was given as $\Delta t = 0.389\ T$, where T is the shortest natural elastic period of vibration of the system. A smaller increment will in general give a more accurate answer, if round off errors do not tend to become critical. An increment of $\Delta t = 0.200\ T$ was used in obtaining the numerical results in this study. Using a smaller value of Δt for a few cases did not change the results significantly.

3.6. Use of Computer

The numerical results presented in this study have been obtained by means of a computer program developed for use on the "CDC 3600" digital computer system of Michigan State University. The program, which is based on the equations and procedures discussed in this chapter, computes the response of a simply supported beam subjected to a single moving load. The moving load may consist of either a single unsprung mass, a single sprung mass, or a single-axle load unit.

Upon being supplied the parameters of the problem to be solved,

the program prints out the following dimensionless quantities at regular intervals of τ (each interval is a multiple of $\Delta\tau$, the interval of numerical integration):

1) the value of τ, which also specifies the position of the load;

2) both the dynamic and static deflections of all the joints of the discrete beam system;

3) the interaction force; and

4) the permanent deformation angles at every joint of the beam.

In addition, at the end of the solution of each problem, the maximum values of the displacements incurred during the passage of the load, and the ordinates of the final shape of the deformed beam are printed out.

The computer time necessary for the solution of a typical problem, including the free vibration response, is about 7 1/2 minutes for $\alpha = 0.10$, and about 4 1/2 minutes for $\alpha = 0.30$.

The format of the parameters to be supplied, and some other details, as well as a copy of the Fortran Program have been compiled in the Appendix.

IV. NUMERICAL RESULTS

4.1. General

The numerical results presented in this chapter comprise the elasto-inelastic dynamic response of simply-supported beams subjected to heavy moving loads. The types of moving loads considered are limited to a single unsprung mass, a single sprung mass, or a single axle load unit consisting of a sprung mass and an unsprung mass. For nearly all the numerical results obtained, the beam is divided into 20 equal panels.

First, typical time history curves of deflections, acceleration, and interaction forces are presented to depict certain typical patterns of the behavior of the beam-load system under critical combinations of the parameters. The objectives are (i) to gain an insight into the physical problem, and (ii) to illustrate certain features in the workings of the mathematical model.

Following the discussion of the history curves, typical shapes of the final deformed beam are shown to illustrate the permanent damage that the beam undergoes due to the passage of the load. After that, the influences of such parameters as the speed and weight of the load, and the inelastic stiffness of the beam on the maximum beam deflection are briefly considered. Finally, the general trends

of the results are compared with certain numerical data available in the existing literature.

4.2. History Curves for Unsprung Mass

The term "history curve" designates a plot of the dimensionless response of the beam as a function of the dimensionless time, τ, which is also a measure of the location of the moving load. As all the variables mentioned in the following discussions are dimensionless, this adjective will be omitted for the sake of simplicity.

In order to form a clear picture of the connection between the beam response and the various parameters, the history curves for an unsprung mass have been grouped together, depending on the combination of the speed parameter α, and the load parameter β. Terms such as "low" and "medium" used in describing the relative values of these parameters within their ranges are, of course, qualitative.

4.2.1. "Low" Speed and "Medium" Load. Figure 7 shows a time history curve of the mid-span ($\bar{x} = 0.5$) deflection, $\bar{y}$, for: $R = 0$, $\alpha = 0.10$, $\beta = 0.90$, and $\gamma = 2.68$. The values of the parameters correspond to the case of an elasto-perfectly plastic beam subjected to a load slightly less than the yield load, moving at a "low" speed (about 25 mph). It is seen that for this set of parameters no inelastic action has taken place. In fact, the dynamic deflection curve is very close to the static deflection curve, which is also shown in the figure.

This curve corresponds to the (static) influence line for mid-span deflection due to the load; it has been computed on the basis that the beam remains perfectly elastic. The free vibration after the load has left the span is also seen to have small amplitudes.

In Figure 8 is plotted the history curve of the interaction force $\bar{P}$, for the same problem as considered in Figure 7. The curve is not smooth; it exhibits many oscillations around the static value. This is a characteristic feature of history curves of $\bar{P}$ for an unsprung mass. The reason is that $\bar{P}$ depends directly on the acceleration of the unsprung mass (see Equation (12')), which, in turn, depends on the accelerations, as well as the velocities (see Equation 5b), of the flexible joints adjacent to the instantaneous position of the load. Although in this case, so far as magnitudes are concerned, the dominating term in the expression for $\bar{P}$ is the constant static or gravitational component, among the time dependent terms those related to accelerations, in general, predominate over those related to velocities. These accelerations generally oscillate a great deal, as illustrated in Figure 9, and bring about the oscillations in $\bar{P}$.

4.2.2. "High" Speed and "Medium" Load. A representative history curve of deflection for this case is shown in Figure 10. The values of the parameters are the same as in the preceding case except that α has been increased to 0.30 (corresponding to about 70 mph). Furthermore, the point under consideration is $\bar{x} = 0.55$, at

which the maximum displacement is larger than that at $\bar{x} = 0.50$. In contrast to the history curve in Figure 7, one may observe that in this case inelastic action has taken place. The equilibrium position of free vibration is below the initial horizontal configuration of the beam, indicating a "permanent set" or permanent deformation. The permanent set is 0.788, and the maximum dynamic deflection is 1.70.

It is also noted from the figure that, although the displacement being considered is for $\bar{x} = 0.55$, its maximum value occurs when $\tau = 0.817$, i.e., when the load is at $\bar{x} = 0.817$. In subsequent discussions, the symbol τ_{max} is used to designate the time at which the maximum dynamic response occurs. Similarly, $\bar{y}_{max}$ denotes the maximum dynamic deflection (at $\tau = \tau_{max}$).

Figure 11 shows the history curve of $\bar{P}$ for the same problem. In general, this curve also exhibits an oscillatory pattern. However, it is to be noted that initially the dynamic $\bar{P}$ curve remains consistently below the static one, for a relatively large interval of τ. Later on, a trend for a gradual increase develops, resulting in values of $\bar{P}$ appreciably larger than the static value. However, as the load is approaching the end of the span, after $\tau = 0.85$, $\bar{P}$ drops suddenly, and even becomes negative. It is to be noted that for physical realization of a negative interaction force, a tensile force would be required to maintain the contact between the moving load and the beam (that is, to keep the load from leaving the surface of

the beam). Thus, the present solution involves a hypothetical tensile force which does not exist in such practical cases as a bridge-vehicle system. However, the effect of such a negative force has been found to be insignificant, since it occurs near the departure end of the beam; and its numerical value is not exceedingly large.

4.2.3. "Medium" Speed and "Heavy" Load. The history curve in Figure 12 corresponds to the displacement at point $\bar{x} = 0.8$ with the following values of parameters: $R = 0$, $\alpha = 0.20$, $\beta = 1.20$, and $\gamma = 3.568$. The distinguishing feature in this case is, of course, the heavier load, which is 20% greater than the yield load. Consequently, as expected, the beam exhibits a behavior quite different than the previous cases. It is worth noting that, while the moving load is on the beam there is no rebound or "snap back" of the beam, but rather a tendency for increasing velocity of the downward movement, and uncontained deformations.

The corresponding $\bar{P}$ curve is shown in Figure 13. For the most part this $\bar{P}$ curve closely resembles the preceding one (Figure 11). However, shortly after the load crosses the third quarter point of the beam, $\bar{P}$ increases very rapidly without a reversal that took place in the preceding case. Near the support, $\bar{P}$ attains an exceedingly large value of 49.38. This behavior is explained as follows.

For an unsprung mass, the value of $\bar{P}$ varies with its vertical acceleration which, as given by Equation 5b, depends on the difference

of $\dot{y}_i$ and $\dot{y}_{i+1}$, and the difference of $\ddot{y}_i$ and $\ddot{y}_{i+1}$. Generally, these differences are relatively small, due to the fact that the corresponding quantities have the same sign. When $\bar{P}$ is on the last (N-th) panel, $\dot{y}_{N+1}$ and $\ddot{y}_{N+1}$ are zero, since the (N+1)-th joint corresponds to the end support. Consequently, the value of $\bar{P}$ depends only on $\dot{y}_N$ and $\ddot{y}_N$.

Under certain combinations of the parameters, such as for the problem being considered, the beam yields a great deal, and the yielding (plastic hinges) moves with the load. When the load is at the last panel, the contribution of $\ddot{y}_N$ to $\bar{P}$ is relatively small, but the yielding of joint N results in large values of $\dot{y}_N$ which apparently is responsible for the large value of $\bar{P}$.

It may be thus conjectured that the large value of $\bar{P}$ in this case could be a consequence of the discrete nature of the beam model. Hence, the numerical results after the load moves on the last panel should be viewed with some caution. However, it is worth noting again that, in general, the major damage to the beam is done before the load passes over that panel.

When the parameters are such that the deformations are contained, i.e., they do not become exceedingly large, the results for $\bar{P}$ for an unsprung mass do not exhibit the kind of behavior described above. One of the parameters that may change the response from an uncontained deformation to a contained one is the stiffness ratio R.

This is considered in the next section.

4.2.4. History Curves for $R > 0$. Retaining the values of all the other parameters in Figure 12 but changing the value of R from 0 to 0.1 yields the history curve of $\bar{y}$ shown in Figure 14. In this case, the beam rebounds before the load has left the span, and $\bar{y}_{max}$ is much less than the one in Figure 12. Thus, at $\bar{x} = 0.8$, when $R = 0$, $\bar{y}_{max} = 12.58$ at $\tau_{max} = 1.000$, and when $R = 0.1$, $\bar{y}_{max} = 2.43$ at $\tau_{max} = 0.833$. This shows that even a small positive value of R causes the deformations to be contained. In passing, it may be pointed out that for the parameters in Figure 14, the absolute maximum $\bar{y}_{max}$ occurs at the point $\bar{x} = 0.6$ (Figure 14 is for $\bar{x} = 0.8$), and has the value of 3.32.

The corresponding history curve of $\bar{P}$ is shown in Figure 15. This curve is similar to the one shown in Figure 11. As the moving load approaches the departure end, $\bar{P}$ attains a relatively large positive value with a subsequent drop to a negative value; and $\bar{P}$ does not build up to any exceedingly large value that appeared in the case of $R = 0$ as shown in Figure 13.

The effect of having an inelastic stiffness is very pronounced for the history curve of $\bar{y}$, shown in Figure 16. The parameters are the same as before, except that R has been increased to 0.5. In this case, the absolute maximum $\bar{y}_{max}$ occurs at $\bar{x} = 0.5$ when $\tau_{max} = 0.641$, and has the value of 1.63. The permanent set at this point of

the beam is 0.309. The value of $\bar{y}_{max}$ at the point $\bar{x} = 0.8$ is 1.02 as compared to the corresponding $\bar{y}_{max} = 12.58$ for R = 0.

4.3. History Curves for Sprung Mass

Figure 17 shows the history curve of point $\bar{x} = 0.5$ when the moving load is a sprung mass. The parameters have the following values: R = 0, $\alpha = 0.20$, $\beta = 1.00$, $\gamma = 2.973$, and $\bar{k} = 33.57$ (this corresponds approximately to the stiffness of the springs of a heavy duty truck). Even though the static value of the load is just equal to P_y, there is a considerable amount of inelastic deformation resulting from its passage. The maximum response $\bar{y}_{max}$ is 2.33 and $\tau_{max} = 0.813$; the permanent set is 1.38.

The history curve of $\bar{P}$ for the above set of parameters is shown in Figure 18. Since in this case the interaction force depends on the vertical deflections rather than the accelerations, the graph for $\bar{P}$ is much smoother in comparison to similar curves for an unsprung mass. However, in this case also, as the load approaches the departure end, $\bar{P}$ attains a relatively large value and drops quickly, but it remains positive as the load leaves the span. This is also true for other data involving sprung loads.

In Figure 19 is plotted the deflection history curve for a case in which considerably large deformations occur. The point considered is at $\bar{x} = 0.7$, and R = 0, $\alpha = 0.20$, $\beta = 1.20$, $\gamma = 3.568$ and $\bar{k} = 33.57$.

The reason for choosing the point $\bar{x} = 0.7$ is that the value of $\bar{y}_{max}$ is largest at that point. It is seen that $\bar{y}_{max} = 10.18$, $\tau_{max} = 0.972$, and the permanent set is 9.14, while at $\bar{x} = 0.8$ the results are $\bar{y}_{max} = 8.87$, $\tau_{max} = 0.964$, and the permanent set is 8.07. It is interesting to note that it is only when the load is about to leave the beam that the structure begins to rebound.

Figure 20 shows the history curve of $\bar{P}$ for the same problem dealt with in Figure 19. Again, the curve is seen to be relatively smooth. As the load approaches the far support, $\bar{P}$ grows considerably, and attains a maximum value of 6.15. This value is still considerably less than the maximum of 49.38 reached by $\bar{P}$ in the unsprung load case shown previously in Figure 13.

4.4. History Curve for a Single-axle Load Unit

A typical history curve of $\bar{y}$ for a beam traversed by a single-axle load unit is shown in Figure 21. The response is for the point $x = 0.6$. The unsprung and sprung part of the moving load are, respectively, 13% and 87% of the total load. All the other parameters are the same as for the proceding problem. It may be observed that the inelastic action which has taken place during the passage of the load over the beam is of considerable magnitude. In this case, $\bar{y}_{max} = 3.68$, $\tau_{max} = 0.825$, and the permanent set is equal to 2.472.

4.5. Final Shape of Deformed Beam

The final shape of the deformed beam is of obvious interest as it represents the apparent damage incurred during the passage of the load. In the present study, this shape is obtained by plotting the final equilibrium position of each flexible joint. This equilibrium position is estimated by taking the average of the maximum and minimum deflections of each joint during free vibrations. This is done sometime after the moving load has left the span, at which time the beam can be assumed to be vibrating elastically.

In the following, shapes of deformed beams are presented for typical sets of parameters and different types of moving loads.

4.5.1. Unsprung Loads. In Figure 22 are shown, for an elastic perfectly plastic beam ($R = 0$), the shapes of three deformed beams traversed by a load $\beta = 1.10$ for three values of α: 0.15, 0.25, and 0.30. The permanent damage is seen to increase with an increase in speed. It is of interest to note that, as the load speed increases, the region of the greatest permanent distortion moves closer to the departure end.

Figure 23a shows the deformed shape of the beam for $\beta = 1.30$. Although the load in this problem is only 18% heavier than the preceding one, the maximum permanent set is 4.9 times larger than that in the preceding case.

The deformed shapes of a beam with an inelastic stiffness

R = 0.5 are shown in Figure 23b for $\beta = 1.20$ and two values of α: 0.10 and 0.20. In this case, in contrast to the elastic perfectly plastic beams, an increase in speed is seen to reduce the permanent damage.

4.5.2. Sprung Load. In Figure 24 are shown typical deformed shapes of an elastic perfectly plastic beam due to a sprung load for the different load speeds as indicated in the figure.

The shapes of the three deformed beams in Figure 24a correspond to a very heavy load $\beta = 1.50$. It is of interest to note that, in contrast to the case of an unsprung load, an increase in speed in this case causes a decrease in the permanent deformation. For this set of parameters, the maximum set occurs, for all three load speeds, at $\bar{x} = 0.7$.

A similar pattern may be observed in the shapes of the deformed beams shown in Figure 24b, which is for a lighter load, $\beta = 1.20$.

4.5.3. Single-axle Load Unit. Some typical shapes of the deformed beam due to a load consisting of a sprung and unsprung mass are shown in Figure 25, for the parameters indicated in the figure.

The two deformed beam shapes in Figure 25a correspond to R = 0 and R = 0.1. It may be observed that a value of R = 0.1 not only cuts down the amount of deformation, but it also causes

the position of the maximum set to shift towards the entry end of the beam.

4.6. Effect of Speed Parameter

For a beam of given geometrical and physical properties, the effect of the speed parameter on the dynamic response is considerable. Its effects on permanent sets have been mentioned in the preceding section. In Figures 26 and 27 are plotted the maximum dynamic deflections of some particular point on the beam as a function of the speed parameter α. The values of the other parameters in each case are also noted in the figures.

Figure 26 shows the effect of α on $\bar{y}_{max}$ for the case of unsprung loads. Figure 26a is for R = 0, and β = 0.90, and Figure 26b for R = 0.1, and β = 1.20. Within the range of values of α for which results have been obtained, both plots indicate that the maximum dynamic deflections increase as α increases.

Similar plots for the case of sprung loads are shown in Figures 27a and 27b, for β = 1.20 and β = 1.50, respectively. An elastic perfectly plastic beam is considered for both figures. Contrary to the results for unsprung loads, in this case the maximum dynamic deflection decreases as α increases. A similar trend was, of course, noted previously in connection with permanent sets.

4.7. Effect of Stiffness Ratio

The importance of the stiffness ratio, R, has already been mentioned (Figure 25). In Figure 28 is plotted the maximum dynamic deflection at $\bar{x} = 0.5$ as a function of R for the case of an unsprung load. It may be observed that a small value of R, say R = 0.1, reduces drastically the value of the deflection. However, the rate of the reduction of the value of the maximum deflection decreases rapidly with an increase in R. For $R > 0.5$, further increases in its value does not result in any significant reduction in the response.

4.8. Effect of Weight of Load

For a beam of given geometrical and physical properties and a fixed value of the speed parameter α, the effect of the weight of the moving load on the response of the beam may be studied by varying β, and simultaneously varying proportionately the parameter γ. Numerical results obtained in this manner are plotted in Figure 29. This figure corresponds to a graph of the quantity $\bar{y}_{max}/\beta$ as a function of β.

The vertical scale in Figure 29 represents the ratio of the maximum dynamic deflection to the maximum static deflection which is found under the assumption of perfect elasticity. As expected, this quantity increases as β increases. However, it is to be noted that the relation is not linear--the rate of increase of $\bar{y}_{max}/\beta$ increases with an increase in β.

V. DISCUSSION, SUMMARY, AND CONCLUSION

5.1. Discussion

5.1.1. Unsprung Load. As mentioned in the Introduction, there have been two analytical studies reported in the literature dealing with the inelastic behavior of beams subjected to moving loads that possess mass. The analysis of Symonds and Neal[11] has included the influence of the mass of the beam, which has been neglected in Parkes' work.[10] However, in both of these studies a rigid-plastic moment-curvature relation has been assumed. It is of interest to compare the results presented in the preceding chapter with those given in these references. Of course, such a comparison can be made only with the data related to elastic perfectly plastic beams subjected to unsprung loads.

A parameter that is present in all existing analyses is the load speed. While the past two works indicated a decrease in the damage to the structure with an increase in speed, results of the present analysis indicate the contrary (see Figure 22).

A result of the present study that is in agreement with an observation made by Symonds and Neal is that a load greater than Parkes' "limit load" of $1.228\,P_y$ can cross a beam. However, it should be pointed out that the ensuing deformations may be very large.

In the numerical computations by Symonds and Neal, the assumption was made that a single plastic hinge existed in the beam at its mid-span. The results of the present study indicate that the point of the greatest plastic deformation has a tendency to move toward the departure end of the beam (see Figure 22).

In order to explain the differences mentioned above, it is to be noted that the present analysis has sacrificed the continuum nature of the structure for a more realistic representation of the deformation characteristics, including the elastic part. Although the previous works are confined to rigid-plastic systems, they have maintained the continuum character of the system. The advantage of either approach depends on the nature of the problem being investigated. For problems in which the loading is prescribed, i.e., unaffected by the deformation of the structure, the elastic part of the deformations may be neglected, if the deformations are large. In the present case of a moving mass, however, the magnitude of the loading is significantly affected by the beam deformation, regardless of it being elastic or inelastic.

It is of interest to note further that under the assumption of a rigid-plastic behavior, there can be no displacements, much less permanent deformations, if β is less than 1.0. On the other hand, it is found in this study that an appreciable amount of permanent damage can be done to a beam, even when β is less than 1.0, e.g. $\beta = 0.90$

(see Figure 10). In this respect, it seems that the approach used in the present study is a significantly more realistic one.

The discrete system, however, has its shortcomings, mainly loss of details and that some of its operations can be justified only on an intuitive physical basis. As a consequence of the rigid-panel assumption, there is on the beam no centrifugal force due to the moving mass, which must be present in a model with continuous flexibility and consequent curvature. This, however, is compensated by the corrections at the joints as discussed in Art. 2.2. Another seemingly questionable phenomenon seen in the discrete model, is the large values of $\bar{P}$ near the departure end of the beam, as discussed in Art. 4.2. Fortunately, as already mentioned, generally this is not too significant so far as the beam deformations are concerned, because it happens near the end of the beam.

5.1.2. Sprung Load. Probably the real advantage of the discrete model used herein is the fact that it can be employed to deal more realistically with more complex problems. In this connection, the sprung load representation of a vehicle, and the analysis of structures with a more general elasto-inelastic moment-curvature relation may be mentioned. It seems simply not practicable to treat such problems from the continuum point of view.

The numerical results obtained in this study seem to indicate that the present approach yields better results for sprung loads than

for unsprung ones. This is on account of the fact that, for sprung loads $\bar{P}$, depends on the deflections, while for unsprung loads it depends on the accelerations, which are not smooth functions (see Art. 4.2). It is also of significance to note that numerical solutions for the sprung mass case are also easier to obtain than those for the unsprung mass case.

5.2. Summary

An analytical study of the elasto-inelastic behavior of beams subjected to moving loads has been presented. The structure analyzed consists of a slender beam resting on rigid supports. The types of moving loads used in this study are a single unsprung mass, a sprung mass, and a combination of a sprung and unsprung mass, referred to as a single-axle load unit.

In obtaining the numerical results, only the case of a simply supported beam traversed by a single load has been considered in this study. The analysis is based on a discrete beam model, consisting of massless rigid panels connected by flexible joints with point mass. The flexibility and mass of the joints are obtained by lumping the corresponding continuous properties of the actual beam. This model facilitates considerations of the nonlinear deformation characteristics of the beam as well as possible non-uniform distribution of the beam mass. The nature of the discrete system, however, gives rise to

discontinuities in the vertical velocities and accelerations which, of course, have been taken into account in the analysis.

The solution of the problem has been carried out by numerical techniques. In nearly all cases, the beam has been divided into 20 equal panels. The numerical results have been obtained by the use of a high speed digital computer. They consist mainly of (i) typical time-history curves for deflections and interaction forces, (ii) final shapes of deformed beams, and (iii) the influence of certain parameters on the beam response. The major findings of this study are summarized as follows:

1) A beam may suffer permanent damage due to the passage of a load whose weight is less than the static yield load.

2) The effect of a positive inelastic stiffness on deformation is of considerable significance; even a small inelastic stiffness reduces the deformations substantially.

3) The inelastic deformations increase at a rapid rate when the load is increased beyond the static yield load. However, loads much heavier than the static yield load can cross the beam, if large deformations are allowed.

4) If permanent deformations occur, with an increase either in the weight or in the speed of the load, the location of the maximum permanent deformation shifts toward the departure end of the beam.

5) The model used in this analysis yields smoother variations in

the interaction force for a sprung load than for an unsprung load.

5.3. Conclusion

In this thesis a procedure for the dynamic analysis of the elasto-inelastic behavior of beams subjected to moving loads is presented. It has been demonstrated that the method is practical, and yields solutions of the physical problem that seemingly cannot be obtained by any other existing method. It may be pointed out also that, although the method has been applied herein to simple beams and single-axle loads only, extension of it to continuous spans and more complex moving load systems should present no difficulty.

Although the numerical results presented in this thesis seem generally reasonable from the physical viewpoint, their validity, strictly speaking, should be verified by experimental data. This verification represents a most important direction for future work for the general problem under consideration. The application of the method of analysis to problems that are more closely related to the present practice in bridge engineering--for example, in the specifications for allowable overloads--should be worthwhile and rewarding.

LIST OF REFERENCES

1. "The Behavior of Long Beams Under Impact Loading," by P. E. Duwez, D. S. Clark, and H. F. Bohnenblust, Journal of Applied Mechanics, Vol. 72, 1950, p. 27.

2. "Impulsive Motion of Elasto-Plastic Beams," by H. H. Bleich and M. G. Salvadori, Trans. ASCE, Vol. 120, 1955, p. 499.

3. "Large Plastic Deformations of Beams Under Transverse Impact," by E. H. Lee and P. S. Symonds, Journal of Applied Mechanics, Vol. 20, No. 1, 1953, p. 151.

4. "Impact of a Cantilever Beam with Strain Rate Sensitivity," by T. C. Ting and P. S. Symonds, Proceedings, the Fourth U.S. National Congress of Applied Mechanics, 1962, p. 1153.

5. "Dynamic Analysis of Elasto-Plastic Structures," by G. V. Berg and D. A. DaDeppo, Journal of Engineering Mechanics Division, ASCE, Vol. 86, No. EM2, April 1960, p. 35.

6. "Response of Elasto-Plastic Structures to Transient Loads," by H. H. Bleich, Transactions, New York Academy of Sciences, Ser. II, Vol. 18, No. 2, December 1955, p. 135.

7. "Dynamic Elasto-Plastic Analysis of Structures," by M. L. Baron, H. H. Bleich, and P. Weidlinger, Journal of Engineering Mechanics Division, ASCE, Vol. 87, No. EM1, February 1961, p. 23.

8. "Discrete Dynamic Models for Elasto-Inelastic Beams," by R. K. Wen and T. Toridis, to be published in the October 1964 issue of the Journal of Engineering Mechanics, ASCE.

9. "Dynamic Behavior of Simple-Span Highway Bridges," by R. K. Wen and A. S. Veletsos, Bulletin 315, 1962, Highway Research Board, Washington, D.C.

10. How To Cross an Unsafe Bridge," by E. W. Parkes, Engineering, Vol. 186, November 7, 1958, pp. 606-608.

11. "Travelling Loads on Rigid-Plastic Beams," by P. S. Symonds and B. G. Neal, Journal of Engineering Mechanics Division, ASCE, Vol. 86, No. EM1, January 1960, p. 79.

12. "Dynamic Analysis of Inelastic Multi-degree Systems," by A. C. Heidebrecht, J. F. Fleming and S. L. Lee, Journal of the Engineering Mechanics Division, ASCE, Vol. 89, No. EM6, December 1963, p. 193.

13. "Vibration Susceptibilities of Various Highway Bridge Types," by L. T. Oehler, Proc. Paper No. 1318, ASCE, Vol. 83, No. ST4, July 1957.

14. "A Method of Computation for Structural Dynamics," by N. M. Newmark, Trans. ASCE, Vol. 127, 1962, p. 1406.

15. "Discussion of a Differential Equation Related to the Breaking of Railway Bridges," by G. G. Stokes, Mathematical and Physical Papers, Cambridge, Vol. 2, p. 179.

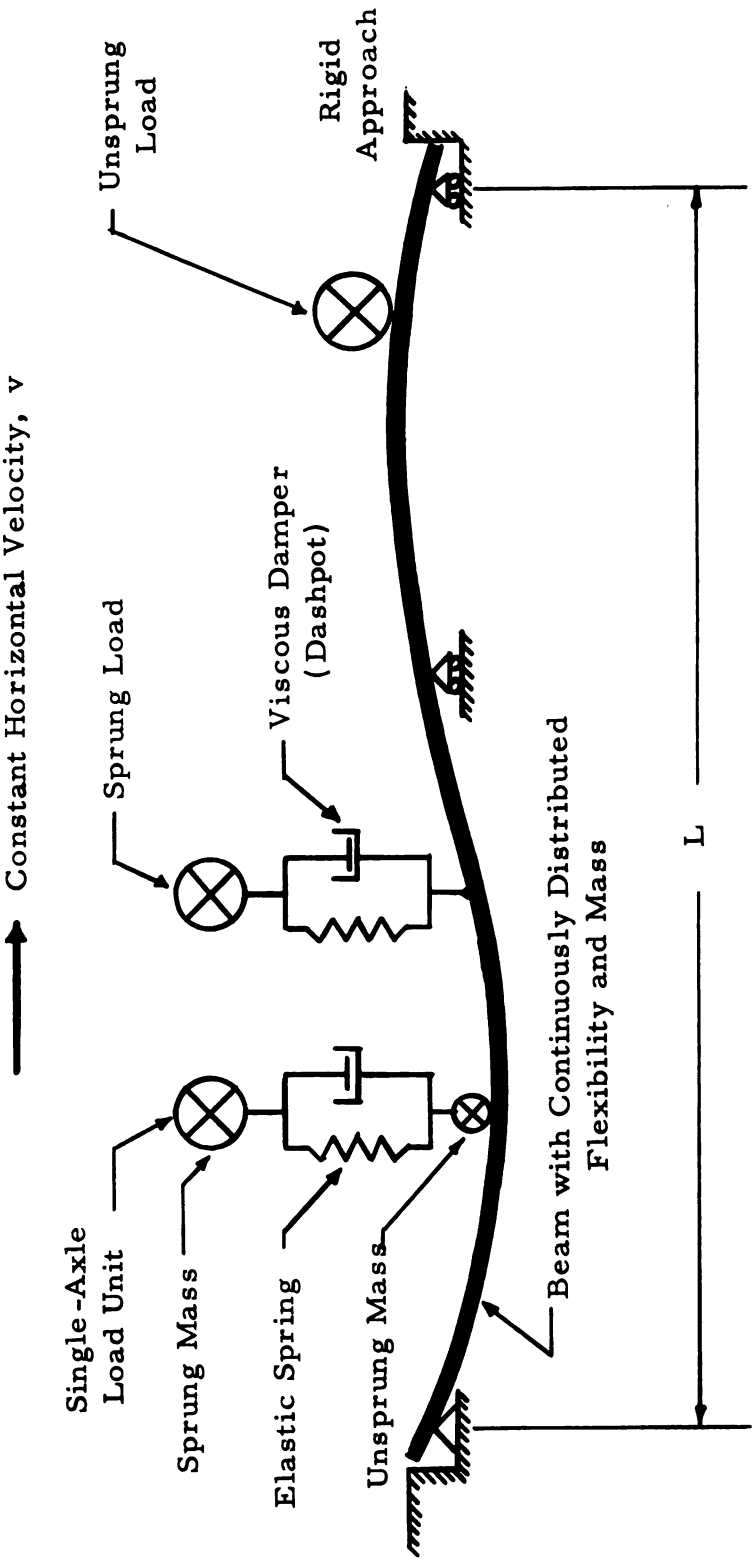

Fig. 1 - -System Considered

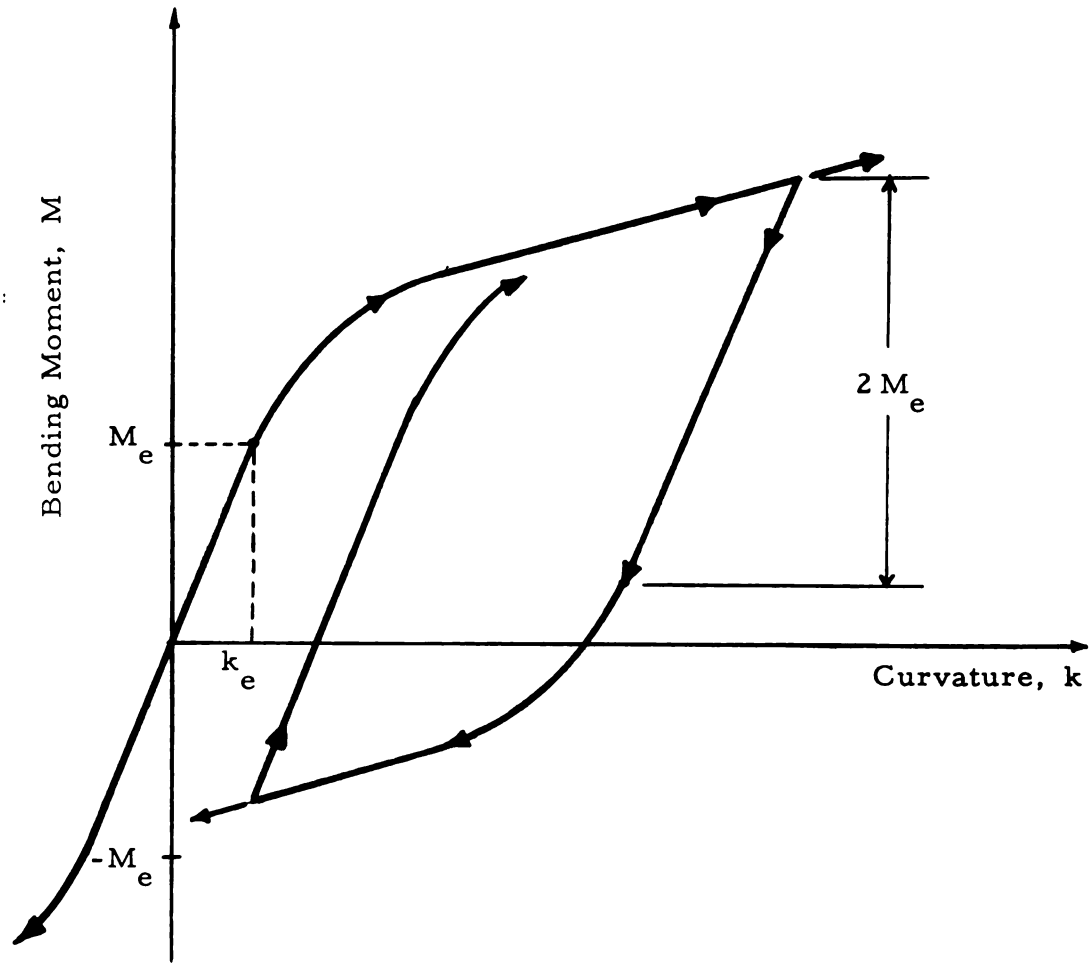

Fig. 2--Nonlinear Bending Moment-Curvature Relation

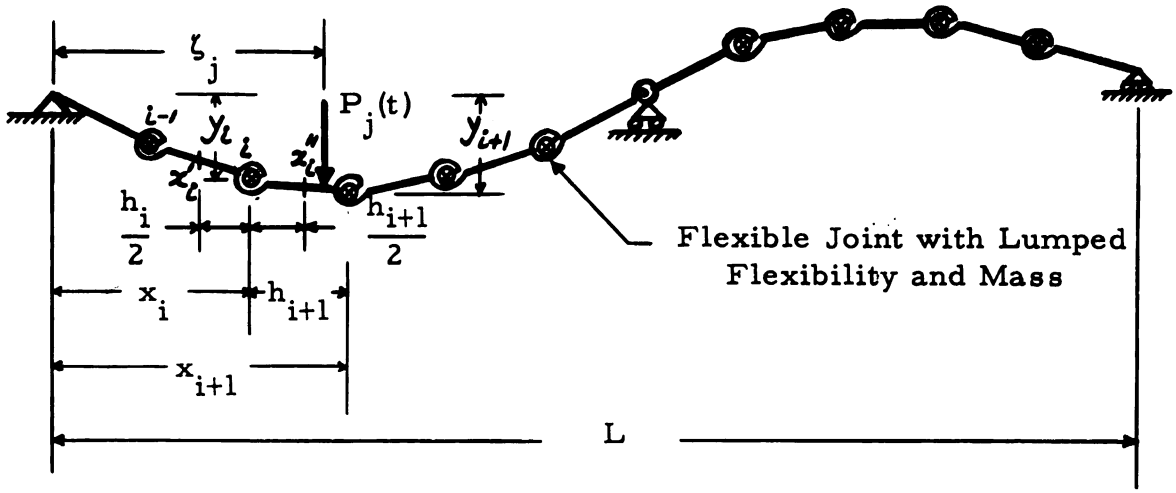

(a) Discrete Beam System

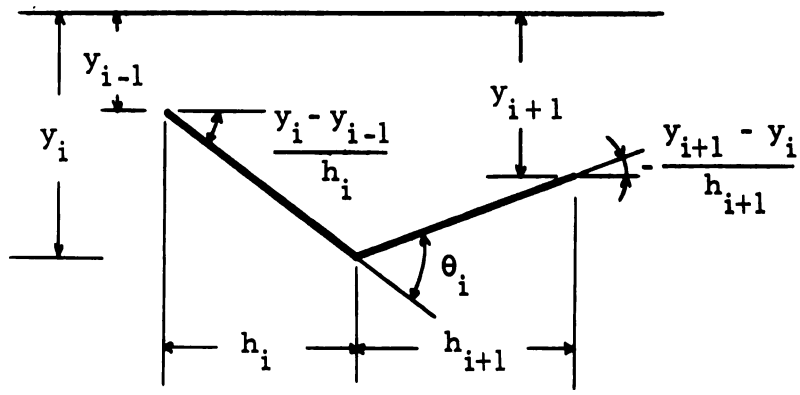

(b) Relation Between y and θ

Fig. 3--Discrete Beam System

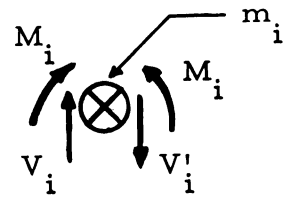

(a) Free Body for Joint (i)

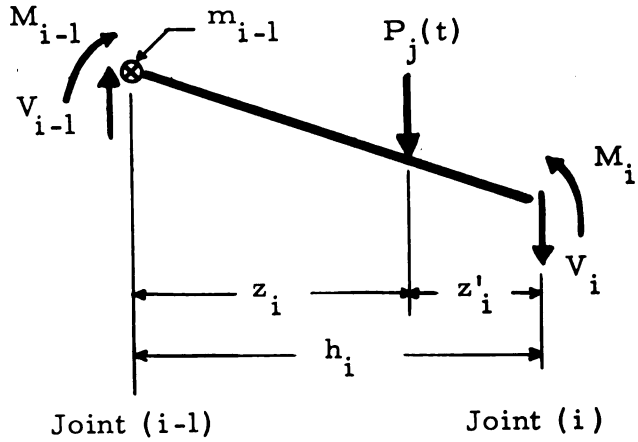

(b) Free Body of Panel (i-1) - (i)

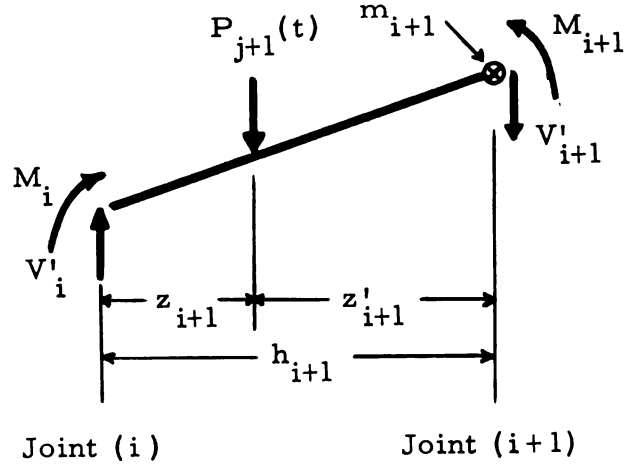

(c) Free Body of Panel (i) - (i+1)

Fig. 4--Free Body Diagrams

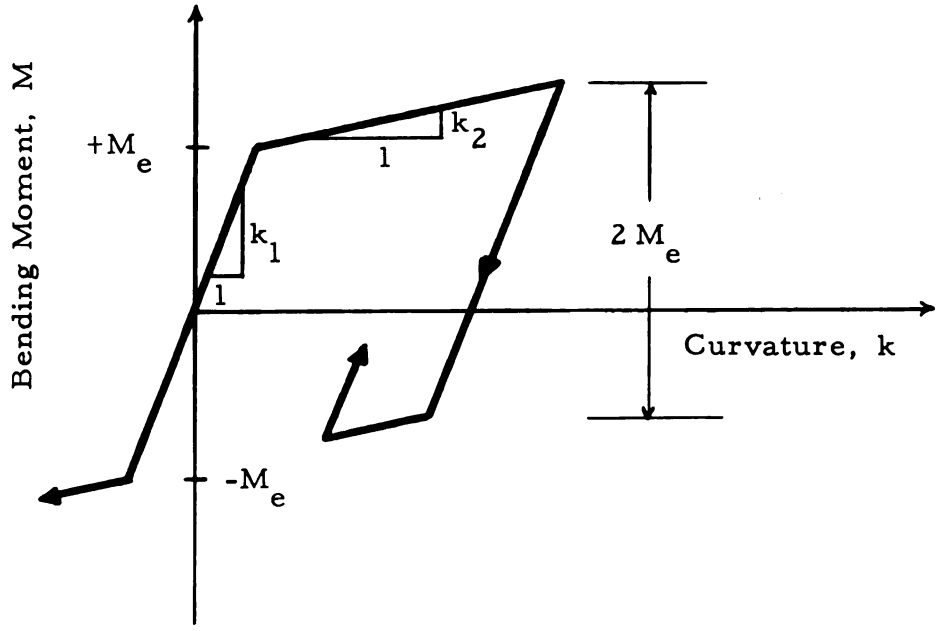

(a) Bilinear Bending Moment-Curvature Relation

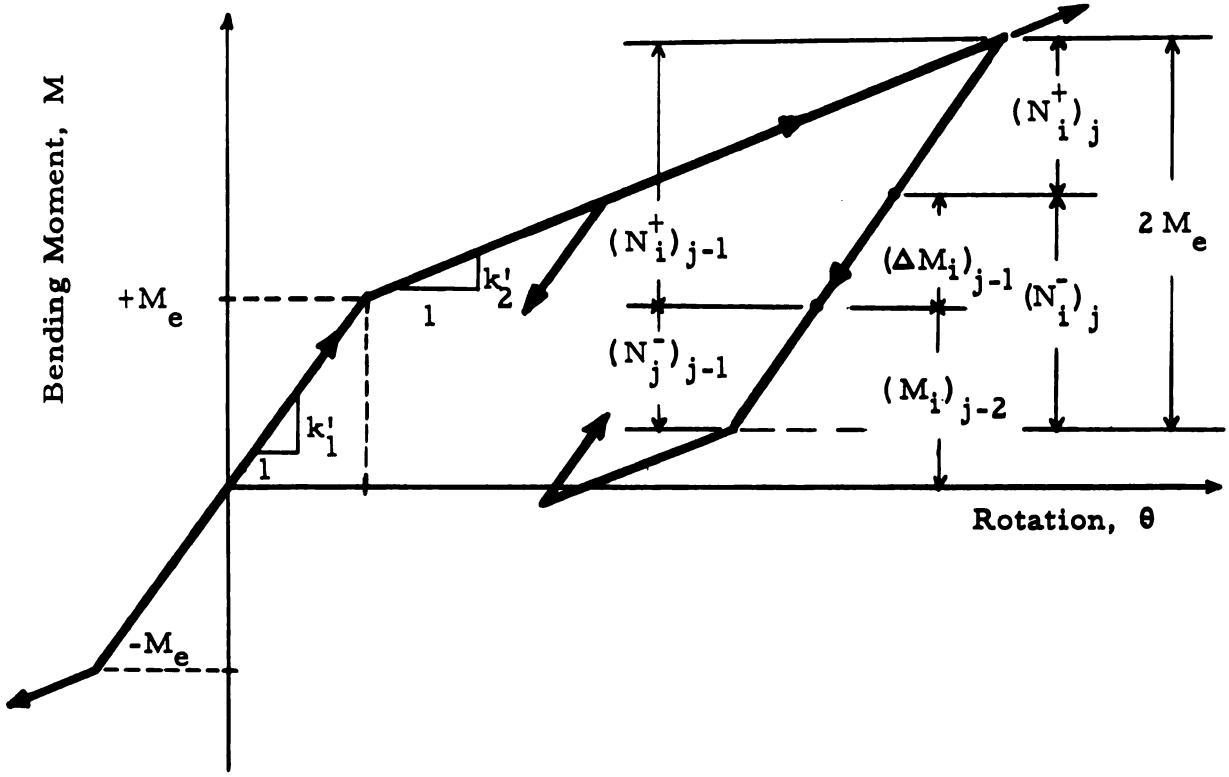

(b) Bilinear Bending Moment-Rotation Relation

Fig. 5--Bilinear Bending Moment-Curvature and Bending Moment--Rotation Diagrams

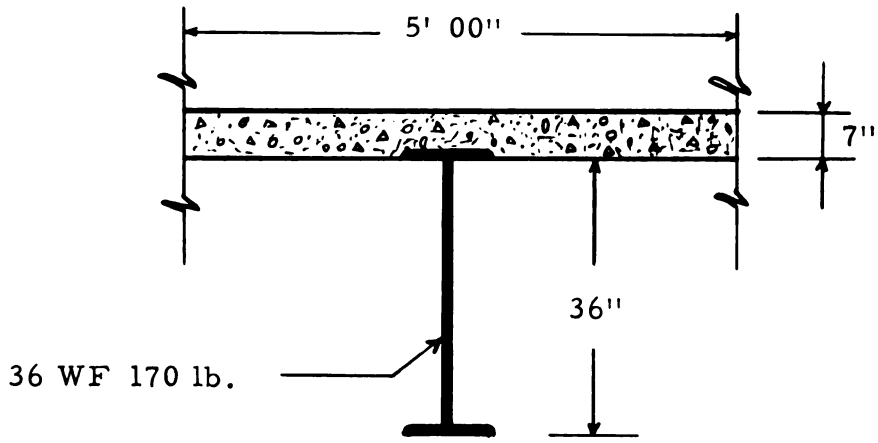

Simply-Supported Beam

Span Length, L = 64.25' c.c.

Steel Section: 36 WF 170 lb. at 5' 0" c.c.

Slab Thickness: 7"

Composite Design

$I_{transformed}$ = 18,270 in.^{4}

$E_{transformed}$ = 30 x 10^6 lb./in.^{2}

σ_{yield} = 33,000 lb./in.^{2}

m(x) = 0.127 lb.-sec.^{2}/in.^{2}

M_e = 2.169 x 10^7 lb./in.

P_y = 1.125 x 10^5 lb.

T_1 = 0.157 sec.

δ = 1.96 in.

Fig. 6--Properties of a Highway Bridge

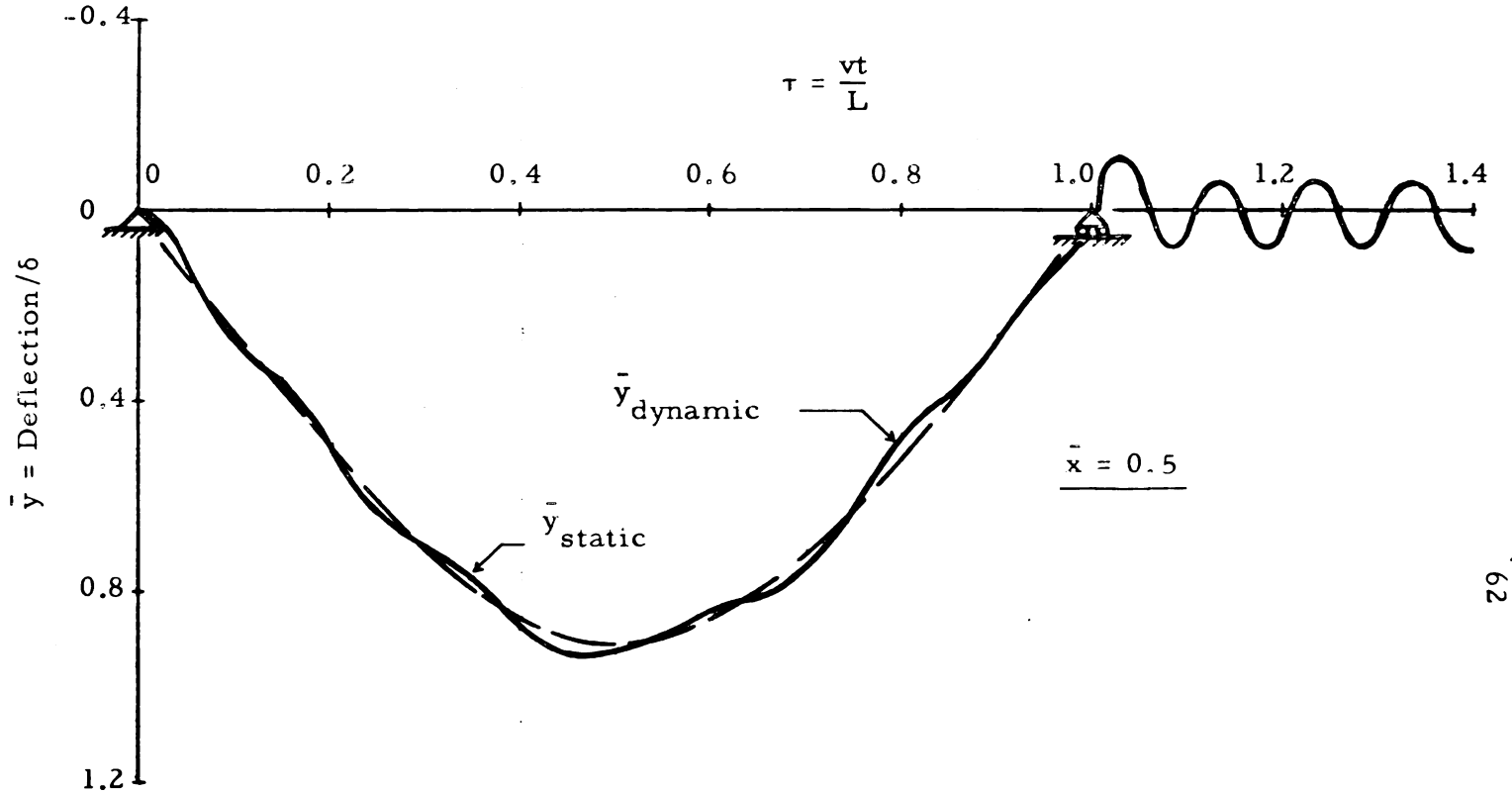

Fig. 7--History Curve of Deflection--Unsprung Mass (R = 0; α = 0.10, β = 0.90, γ = 2.676)

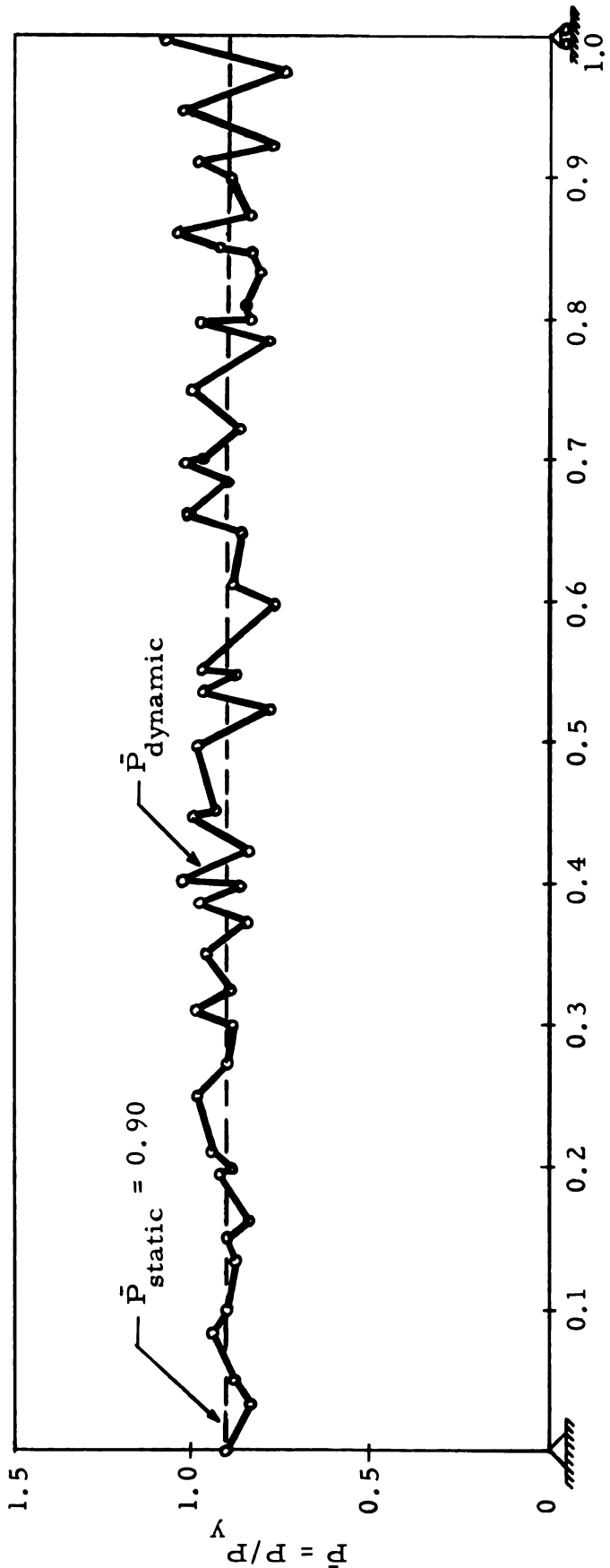

Fig. 8--History Curve of Interaction Force--Unsprung Mass ($R = 0$, $\alpha = 0.10$, $\beta = 0.90$, $\gamma = 2.676$)

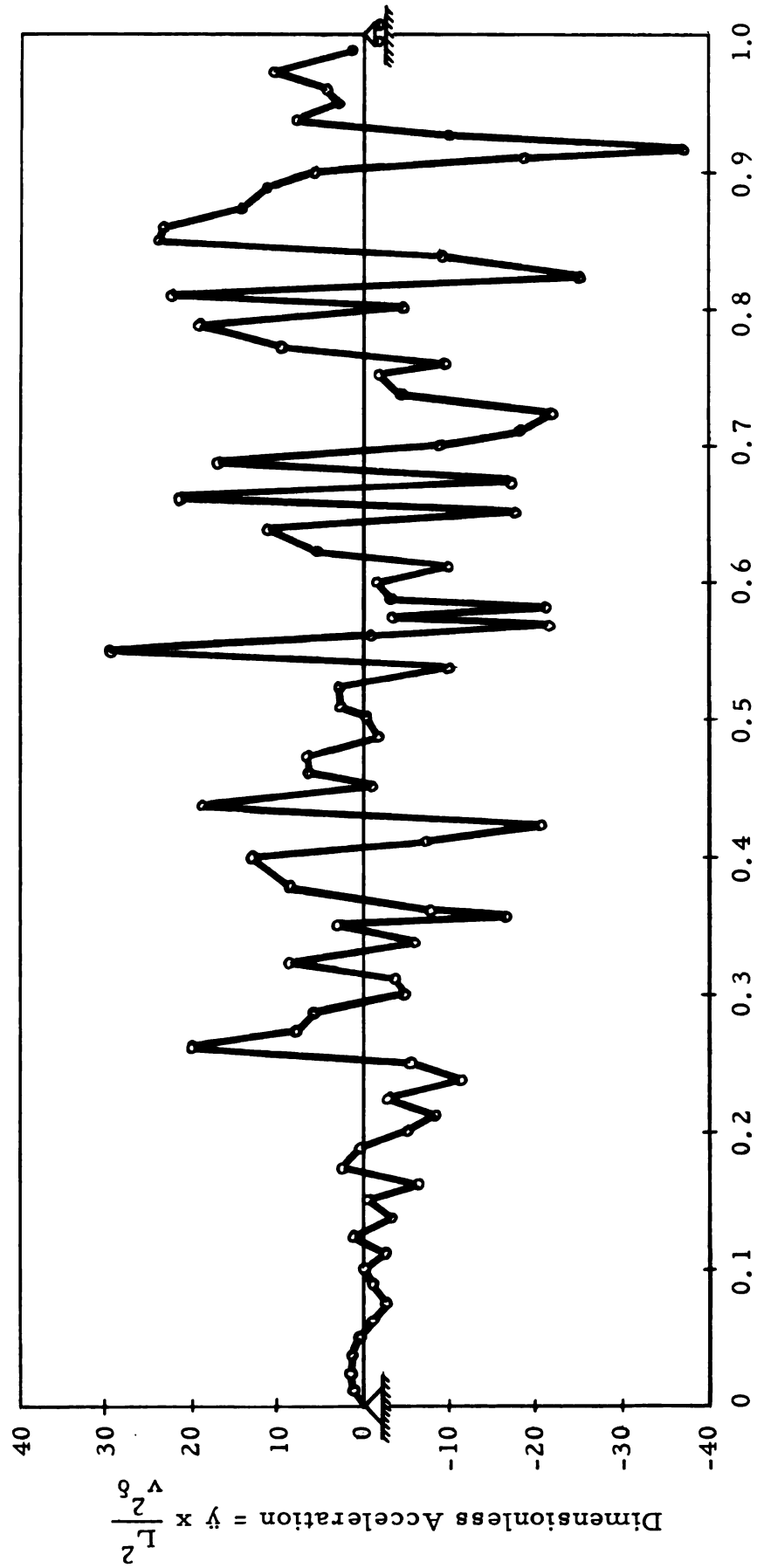

Fig. 9--History Curve of Acceleration--Unsprung Mass ($R = 0$, $\alpha = 0.10$, $\beta = 0.90$, $\gamma = 2.676$)

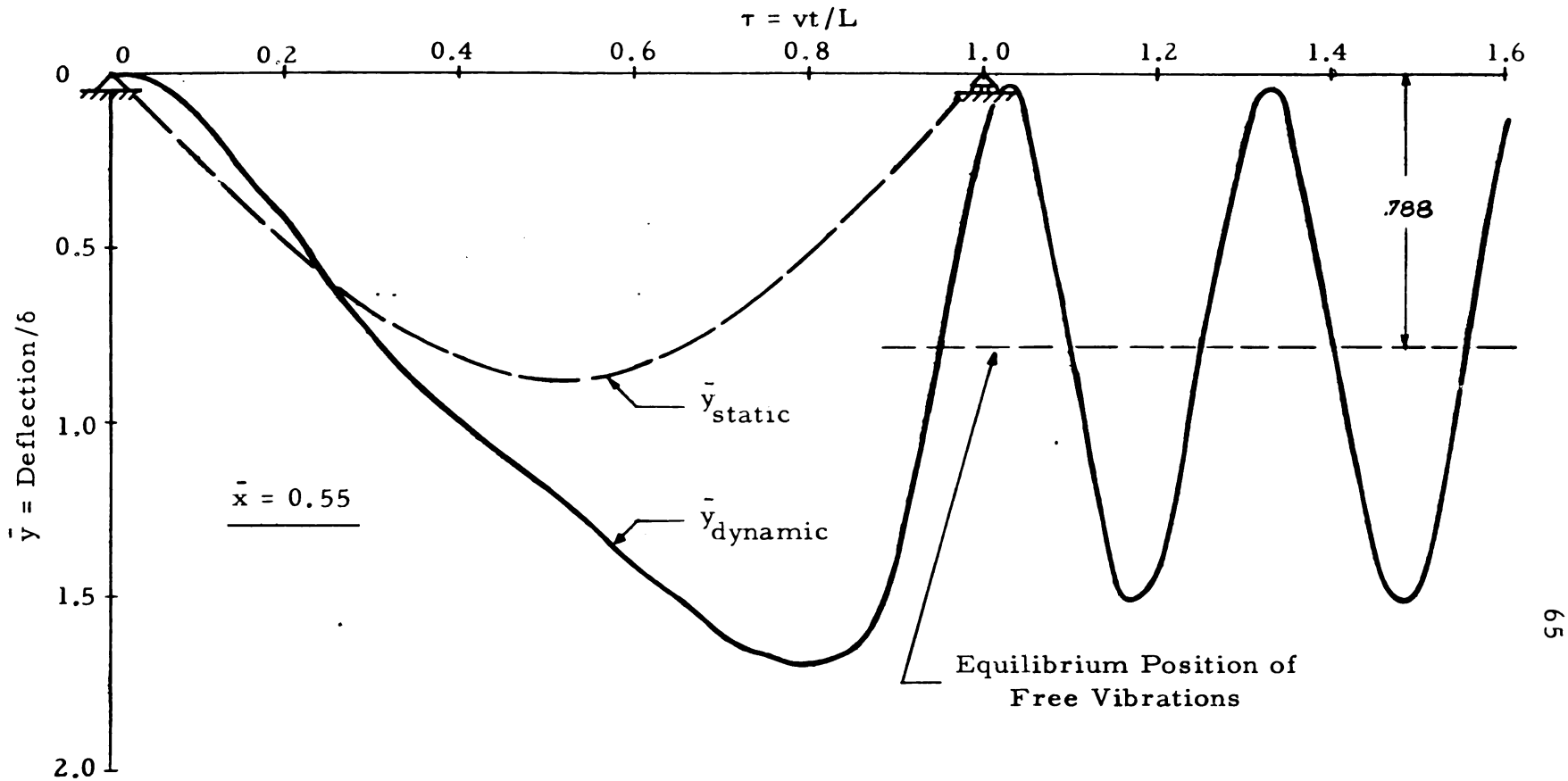

Fig. 10--History Curve of Deflection--Unsprung Mass (R = 0, a = 0.30, β = 0.90, γ = 2.676)

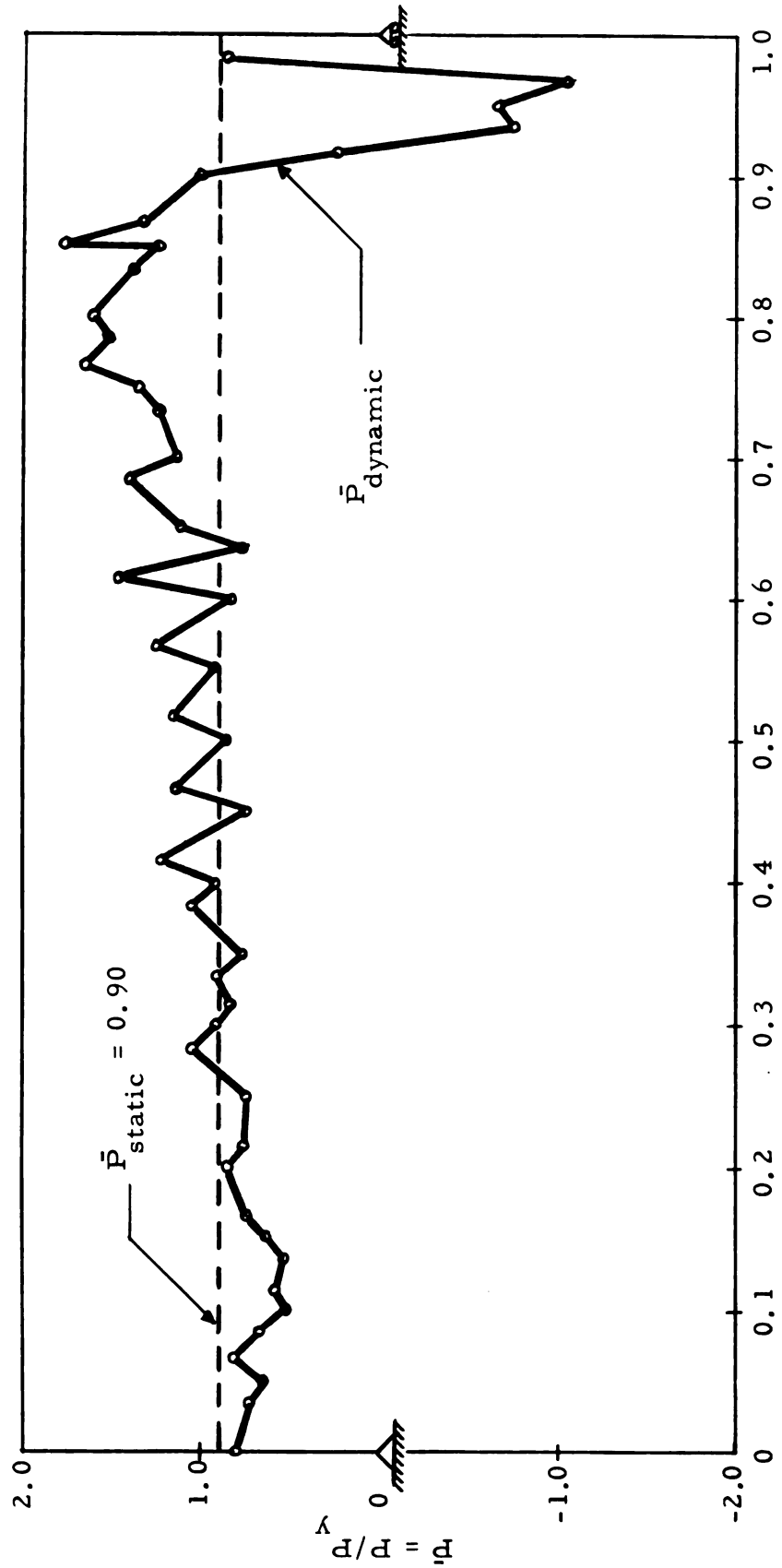

Fig. 11--History Curve of Interaction Force--Unsprung Mass (R = 0, α = 0.30, β = 0.90, γ = 2.676)

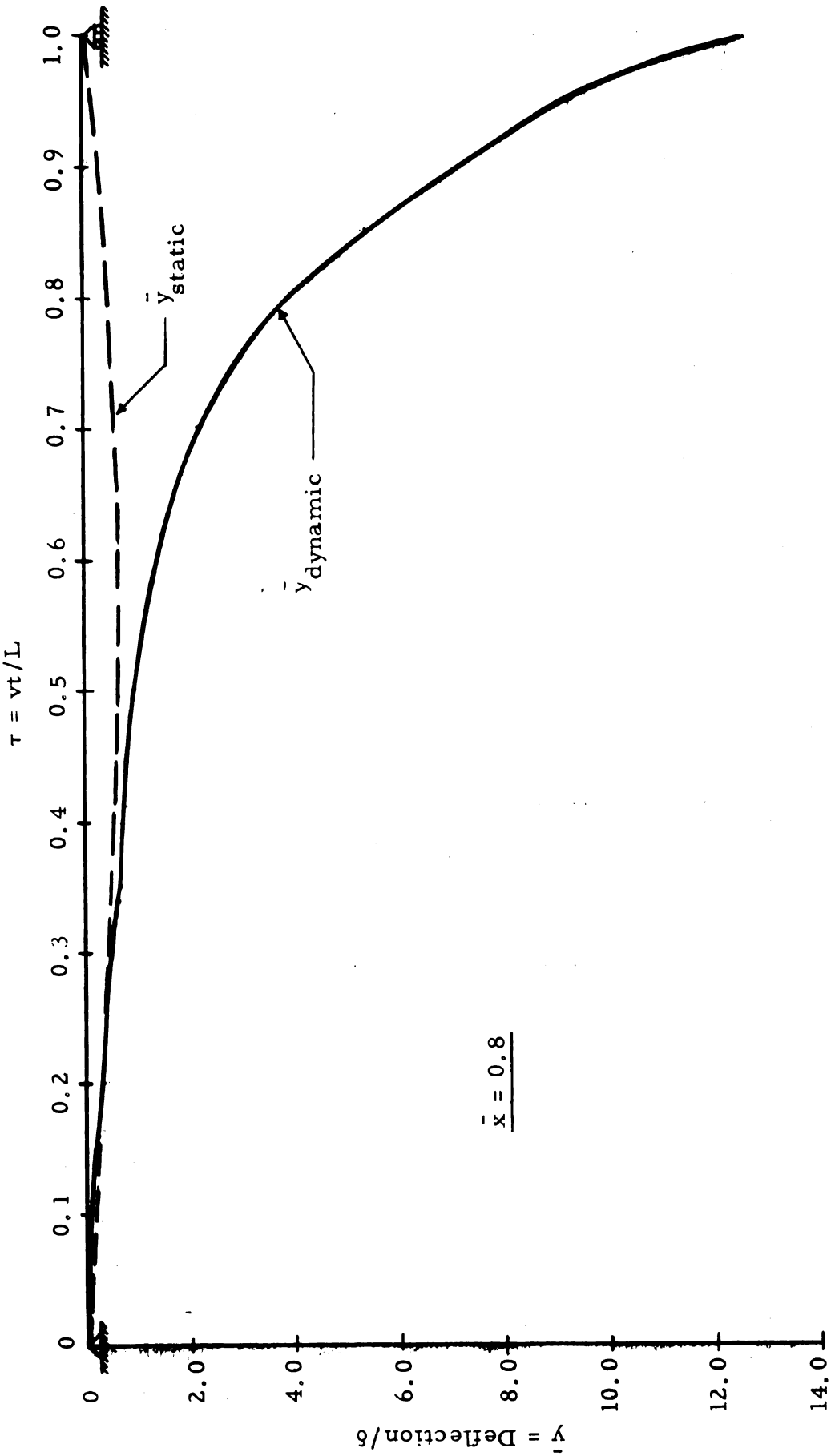

Fig. 12--History Curve of Deflection--Unsprung Mass ($R = 0$, $\alpha = 0.20$, $\beta = 1.20$, $\gamma = 3.568$)

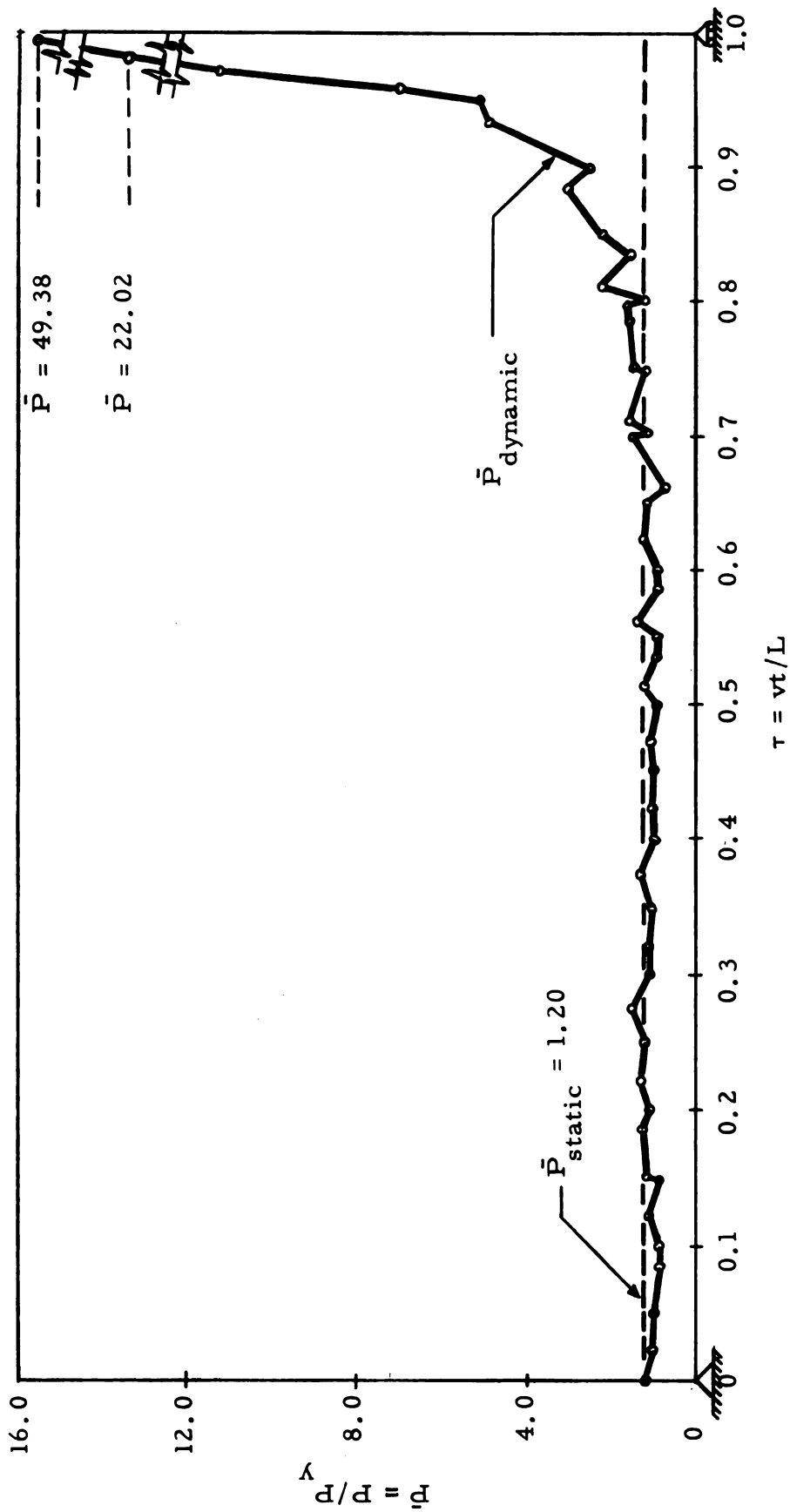

Fig. 13--History Curve of Interaction Force--Unsprung Mass ($R = 0$, $\alpha = 0.20$, $\beta = 1.20$, $\gamma = 3.568$)

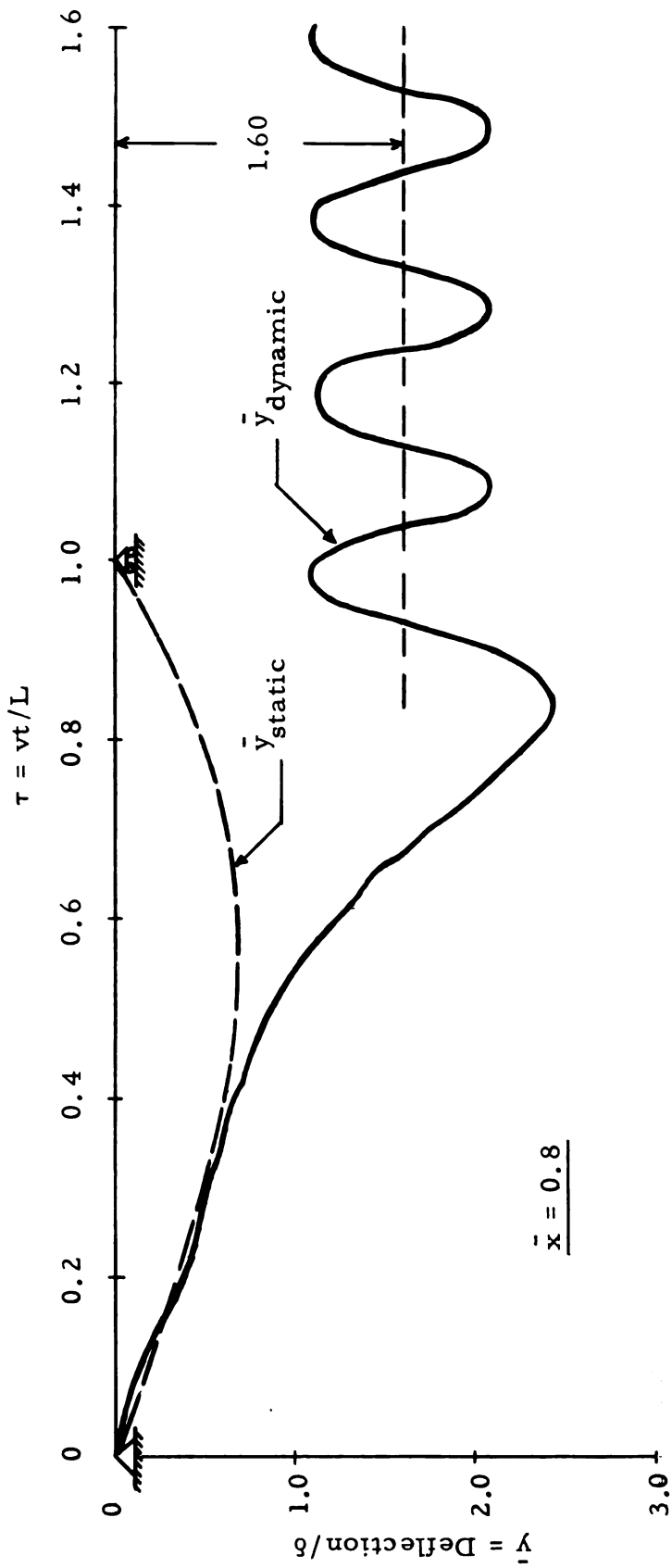

Fig. 14--History Curve of Deflection--Unsprung Mass ($R = 0.1$, $\alpha = 0.20$, $\beta = 1.20$, $\gamma = 3.568$)

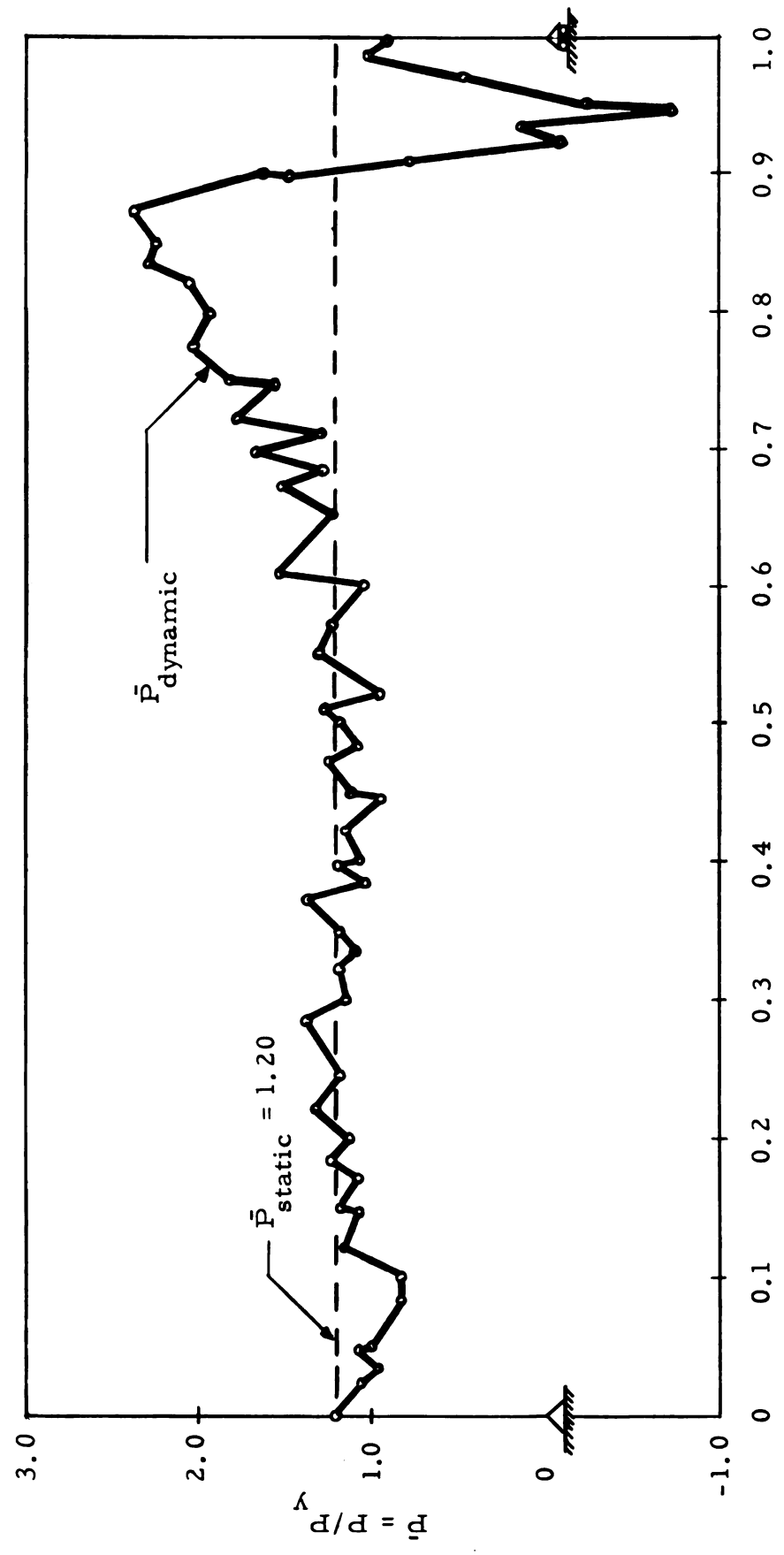

Fig. 15--History Curve of Interaction Force--Unsprung Mass ($R = 0.1$, $\alpha = 0.20$, $\beta = 1.20$, $\gamma = 3.568$)

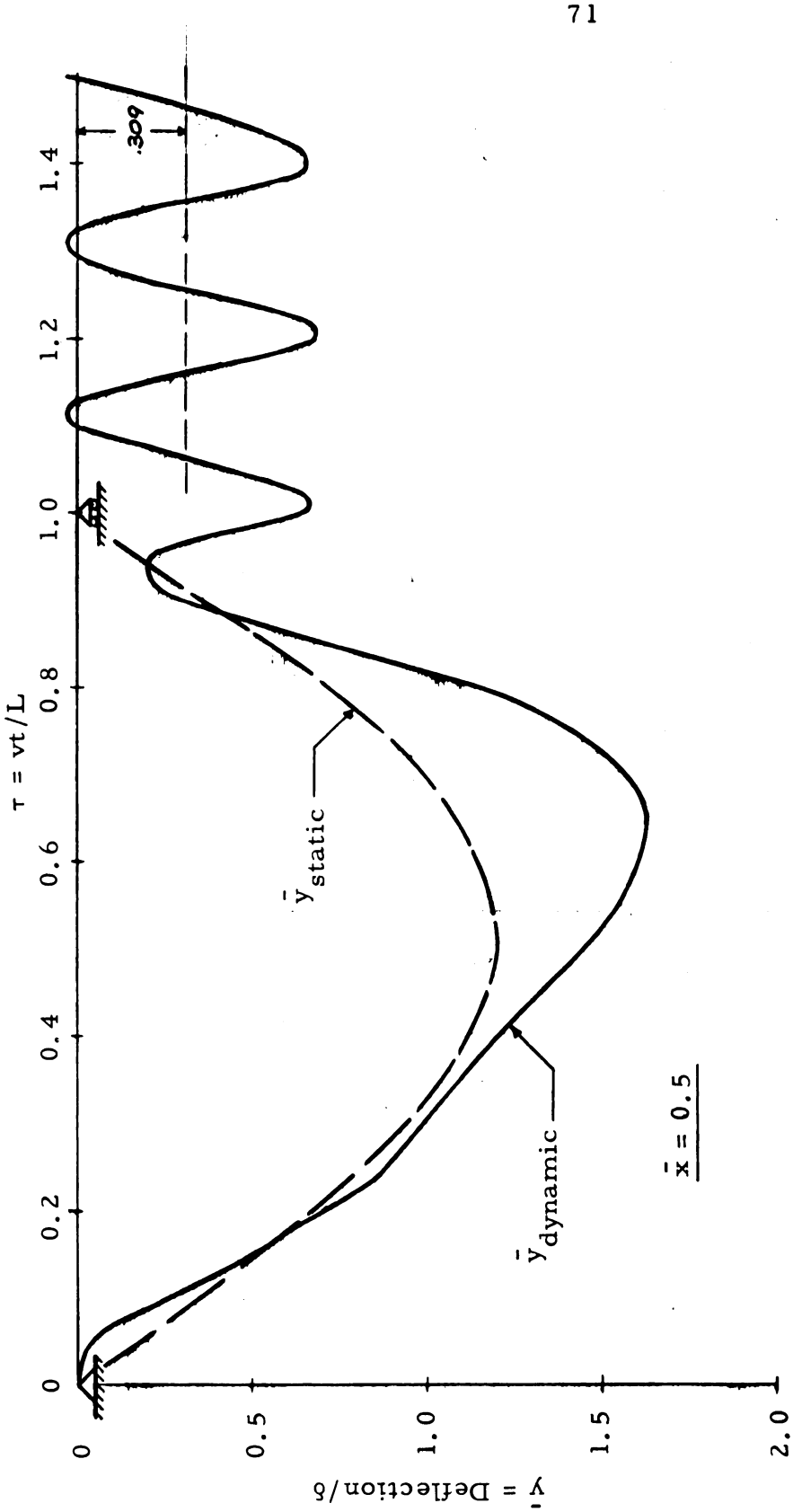

Fig. 16--History Curve of Deflection--Unsprung Mass (R = 0.5, α = 0.20, β = 1.20, γ = 3.568)

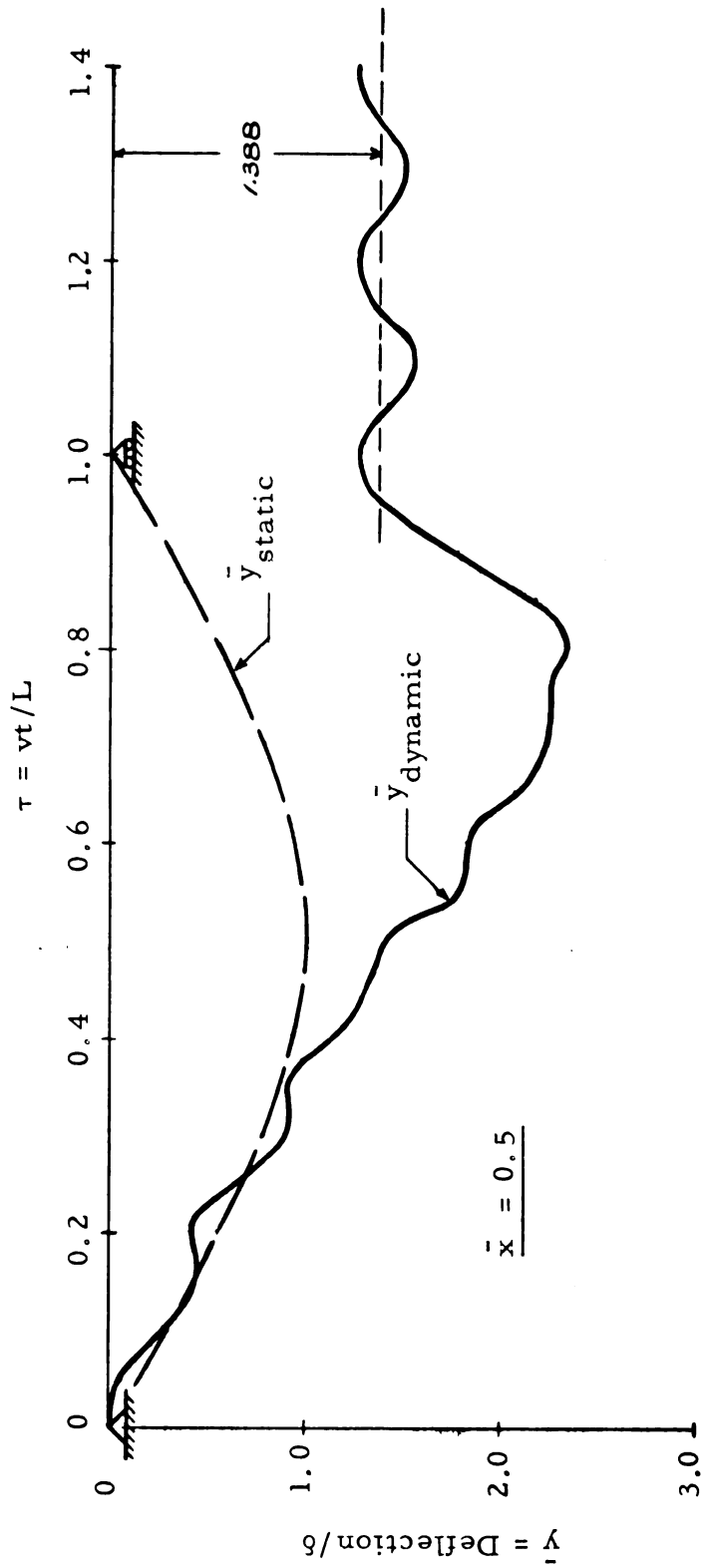

Fig. 17--History Curve of Deflection--Sprung Mass ($R = 0$, $\alpha = 0.20$, $\beta = 1.00$, $\gamma = 2.973$, $\bar{k} = 33.57$)

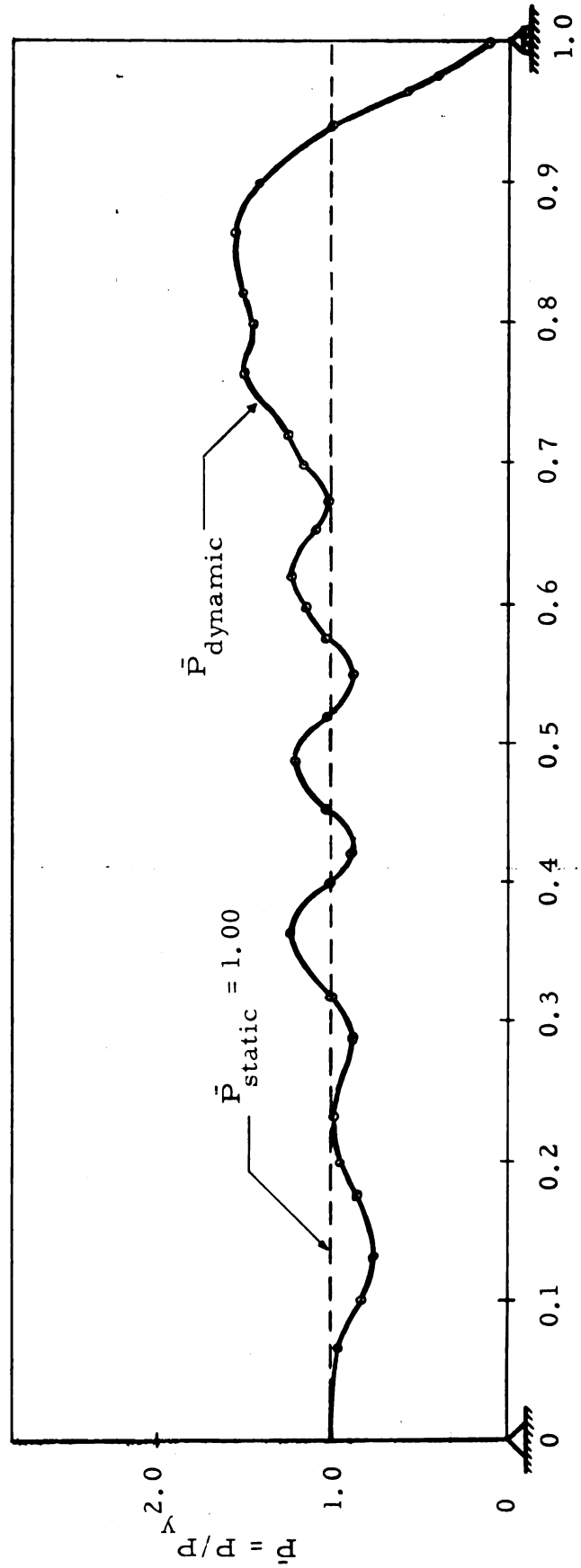

Fig. 18--History Curve of Interaction Force--Sprung Mass ($R = 0$, $\alpha = 0.20$, $\beta = 1.00$, $\gamma = 2.973$, $\bar{k} = 33.57$)

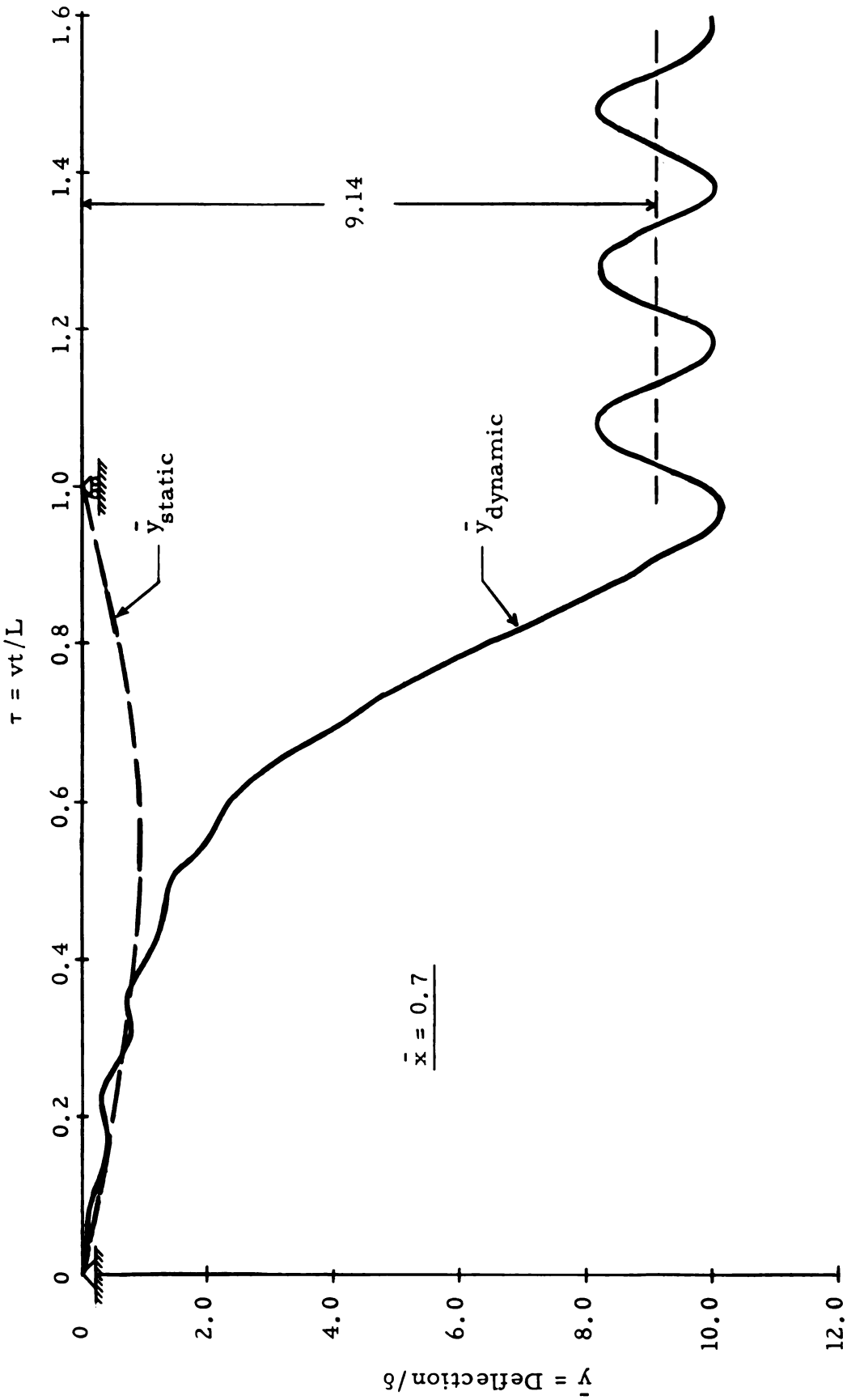

Fig. 19--History Curve of Deflection--Sprung Mass ($R = 0$, $\alpha = 0.20$, $\beta = 1.20$, $\gamma = 3.568$, $\bar{k} = 33.57$)

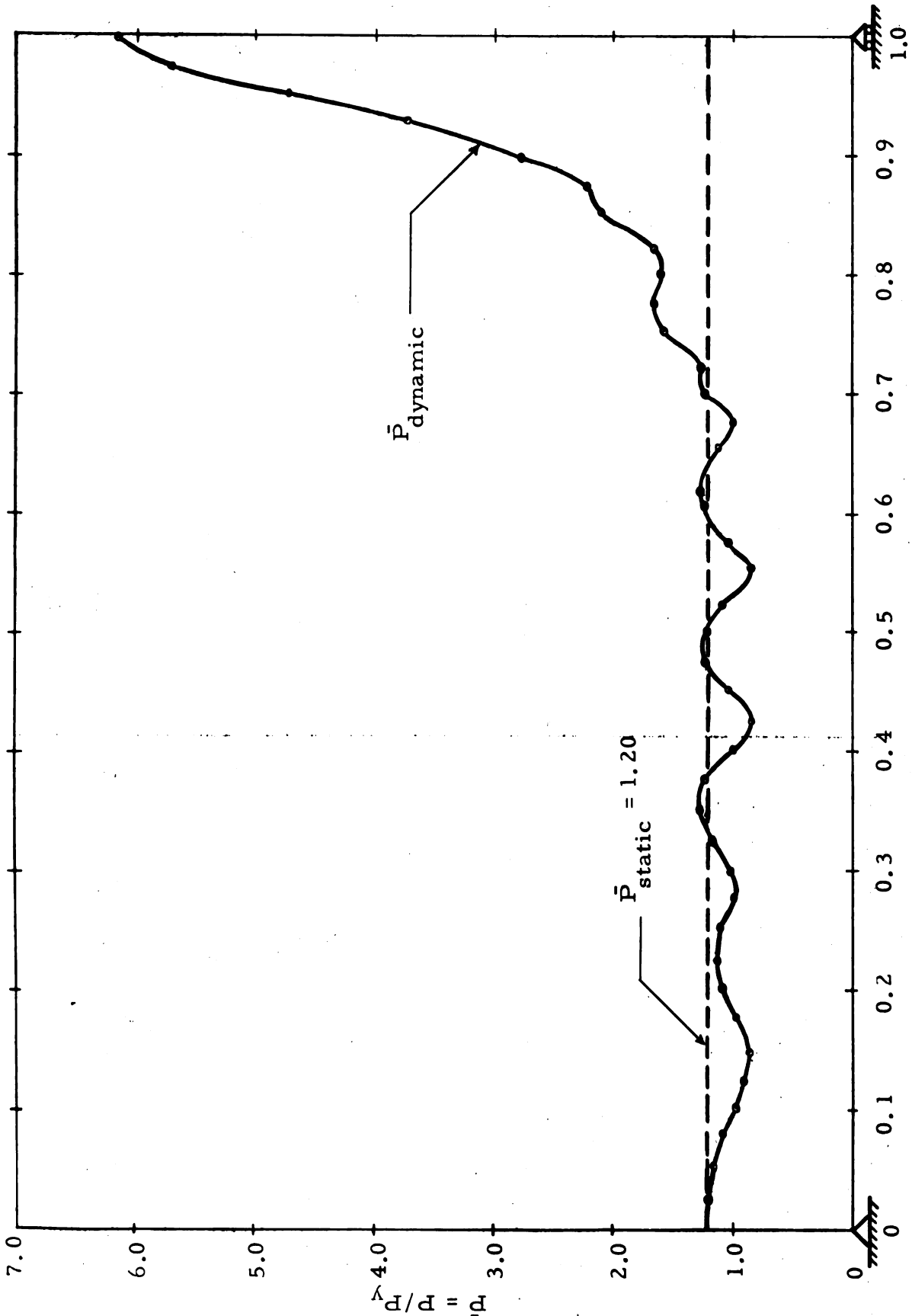

Fig. 20--History Curve of Interaction Force--Sprung Mass (R = 0, α = 0.20, β = 1.20, γ = 3.568, $\bar{k}$ = 33.57)

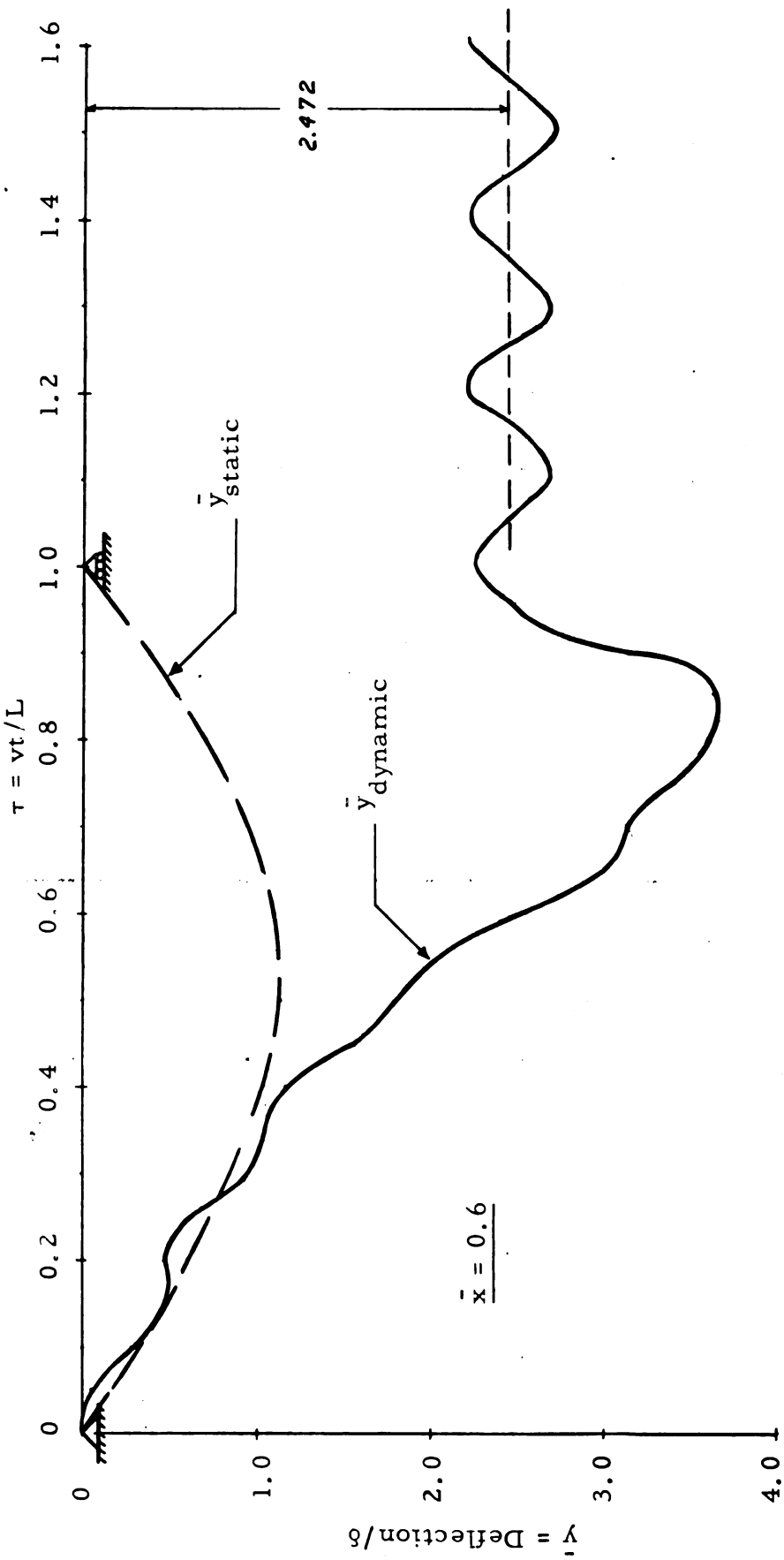

Fig. 21--History Curve of Deflection--Single-Axle Load Unit ($R = 0.1$, $\alpha = 0.20$, $\beta = 1.20$, $\gamma = 3.568$, $\lambda = 0.132$, $\bar{k} = 33.57$)

R = 0, β = 1.10, γ = 3.271

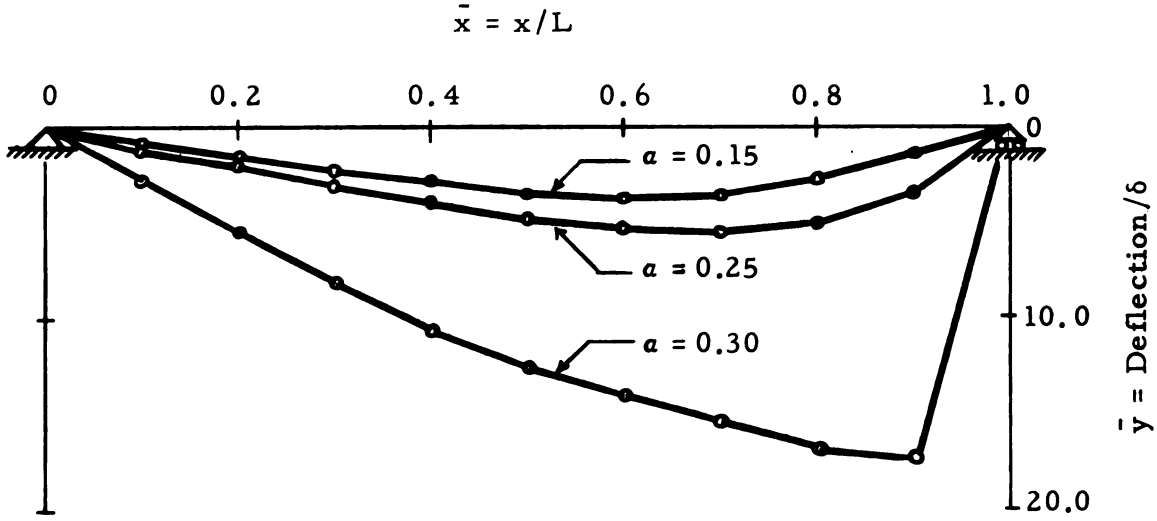

Fig. 22--Deformed Beam Shapes--Unsprung Mass

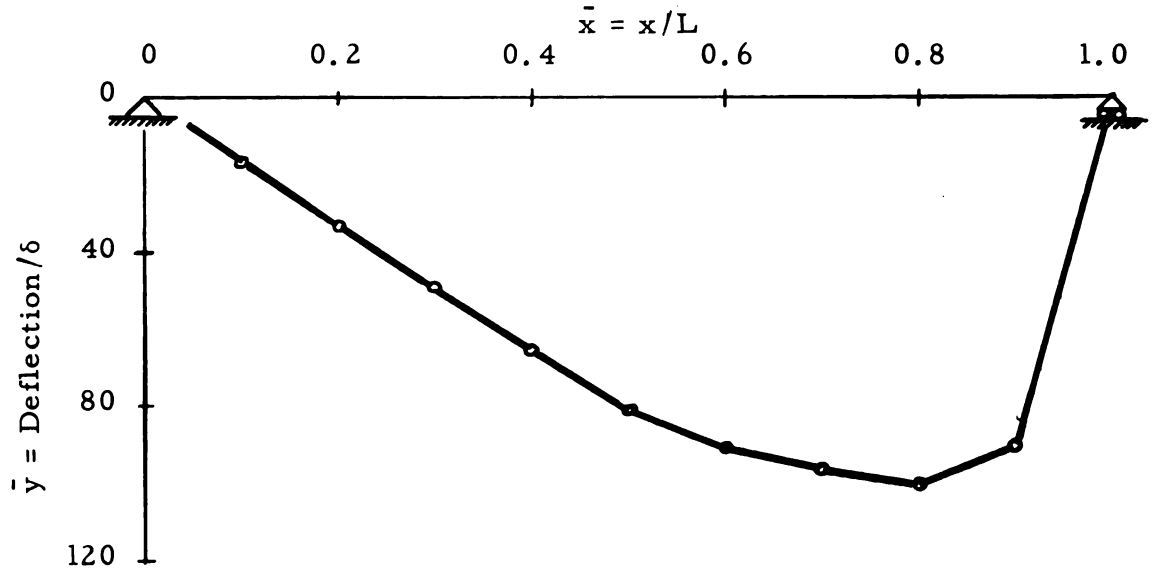

(a) Permanent Sets for R = 0, α = 0.10, β = 1.30, γ = 3.865

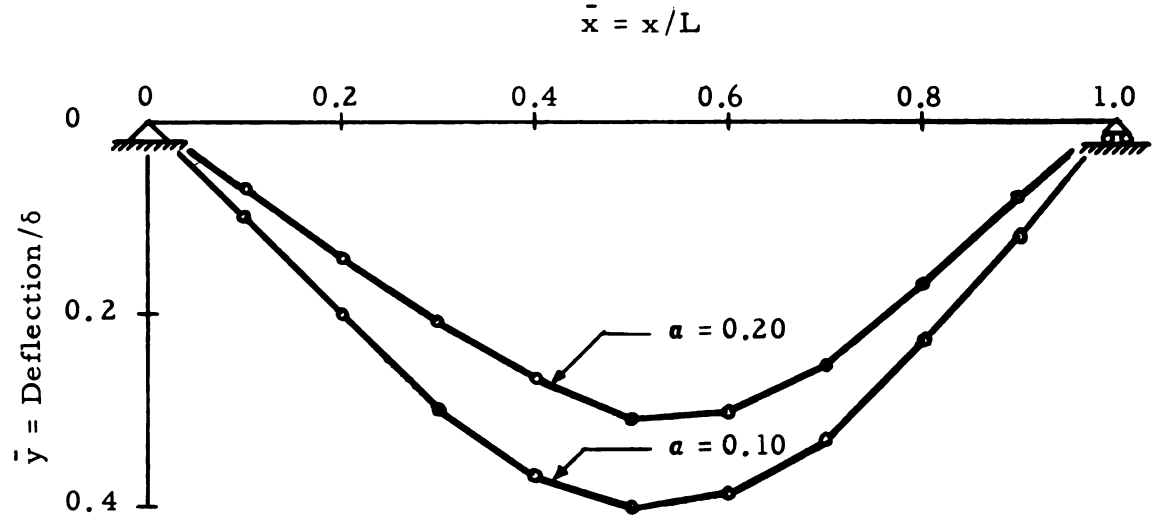

(b) Permanent Sets for R = 0.5, β = 1.20, γ = 3.568

Fig. 23--Deformed Beam Shapes--Unsprung Mass

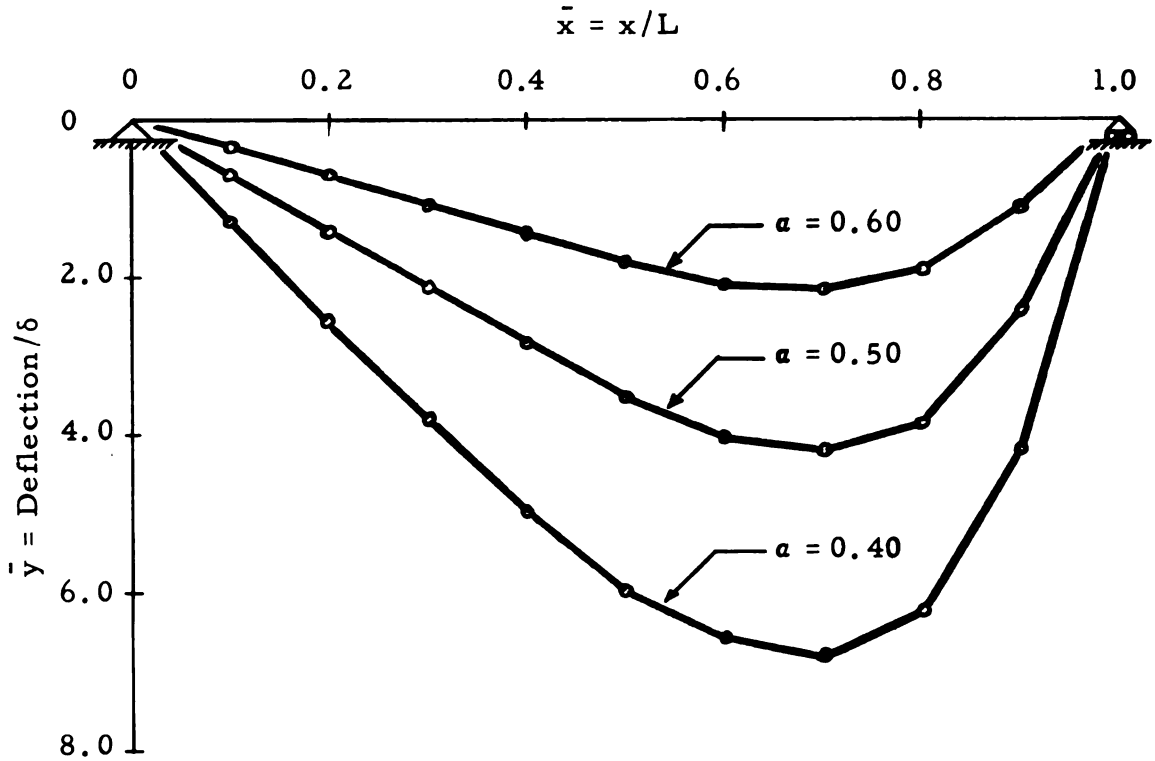

(a) Permanent Sets for R = 0, β = 1.50, γ = 4.460, $\bar{k}$ = 33.57

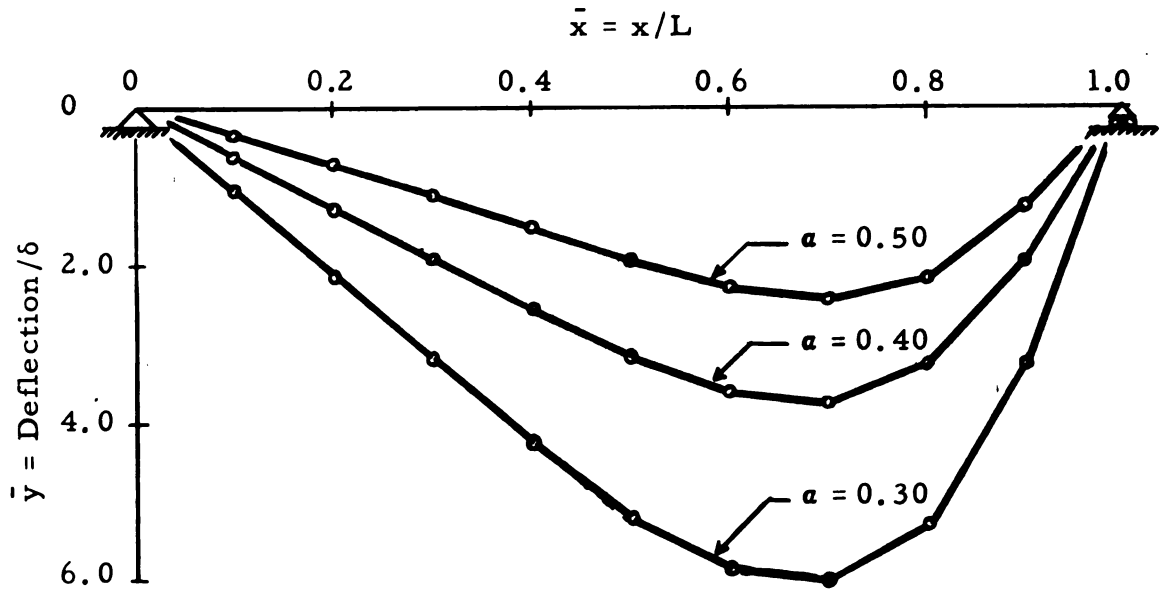

(b) Permanent Sets for R = 0, β = 1.20, γ = 3.568, $\bar{k}$ = 33.57

Fig. 24--Deformed Beam Shapes--Sprung Mass

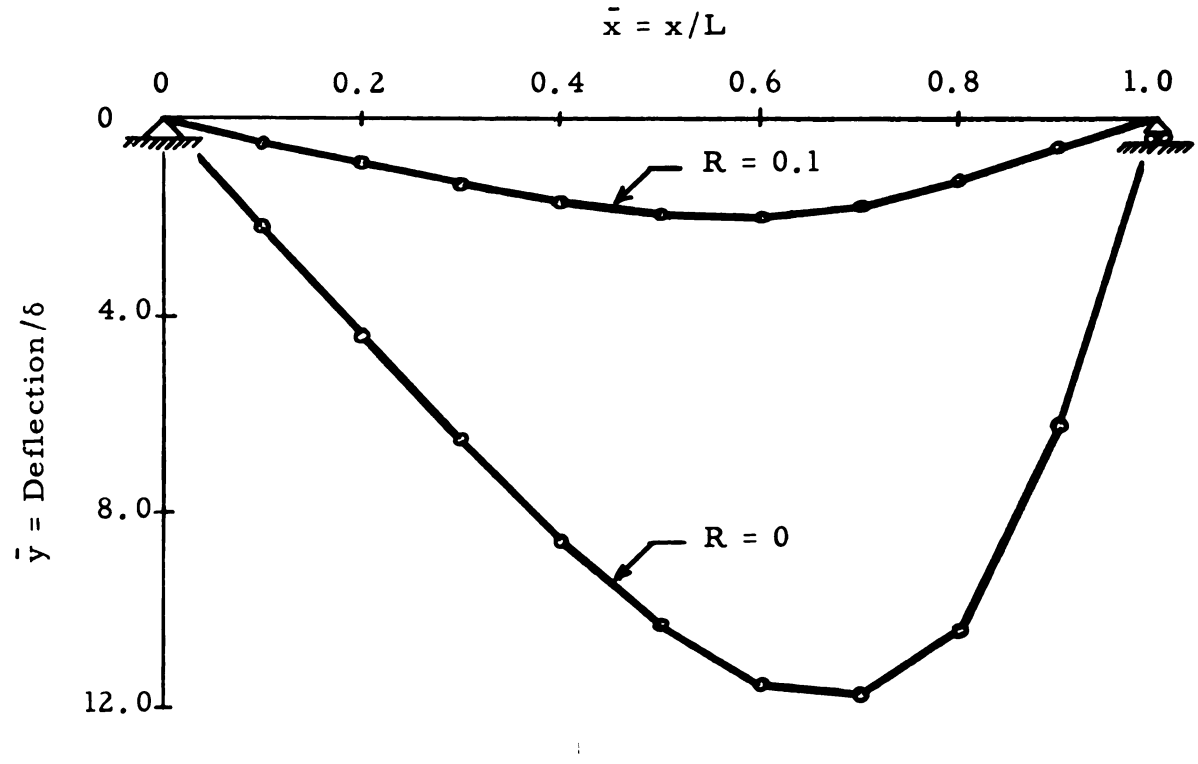

(a) Permanent Sets for
$\alpha = 0.15$, $\beta = 1.20$, $\gamma = 0.472$, $\lambda = 0.132$, $\bar{k} = 33.57$

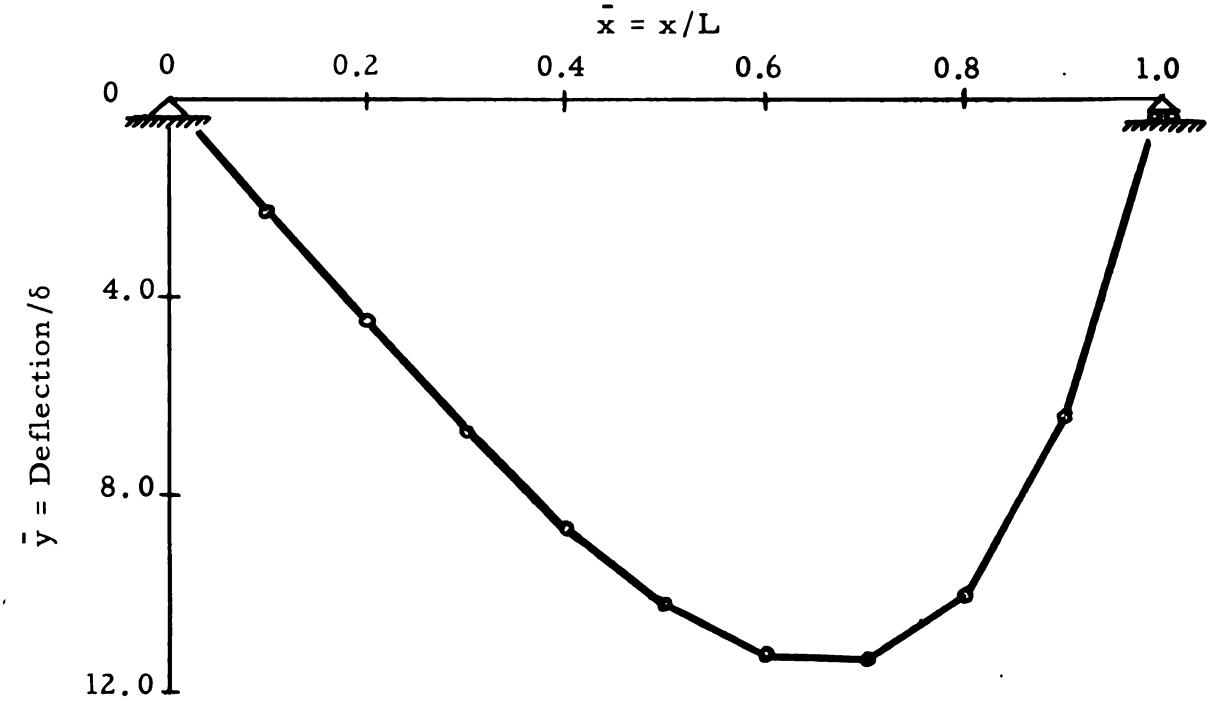

(b) Permanent Sets for R = 0, $\alpha = 0.20$,
$\beta = 1.20$, $\gamma = 0.472$, $\lambda = 0.132$, $\bar{k} = 33.57$

Fig. 25--Deformed Beam Shapes--Single-Axle Load Unit

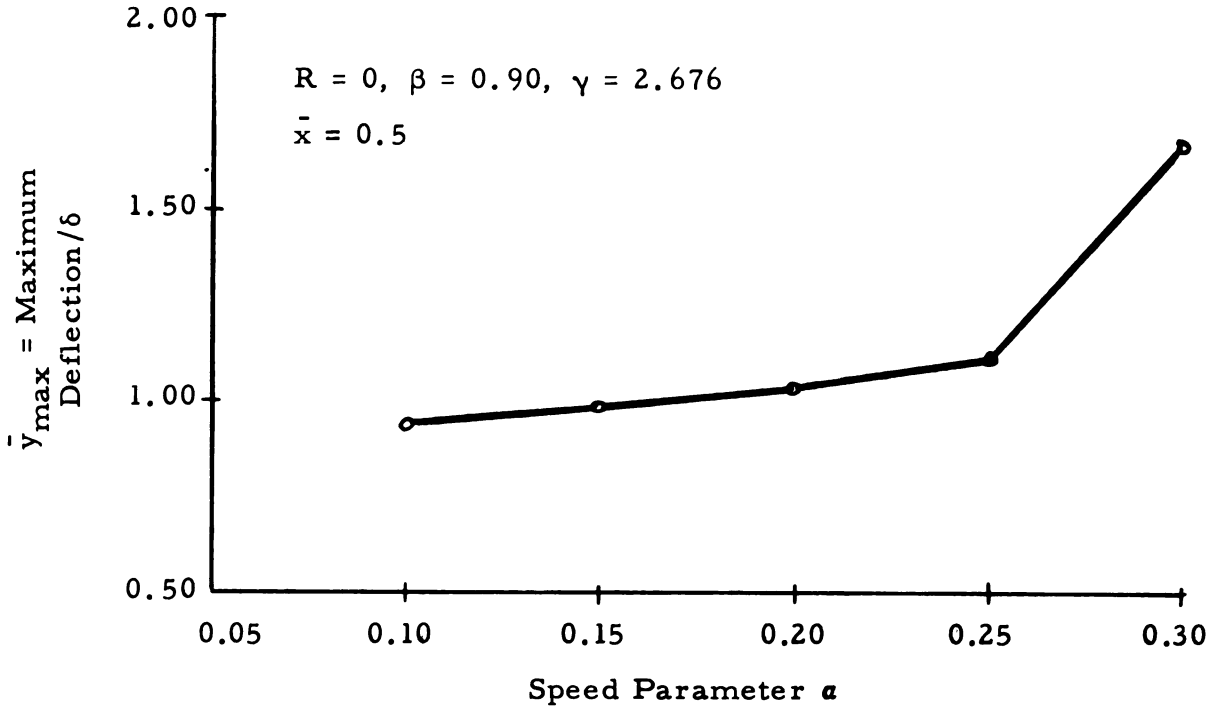

(a) Effect of a on Maximum Deflections ($R = 0$, $\beta = 0.90$)

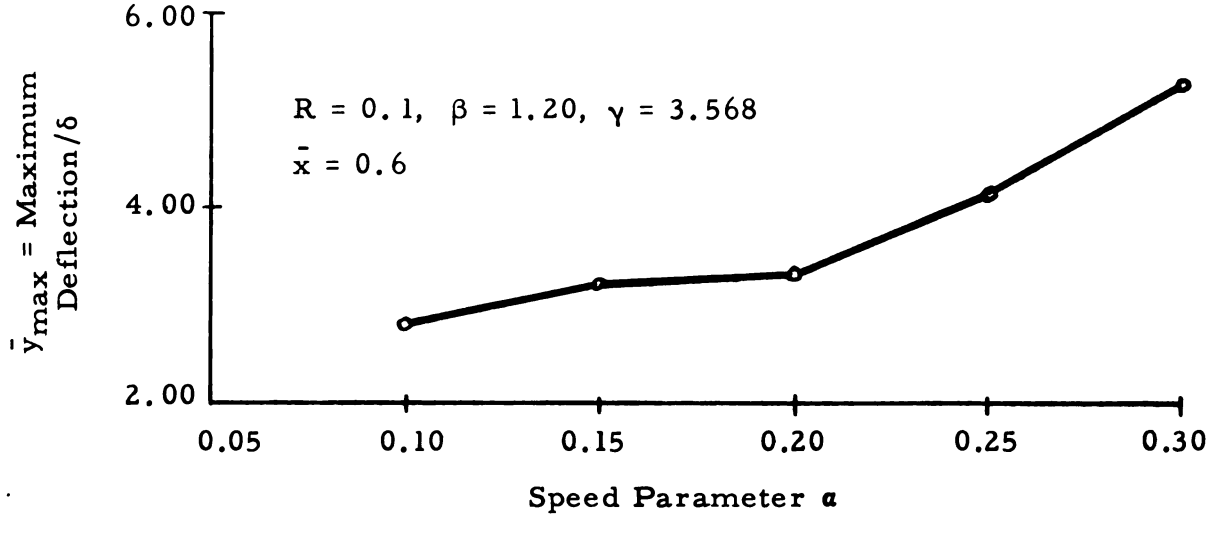

(b) Effect of a on Maximum Deflections ($R = 0.1$, $\beta = 1.20$)

Fig. 26--Effect of Speed on Maximum Deflections--Unsprung Mass

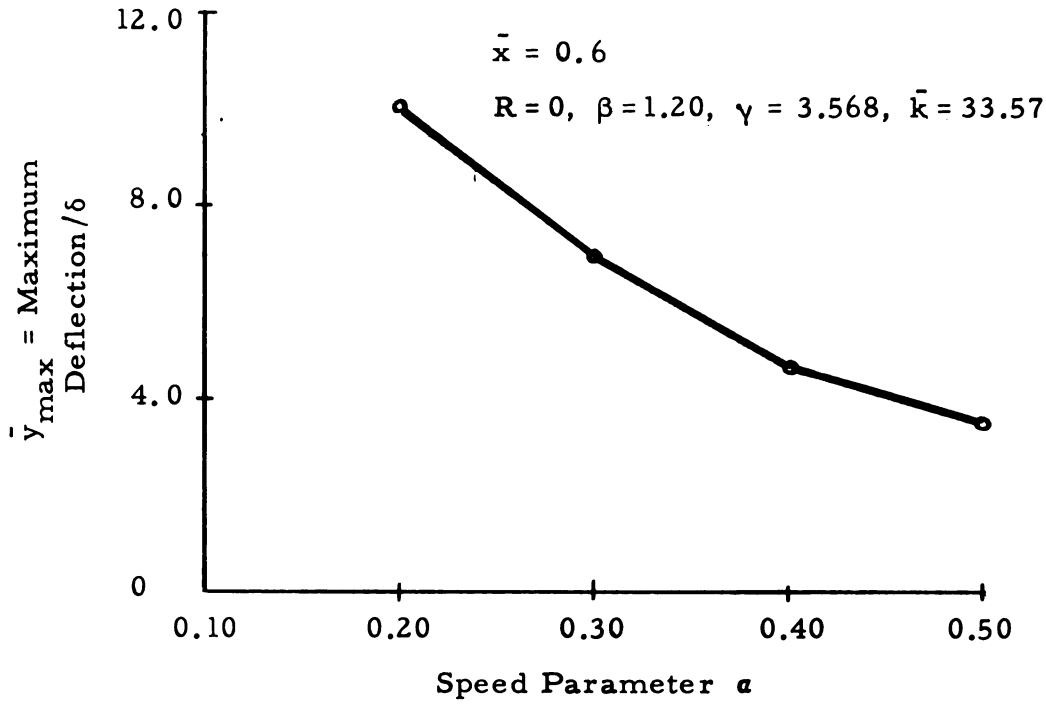

(a) Effect of a on Maximum Deflections
(R = 0, β = 1.20)

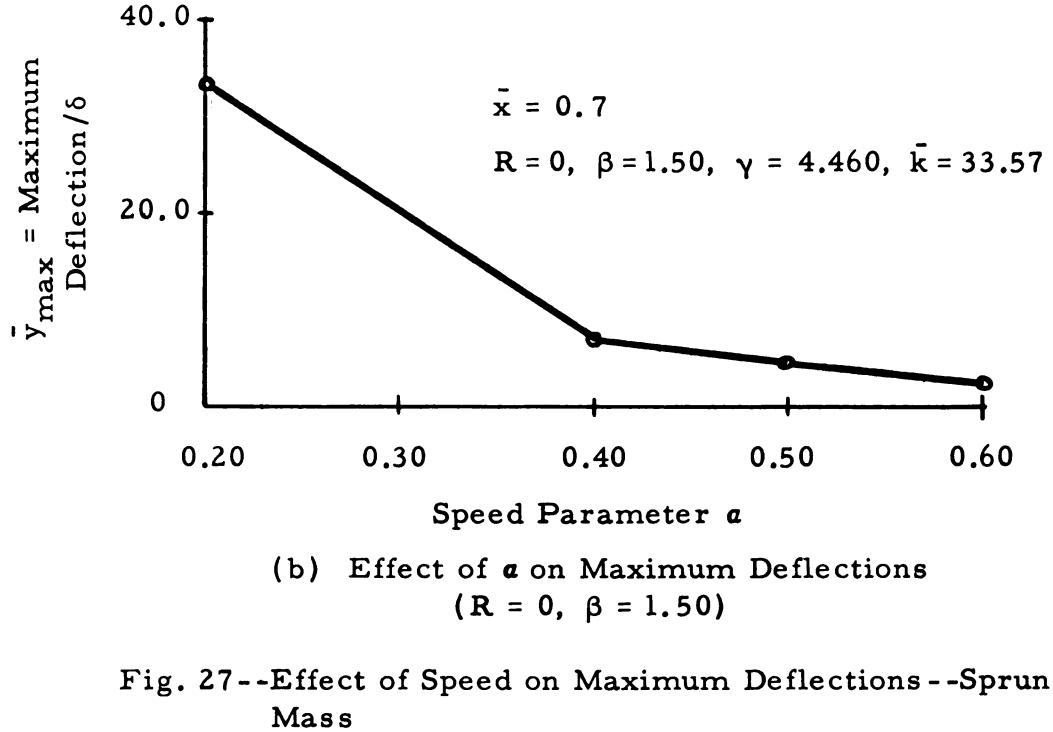

(b) Effect of a on Maximum Deflections
(R = 0, β = 1.50)

Fig. 27--Effect of Speed on Maximum Deflections--Sprung Mass

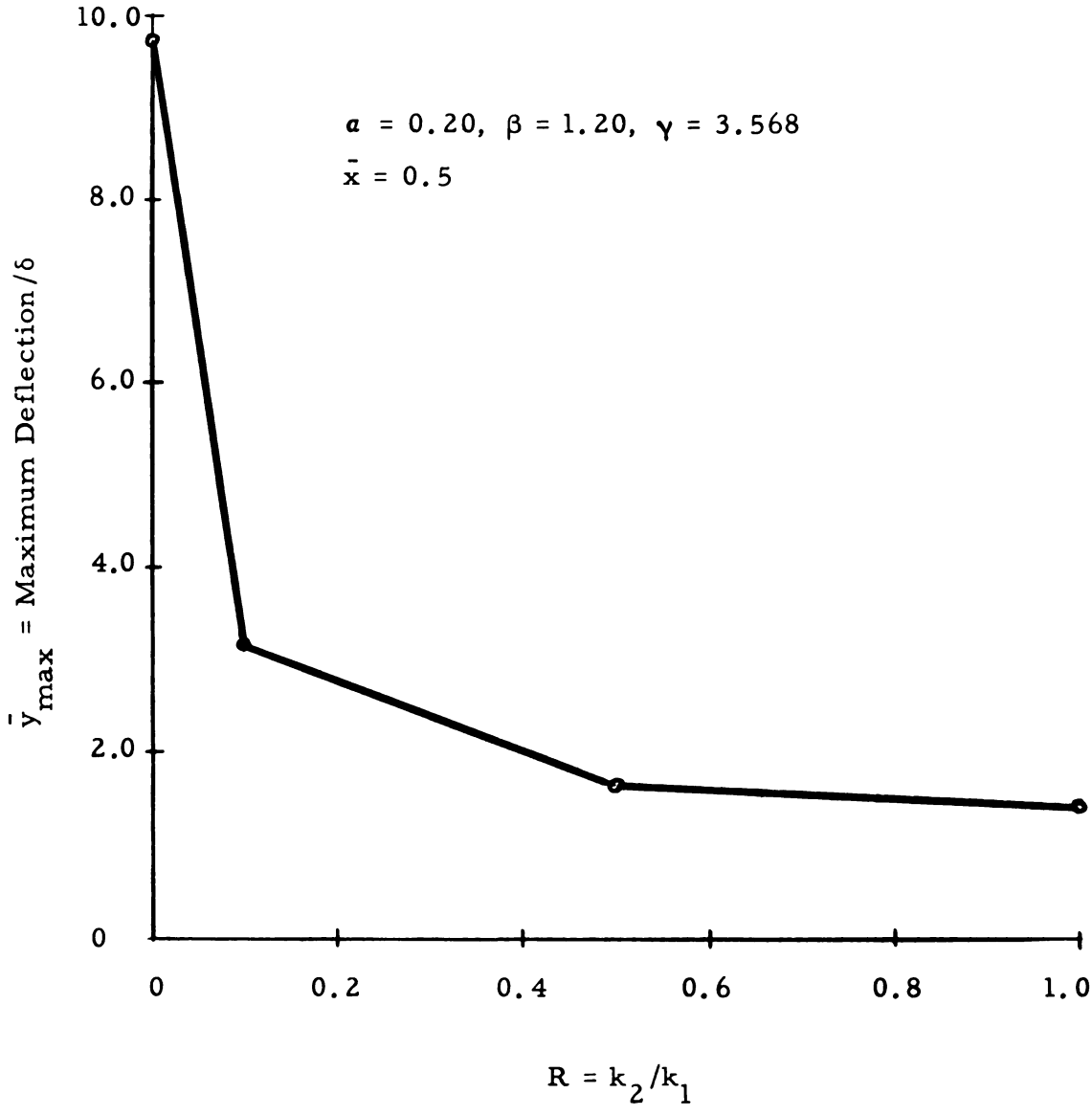

Fig. 28--Effect of R on Maximum Deflections--Unsprung Mass

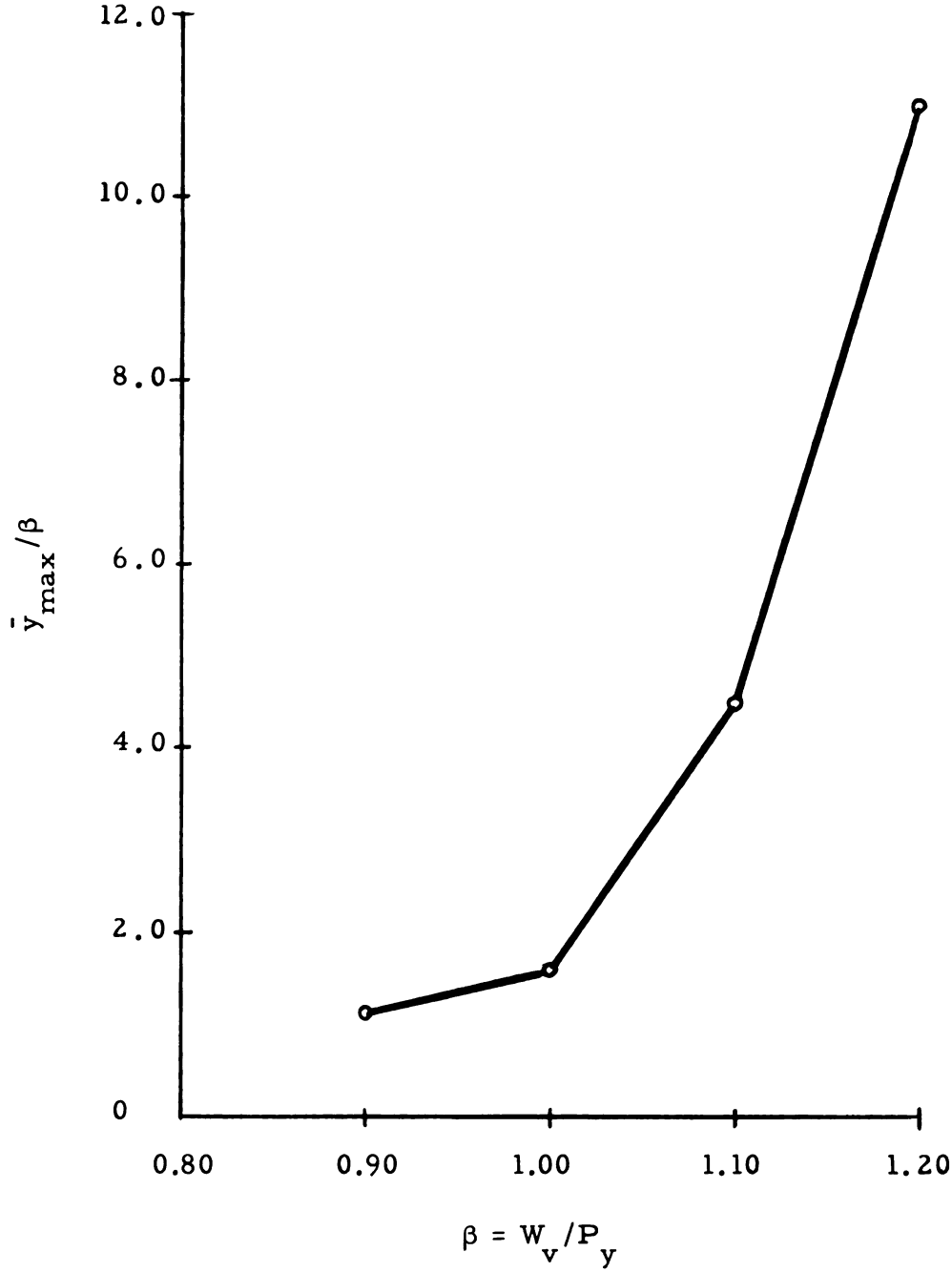

Fig. 29--Effect of Weight of Vehicle on Maximum Deflections--Unsprung Mass

APPENDIX

COMPUTER PROGRAM

Presented in this Appendix are the computer programs used in this study and certain information useful to a potential user.

1. Parameters of the Problem

The programs can be used to solve a series of numerical problems involving a range of values of the parameter α. The parameters are:

R = $R(=k_2/k_1)$

TALPHA = initial value of α

TBETA = β

TGAMMA = γ

TLAMBDA = λ

TKBAR = $\bar{k}$

TCER = increment in α

TMED = 0.98 times the final value of α

NP = an integer such that NP times $\Delta\tau$ is the interval between print-outs.

2. Computer Time

The computer time required for the solution of a given problem

depends primarily on the value of a. The approximate amounts of computer time necessary for some typical values of a are listed below:

1) for $a = 0.10$, 7 1/2 minutes

2) for $a = 0.20$, 5 minutes

3) for $a = 0.30$, 4 1/2 minutes

4) for $a = 0.40$, 4 minutes

3. Identification of Important Variables in the Program

TTAU = τ

ZBAR = $\bar{z}$

REMD = $\bar{z}'$

DPA(I) = $[\delta\pi^2/1.25]\,\bar{y}_i$

VEA(I) = $[\delta\pi^2/1.25]\,d\bar{y}_i/d\tau$

ACA(I) = $[\delta^2\pi^2/1.25]\,d^2\bar{y}_i/d\tau^2$

SYA = $[\delta\pi^2/1.25]\,\bar{w}$

VSA = $[\delta\pi^2/1.25]\,d\bar{w}/d\tau$

ASA = $[\delta^2\pi^2/1.25]\,d^2\bar{w}/d\tau^2$

ANGLA(I) = $\bar{\theta}_i$

BMA(I) = $\bar{M}_i$

AMM = $\pi^2/1.25 \times d^2\bar{y}_\zeta/d\tau^2$

PBAR = $\bar{P}$

4. Quantities Printed Out

At the start of the program N, NP, and $\Delta\tau$ are printed out. During the process of solution, the following quantities are printed out at regular intervals as determined by NP:

1) τ

2) $(\bar{y}_i)_{\text{dynamic}}$

3) $\bar{P}$

4) $(\bar{y}_i)_{\text{static}}$

5) $(\bar{\theta}_i)_{\text{permanent}}$ $(= \bar{\theta}_i - \bar{M}_i/k_1')$

In addition, in the case of a single-axle load unit, the acceleration of the unsprung mass and the spring force are printed out simultaneously with $\bar{P}$.

At the end of the problem, the following quantities are printed out:

1) absolute maximum $\bar{y}_i$

2) τ_i corresponding to absolute maximum $\bar{y}_i$

3) numerical values of parameters

4) maximum $\bar{y}_i$ during free vibration

5) minimum $\bar{y}_i$ during free vibration

6) $\bar{y}_i$ corresponding to the final shape of the deformed beam

7) $\bar{\theta}_i$ corresponding to the final angles of the

deformed beam

8) maximum value of $\bar{P}$

9) τ corresponding to the maximum value of $\bar{P}$

10) minimum value of $\bar{P}$

11) τ corresponding to the minimum value of $\bar{P}$

```
C
C     *****  COMPUTER  PROGRAM  ******
C
C
C
      PROGRAM  MOVLINK
C
C     *****  UNSPRUNG  MASS  *****
C
      DIMENSION ACA(35),ACB(35),ACD(35),VEA(35),VEB(35),DPA(35),DPB(35),
     1DDP(35),BMA(35),BMB(35),TMPA(35),TMPB(35),TMNA(35),TMNB(35),DPAMX
     2(35),TMAX(35),ANGLA(35),ANGLB(35),DA(35),P(35),DPS(35),DIF(35),
     3STDE(35),SOF(35),EF(35),THPL(35),RAC(35)
      N=20
      M=20
      TOLER=0.00000005
      BETA=0.
      ZN=N
C
C
C     *****  PARAMETERS  *****
      R=0.
      TALPHA=0.30
      TBETA=0.90
      TGAMMA=2.6761
C
      TCER=0.10
      TMED=0.39
      NP=N**2/4
C
C
      RK=R
      VBAR=TALPHA*ZN
      TMED=TMED*ZN
      CER=0.
      FBAR=0.5*TBETA
      R=TGAMMA*ZN
C
C     *****  CLEAR  OR  SET  STORAGE  *****
 1001 VBAR=VBAR+CER
      RANGE=ZN/VBAR
      NN=N+2
      DO 2 I=1,NN
      ANGLA(I)=0.0
      ACA(I)=0.0
```

```
      ACD(I)=0.0
      VEA(I)=0.0
      VEB(I)=0.0
      DPA(I)=0.0
      DPB(I)=0.0
      BMA(I)=0.0
      BMB(I)=0.0
      DPAMX(I)=0.0
      TMPA(I)=1.0
      TMPB(I)=1.0
      TMNA(I)=1.0
    2 TMNB(I)=1.0
      KT=1
      TKN=1.0
      TNLE=0.
      TAU=0.0
      VN=N-1
      DELTA=0.2/VN**2
      STFA=40.*ZN**2/(384.*3.141592654**2)
      STEP=RANGE/(DELTA*ZN)
      ISTEP=STEP
      STEP=ISTEP
      DELTA=RANGE/(STEP*ZN)
      RANGE=RANGE+5.0
      TAPN=1.0/VBAR
      PRINT 1000,N,NP,DELTA
 1000 FORMAT(1H0,I2,5X,I3,5X,F12.10)
      TERC=VBAR/ZN
      AGR=2.*FBAR
      PHYS=R/ZN
      PRINT 278,RK,TERC,AGR,PHYS
  278 FORMAT(1H0,4F10.5)
      GBAR=8.*38.4*ZN*FBAR/R
      PBMA=(R*GBAR/ZN)/153.6
      PBMI=(R*GBAR/ZN)/153.6
      TPMA=0.
      TPMI=0.
      TLENG=1.0/ZN
      TMEAS=TLENG
      IOT=1
    7 IN=NP
    4 TAU=TAU+DELTA
      ZBAR=VBAR*TAU
      IF(RANGE-TAU) 10,10,300
C
```

```
C     ***** PRINT MAXIMUM VALUES AND DEFORMED SHAPE *****
     10 PRINT 21
        PRINT 271,(DPAMX(I),I=2,11)
        PRINT 98,(DPAMX(I),I=12,N)
        PRINT 271,(TMAX(I),I=2,11)
        PRINT 98,(TMAX(I),I=12,N)
        PRINT 278,RK,TERC,AGR,PHYS
        PRINT 271,(SOF(I),I=2,11)
        PRINT 98,(SOF(I),I=12,N)
        PRINT 271,(EF(I),I=2,11)
        PRINT 98,(EF(I),I=12,N)
        DO 279  I=K,J
    279 SOF(I)=0.5*(SOF(I)+EF(I))
        PRINT 271,(SOF(I),I=2,11)
        PRINT 98,(SOF(I),I=12,N)
     20 FORMAT(1H0,9F10.5)
     21 FORMAT(1H0,10X,31H END. MAX. DISPLACEMT. AND TIME)
        DO 270 I=2,N
        THPL(I)=ANGLA(I)-BMA(I)/STFA
    270 THPL(I)=THPL(I)/3.141592654**2
        PRINT 271,(THPL(I),I=2,11)
        PRINT 20,(THPL(I),I=12,N)
    271 FORMAT(1H0,10F10.5)
        PRINT 97,PBMA
        PRINT 97,TPMA
        PRINT 97,PBMI
        PRINT 97,TPMI
        NP=7*NP/12
        CER=TCER*ZN
        IF(TMED-VBAR)1002,1001,1001
   1002 STOP
C
C       LOCATION OF MOVING MASS
    300 IF(TKN-ZBAR)296,298,299
    299 GAM=ZBAR+0.01*DELTA*VBAR
        IF(TKN-GAM) 298,298,302
    302 ZBAR=ZBAR-TNLE
        ASSIGN 290 TO LIL
        GO TO 5
    298 ZBAR=TKN-TNLE
    297 ASSIGN 291 TO LIL
        GO TO 5
    296 ZET=ZBAR-0.01*DELTA*VBAR
        IF(TKN-ZET) 301,298,298
    301 TKN=TKN+1.0
```

```
      TNLE=TNLE+1.0
      KT=KT+1
      GO TO 302
C
C     ***** INTEGRATE BY BETA METHOD *****
    5 DO 102 I=2,M
      ACB(I)=ACD(I)
      X=0.5*ACB(I)+0.5*ACA(I)
      VEB(I)=VEA(I)+X
      X=0.5*ACA(I)-BETA*ACA(I)
      DDP(I)=VEA(I)+X+BETA*ACB(I)
  102 DPB(I)=DPA(I)+DDP(I)
      DPB(N+2)=DPB(N)
C
C     ***** COMPUTE ANGLE OF ROTATION *****
      DO 18 I=2,M
      ANGLB(I)=-DPB(I-1)+2.0*DPB(I)-DPB(I+1)
   18 DA(I)=ANGLB(I)-ANGLA(I)
C
CC    ***** COMPUTE BENDING MOMENT *****
      DO 79 I=2,M
      IF(DA(I)) 50,50,65
   50 IF(TMNA(I)+STFA*DA(I)) 51,52,55
   51 C=RK
      GO TO 53
   52 C=0.0
   53 TMNB(I)=0.0
      X=STFA*DA(I)+TMNA(I)
      BMB(I)=BMA(I)-TMNA(I)+C*X
      GO TO 56
   55 TMNB(I)=TMNA(I)+STFA*DA(I)
      BMB(I)=BMA(I)+STFA*DA(I)
   56 TMPB(I)=2.0-TMNB(I)
      GO TO 79
   65 IF(TMPA(I)-STFA*DA(I)) 70,71,75
   70 C=RK
      GO TO 73
   71 C=0.0
   73 TMPB(I)=0.0
      X=STFA*DA(I)-TMPA(I)
      BMB(I)=BMA(I)+TMPA(I)+C*X
      GO TO 76
   75 TMPB(I)=TMPA(I)-STFA*DA(I)
      BMB(I)=BMA(I)+STFA*DA(I)
   76 TMNB(I)=2.0-TMPB(I)
```

```
   79 CONTINUE
C
C       ***** AUXILIARY ROUTINE *****
        DO 23 I=2,N
        X=ZN**2*(BMB(I-1)-2.0*BMB(I)+BMB(I+1))
   23 ACD(I)=DELTA*38.4*DELTA*X
        IF(N-KT) 310,322,322
  322 IF(KT-1) 304,304,305
  304 X=1.0/(1.0+R*ZBAR**2)
        ACD(KT+1)=X*DELTA*(38.4*ZN*(ZN*(BMB(KT)-2.0*BMB(KT+1)+BMB(KT+2))+
       18.0*FBAR*ZBAR)*DELTA-2.0*R*VBAR*ZBAR*VEB(KT+1))
        GO TO 310
  305 IF(KT-N) 306,307,308
  308 PRINT 309
  309 FORMAT(1H2,10X,12HKT=TOO LARGE)
  307 REMD=1.0-ZBAR
        X=1.0/(1.0+R*REMD**2)
        Y=BMB(KT-1)-2.0*BMB(KT)+BMB(KT+1)
        ACD(KT)=X*DELTA*(38.4*ZN*DELTA*(ZN*Y+8.0*FBAR*REMD)-2.0*R*VBAR*
       1REMD*(VEB(KT+1)-VEB(KT)))
        GO TO 310
  306 REMD=1.0-ZBAR
        S=1.0/R+REMD-ZBAR*REMD
        T=R*(ZBAR*REMD)**2
        U=R*ZBAR**2
        V=1.0/(1.0-T/S+U)
        W=BMB(KT-1)-2.0*BMB(KT)+BMB(KT+1)
        X=ZN**2*ZBAR*REMD*W
        Y=ZN*ZBAR*REMD**2*FBAR
        Z=BMB(KT)-2.0*BMB(KT+1)+BMB(KT+2)
        YE=2.0*R*VBAR*ZBAR*(REMD**2/S-1.0)*(VEB(KT+1)-VEB(KT))
        ACD(KT+1)=V*DELTA*(38.4*ZN**2*Z+8.0*38.4*ZN*FBAR*ZBAR-38.4*X/S-8.0
       1*38.4*Y/S)*DELTA+V*DELTA*YE
        TIM=1.0/(1.0+R*REMD-R*ZBAR*REMD)
        ACD(KT)=TIM*(DELTA*(38.4*ZN**2*W+8.0*38.4*ZN*FBAR*REMD)*DELTA
       1-R*ZBAR*REMD*ACD(KT+1)-2.0*DELTA*R*VBAR*REMD*(VEB(KT+1)-VEB(KT)))
  310 DO 35 I=2,N
        X=0.5*(ACD(I)+ACA(I))
   35 VEB(I)=VEA(I)+X
        GO TO LIL
  290 ADAC=0.
        AUT=0.
        YOJ=0.
        GO TO 289
  291 AUT=-DELTA*R*VBAR*(DPB(KT+2)-2.*DPB(KT+1)+DPB(KT))/(1.+R)
```

```
      ADAC=-2.*R*VBAR*(VEB(KT+2)-2.*VEB(KT+1)+VEB(KT)-AUT)*DELTA/(1.+R)
      YOJ=(2.*VBAR/(1.+R))*(VEB(KT+2)-2.*VEB(KT+1)+VEB(KT)-AUT)*DELTA
      IF(N-KT)425,426,426
  425 GO TO 289
  426 ZIB=0.
  289 LOT=KT+1
      IF(N-LOT) 288,287,287
  287 ACD(KT+1)=ACD(KT+1)+ADAC
      VEB(KT+1)=VEB(KT+1)+AUT
C
C
  288 IF(N-KT) 40,254,254
  254 AMM=ACD(KT)/DELTA**2+2.*VBAR*(VEB(KT+1)-AUT-VEB(KT))/DELTA
     1+(ZBAR/DELTA)*(ACD(KT+1)-ADAC-ACD(KT))/DELTA
      TYOJ=YOJ/DELTA**2
      AMM=AMM+TYOJ
      PBAR=(R*(GBAR-AMM)/ZN)/153.6
C
C    ***** PREPARE FOR NEXT STEP OF INTEGRATION *****
   40 DO 45 I=2,M
      BMA(I)=BMB(I)
      TMPA(I)=TMPB(I)
      TMNA(I)=TMNB(I)
      ACA(I)=ACD(I)
      VEA(I)=VEB(I)
      DPA(I)=DPB(I)
      ANGLA(I)=ANGLB(I)
   45 CONTINUE
C
C    ***** COMPUTE MAXIMUM RESPONSE *****
      J=N
      K=2
      SIK=ZN/VBAR+3.
      IF(TAU-SIK) 1101,285,285
 1101 DO 109 I=K,J
      DPS(I)=1.25*DPA(I)/3.141592654**2
      SOF(I)=DPS(I)
      EF(I)=DPS(I)
      IF(DPS(I)-DPAMX(I)) 109,109,112
  112 DPAMX(I)=DPS(I)
      TMAX(I)=TAU*VBAR/ZN
  109 CONTINUE
      IF(PBMA-PBAR)261,262,262
  261 PBMA=PBAR
      TPMA=TAU*VBAR/ZN
```

```
  262 IF(PBMI-PBAR)264,264,263
  263 PBMI=PBAR
      TPMI=TAU*VBAR/ZN
  264 GO TO 48
  285 DO 280 I=K,J
      DPS(I)=1.25*DPA(I)/3.141592654**2
      IF(SOF(I)-DPS(I)) 283,282,282
  283 SOF(I)=DPS(I)
  282 IF(EF(I)-DPS(I)) 280,280,281
  281 EF(I)=DPS(I)
  280 CONTINUE
C
C     ***** TEST TIME TO PRINT *****
   48 IF(IN-1)  115,115,16
   16 IN=IN-1
      GO TO 4
  115 TTAU=TAU*VBAR/ZN
      PRINT 97,TTAU
      PRINT 271,(DPS(I),I=2,11)
      PRINT 98,(DPS(I),I=12,N)
   97 FORMAT(1H0,F12.7)
   98 FORMAT(1H0,9F10.5)
      IF(TAU-ZN/VBAR)266,266,267
  266 PRINT 260,PBAR
  260 FORMAT(1H0,5HPBAR=F10.6)
  267 ZIB=0.
C
C     ***** STATIC DEFLECTION *****
      IF(N-KT) 324,323,323
  323 ABAR=(ZBAR+TNLE)/ZN
      IF(1.0-ABAR) 398,399,399
  398 PRINT 397
  397 FORMAT(1H2,20HABAR=LARGER THAN ONE)
  399 IF(TMEAS-ABAR) 400,401,401
  400 TMEAS=TMEAS+TLENG
      IOT=IOT+1
      GO TO 401
  401 BBAR=1.0-ABAR
      DIST=0.
      REMD=0.
      DO 802 I=2,IOT
      DIST=DIST+TLENG
  802 DIF(I)=12.8*BBAR*DIST*(ABAR*(BBAR+1.0)-DIST**2)
      TIT=IOT
      DIST=TIT*TLENG-TLENG
```

```
      JJ=IOT+1
      DO 803 I=JJ,N
      DIST=DIST+TLENG
      REMD=1.0-DIST
  803 DIF(I)=12.8*ABAR*REMD*(BBAR*(ABAR+1.0)-REMD**2)
      DO 804 I=2,N
  804 STDE(I)=1.25*FBAR*DIF(I)
      J=N
      K=2
      PRINT 271,(STDE(I),I=2,11)
      PRINT 98,(STDE(I),I=12,N)
      DO 570 I=2,N
      THPL(I)=ANGLA(I)-BMA(I)/STFA
  570 THPL(I)=THPL(I)/3.141592654**2
      PRINT 271,(THPL(I),I=2,11)
      PRINT 20,(THPL(I),I=12,N)
  324 GO TO 7
      END
      END

C
C
      PROGRAM  MOVLINK
C     *****  SPRUNG  MASS  *****
      DIMENSION ACA(35),ACB(35),ACD(35),VEA(35),VEB(35),DPA(35),DPB(35),
     1DDP(35),BMA(35),BMB(35),TMPA(35),TMPB(35),TMNA(35),TMNB(35),DPAMX
     2(35),TMAX(35),ANGLA(35),ANGLB(35),DA(35),P(35),DPS(35),DIF(35),
     3STDE(35),SOF(35),EF(35),THPL(35),RAC(35)
      N=20
      M=20
      TOLER=0.00000005
      BETA=0.
      ZN=N
C
C
C     *****  PARAMETERS  *****
      R=0.
      TALPHA=0.20
      TBETA=1.20
      TGAMMA=3.5681
      TKBAR=33.573
C
      TCER=0.10
      TMED=0.29
      NP=N**2/4
```

```
C
C
      RK=R
      VBAR=TALPHA*ZN
      TMED=TMED*ZN
      CER=0.
      FBAR=0.5*TBETA
      QS=TGAMMA*ZN
      SK=TKBAR*ZN
C
C     *****  CLEAR  OR  SET  STORAGE  *****
 1001 VBAR=VBAR+CER
      RANGE=ZN/VBAR
      NN=N+2
      DO 2 I=1,NN
      ANGLA(I)=0.0
      ACA(I)=0.0
      ACD(I)=0.0
      VEA(I)=0.0
      VEB(I)=0.0
      DPA(I)=0.0
      DPB(I)=0.0
      BMA(I)=0.0
      BMB(I)=0.0
      DPAMX(I)=0.0
      TMPA(I)=1.0
      TMPB(I)=1.0
      TMNA(I)=1.0
    2 TMNB(I)=1.0
      SYA=0.
      VSA=0.
      ASI=0.
      KT=1
      TKN=1.0
      TNLE=0.
      TAU=0.0
      AMM=0.
      TIM=0.
      VN=N-1
      DELTA=0.2/VN**2
      STFA=40.*ZN**2/(384.*3.141592654**2)
      RANGE=RANGE+5.0
      TAPN=1.0/VBAR
      PRINT 1000,N,NP,DELTA
 1000 FORMAT(1H0,I2,5X,I3,5X,F12.10)
```

```
      TERC=VBAR/ZN
      PRINT 278,RK,TERC,TBETA,TGAMMA,TKBAR
  278 FORMAT(1H0,5F10.5)
      GBAR=8.*38.4*ZN*FBAR/QS
      PBMA=(QS*GBAR/ZN)/153.6
      PBMI=(QS*GBAR/ZN)/153.6
      TPMA=0.
      TPMI=0.
      TLENG=1.0/ZN
      TMEAS=TLENG
      IOT=1
    7 IN=NP
    4 TAU=TAU+DELTA
      ZBAR=VBAR*TAU
      TTAU=TAU*VBAR/ZN
      IF(RANGE-TAU) 10,10,300
C
C
C     ***** PRINT MAXIMUM VALUES AND DEFORMED SHAPE *****
   10 PRINT 21
      PRINT 271,(DPAMX(I),I=2,11)
      PRINT 98,(DPAMX(I),I=12,N)
      PRINT 271,(TMAX(I),I=2,11)
      PRINT 98,(TMAX(I),I=12,N)
      PRINT 278,RK,TERC,TBETA,TGAMMA,TKBAR
      PRINT 271,(SOF(I),I=2,11)
      PRINT 98,(SOF(I),I=12,N)
      PRINT 271,(EF(I),I=2,11)
      PRINT 98,(EF(I),I=12,N)
      DO 279  I=K,J
  279 SOF(I)=0.5*(SOF(I)+EF(I))
      PRINT 271,(SOF(I),I=2,11)
      PRINT 98,(SOF(I),I=12,N)
   20 FORMAT(1H0,9F10.5)
   21 FORMAT(1H0,10X,31H END. MAX. DISPLACEMT. AND TIME)
      DO 270 I=2,N
      THPL(I)=ANGLA(I)-BMA(I)/STFA
  270 THPL(I)=THPL(I)/3.141592654**2
      PRINT 271,(THPL(I),I=2,11)
      PRINT 20,(THPL(I),I=12,N)
  271 FORMAT(1H0,10F10.5)
      PRINT 97,PBMA
      PRINT 97,TPMA
      PRINT 97,PBMI
      PRINT 97,TPMI
```

```
      NP=7*NP/12
      CER=TCER*ZN
      IF(TMED-VBAR)1002,1001,1001
 1002 STOP
C
C     LOCATION  OF  MOVING  MASS
  300 IF(TKN-ZBAR)301,302,302
  302 ZBAR=ZBAR-TNLE
      GO TO 5
  301 TKN=TKN+1.
      TNLE=TNLE+1.
      KT=KT+1
      IF(ZN-TKN)321,302,302
  321 GO TO 302
C
C     *****  INTEGRATE  BY  BETA  METHOD  *****
    5 DO 102 I=2,M
      ACB(I)=ACD(I)
      X=0.5*ACB(I)+0.5*ACA(I)
      VEB(I)=VEA(I)+X
      X=0.5*ACA(I)-BETA*ACA(I)
      DDP(I)=VEA(I)+X+BETA*ACB(I)
  102 DPB(I)=DPA(I)+DDP(I)
      DPB(N+2)=-DPB(N)
      VEB(N+2)=-VEB(N)
      ASB=ASI
      VSB=VSA+0.5*(ASB+ASI)
      SYB=SYA+VSA+0.5*ASI+BETA*(ASB-ASI)
C
C     *****  COMPUTE  ANGLE  OF  ROTATION  *****
      DO 18 I=2,M
      ANGLB(I)=-DPB(I-1)+2.0*DPB(I)-DPB(I+1)
   18 DA(I)=ANGLB(I)-ANGLA(I)
C
CC    *****  COMPUTE  BENDING  MOMENT  *****
      DO 79 I=2,M
      IF(DA(I)) 50,50,65
   50 IF(TMNA(I)+STFA*DA(I)) 51,52,55
   51 C=RK
      GO TO 53
   52 C=0.0
   53 TMNB(I)=0.0
      X=STFA*DA(I)+TMNA(I)
      BMB(I)=BMA(I)-TMNA(I)+C*X
      GO TO 56
```

```
   55 TMNB(I)=TMNA(I)+STFA*DA(I)
      BMB(I)=BMA(I)+STFA*DA(I)
   56 TMPB(I)=2.0-TMNB(I)
      GO TO 79
   65 IF(TMPA(I)-STFA*DA(I)) 70,71,75
   70 C=RK
      GO TO 73
   71 C=0.0
   73 TMPB(I)=0.0
      X=STFA*DA(I)-TMPA(I)
      BMB(I)=BMA(I)+TMPA(I)+C*X
      GO TO 76
   75 TMPB(I)=TMPA(I)-STFA*DA(I)
      BMB(I)=BMA(I)+STFA*DA(I)
   76 TMNB(I)=2.0-TMPB(I)
   79 CONTINUE
C
C       *****  AUXILIARY  ROUTINE  *****
      DO 23 I=2,N
      X=ZN**2*(BMB(I-1)-2.0*BMB(I)+BMB(I+1))
   23 ACD(I)=DELTA*38.4*DELTA*X
      IF(N-KT) 310,322,322
  322 REMD=1.-ZBAR
      YM1=DPB(KT)+ZBAR*(DPB(KT+1)-DPB(KT))
      IF(KT-1)500,500,501
  500 W=-2.*BMB(KT)+BMB(KT+1)
      GO TO 502
  501 W=BMB(KT-1)-2.*BMB(KT)+BMB(KT+1)
  502 Z=BMB(KT)-2.*BMB(KT+1)+BMB(KT+2)
      ACD(KT)=38.4*ZN*DELTA*(ZN*W+8.*FBAR*REMD)*DELTA
     1+SK*DELTA*(SYB-YM1)*REMD*DELTA
      ACD(KT+1)=38.4*ZN*DELTA*(ZN*Z+8.*FBAR*ZBAR)*DELTA
     1+SK*DELTA*(SYB-YM1)*ZBAR*DELTA
      ACD(1)=0.
      ACD(N+1)=0.
      ASD=-(DELTA*(SK*(SYB-YM1))/QS)*DELTA
  310 DO 35 I=2,N
      X=0.5*(ACD(I)+ACA(I))
   35 VEB(I)=VEA(I)+X
      VSB=VSA+0.5*(ASD+ASI)
      PBAR=((QS*GBAR+SK*(SYB-YM1))/ZN)/153.6
C
C     *****  PREPARE  FOR  NEXT  STEP  OF  INTEGRATION  *****
   40 DO 45 I=2,M
      BMA(I)=BMB(I)
```

```
      TMPA(I)=TMPB(I)
      TMNA(I)=TMNB(I)
      ACA(I)=ACD(I)
      VEA(I)=VEB(I)
      DPA(I)=DPB(I)
      ANGLA(I)=ANGLB(I)
   45 CONTINUE
      ASI=ASD
      VSA=VSB
      SYA=SYB
C
C     ***** COMPUTE MAXIMUM RESPONSE *****
      J=N
      K=2
      SIK=ZN/VBAR+3.
      IF(TAU-SIK) 1101,285,285
 1101 DO 109 I=K,J
      DPS(I)=1.25*DPA(I)/3.141592654**2
      SOF(I)=DPS(I)
      EF(I)=DPS(I)
      IF(DPS(I)-DPAMX(I)) 109,109,112
  112 DPAMX(I)=DPS(I)
      TMAX(I)=TAU*VBAR/ZN
  109 CONTINUE
      IF(TAU-ZN/VBAR)510,510,264
  510 ZIB=0.
      IF(PBMA-PBAR)261,262,262
  261 PBMA=PBAR
      TPMA=TAU*VBAR/ZN
  262 IF(PBMI-PBAR)264,264,263
  263 PBMI=PBAR
      TPMI=TAU*VBAR/ZN
  264 GO TO 48
  285 DO 280 I=K,J
      DPS(I)=1.25*DPA(I)/3.141592654**2
      IF(SOF(I)-DPS(I)) 283,282,282
  283 SOF(I)=DPS(I)
  282 IF(EF(I)-DPS(I)) 280,280,281
  281 EF(I)=DPS(I)
  280 CONTINUE
C
C     ***** TEST TIME TO PRINT *****
   48 IF(IN-1)  115,115,16
   16 IN=IN-1
      GO TO 4
```

```
  115 TTAU=TAU*VBAR/ZN
      PRINT 97,TTAU
      PRINT 271,(DPS(I),I=2,11)
      PRINT 98,(DPS(I),I=12,N)
   98 FORMAT(1H0,9F10.5)
   97 FORMAT(1H0,F12.7)
      IF(TAU-ZN/VBAR)266,266,267
  266 PRINT 260,PBAR
  260 FORMAT(1H0,5HPBAR=F10.6)
  267 ZIB=0.
C
C     ***** STATIC DEFLECTION *****
      IF(N-KT) 324,323,323
  323 ABAR=(ZBAR+TNLE)/ZN
      IF(1.0-ABAR) 398,399,399
  398 PRINT 397
  397 FORMAT(1H2,20HABAR=LARGER THAN ONE)
  399 IF(TMEAS-ABAR) 400,401,401
  400 TMEAS=TMEAS+TLENG
      IOT=IOT+1
      GO TO 401
  401 BBAR=1.0-ABAR
      DIST=0.
      REMD=0.
      DO 802 I=2,IOT
      DIST=DIST+TLENG
  802 DIF(I)=12.8*BBAR*DIST*(ABAR*(BBAR+1.0)-DIST**2)
      TIT=IOT
      DIST=TIT*TLENG-TLENG
      JJ=IOT+1
      DO 803 I=JJ,N
      DIST=DIST+TLENG
      REMD=1.0-DIST
  803 DIF(I)=12.8*ABAR*REMD*(BBAR*(ABAR+1.0)-REMD**2)
      DO 804 I=2,N
  804 STDE(I)=1.25*FBAR*DIF(I)
      J=N
      K=2
      PRINT 271,(STDE(I),I=2,11)
      PRINT 98,(STDE(I),I=12,N)
      DO 570 I=2,N
      THPL(I)=ANGLA(I)-BMA(I)/STFA
  570 THPL(I)=THPL(I)/3.141592654**2
      PRINT 271,(THPL(I),I=2,11)
      PRINT 20,(THPL(I),I=12,N)
```

```
  324 GO TO 7
      END
      END

C
      PROGRAM MOVLINK
C
C    ***** SINGLE AXLE LOAD UNIT *****
C
      DIMENSION ACA(35),ACB(35),ACD(35),VEA(35),VEB(35),DPA(35),DPB(35),
     1DDP(35),BMA(35),BMB(35),TMPA(35),TMPB(35),TMNA(35),TMNB(35),DPAMX
     2(35),TMAX(35),ANGLA(35),ANGLB(35),DA(35),P(35),DPS(35),DIF(35),
     3STDE(35),SOF(35),EF(35),THPL(35)
      N=10
      M=10
      TOLER=0.00000005
      BETA=0.
      ZN=N
C
C
C    ***** PARAMETERS *****
      R=0.1
      TALPHA=0.20
      TBETA=1.20
      TGAMMA=3.5681
      TLAMDA=0.1323
      TKBAR=33.573
C
      TCER=0.10
      TMED=0.29
      NP=N**2/4
C
      RK=R
      VBAR=TALPHA*ZN
      TMED=TMED*ZN
      CER=0.
      FBAR=0.5*TBETA
      R=TLAMDA*TGAMMA*ZN
      QS=TGAMMA*ZN-R
      SK=TKBAR*ZN
      DC=0.
C
C     ***** CLEAR OR SET STORAGE *****
 1001 VBAR=VBAR+CER
      RANGE=ZN/VBAR
```

```
      NN=N+2
      DO 2 I=1,NN
      ANGLA(I)=0.0
      ACA(I)=0.0
      ACD(I)=0.0
      VEA(I)=0.0
      VEB(I)=0.0
      DPA(I)=0.0
      DPB(I)=0.0
      BMA(I)=0.0
      BMB(I)=0.0
      DPAMX(I)=0.0
      TMPA(I)=1.0
      TMPB(I)=1.0
      TMNA(I)=1.0
    2 TMNB(I)=1.0
      SYA=0.
      VSA=0.
      ASI=0.
      KT=1
      TKN=1.0
      TNLE=0.
      TAU=0.0
      VN=N-1
      DELTA=0.2/VN**2
      STFA=40.*ZN**2/(384.*3.141592654**2)
      STEP=RANGE/(DELTA*ZN)
      ISTEP=STEP
      STEP=ISTEP
      DELTA=RANGE/(STEP*ZN)
      RANGE=ZN/VBAR+5.
      TAPN=1.0/VBAR
      PRINT 1000,N,NP,DELTA
 1000 FORMAT(1H0,I2,5X,I3,5X,F12.10)
      TERC=VBAR/ZN
      PRINT 278,RK,TERC,TBETA,TGAMMA,TLAMDA,TKBAR
  278 FORMAT(1H0,6F10.5)
      GBAR=8.*38.4*ZN*FBAR/(QS+R)
      PBMA=((QS+R)*GBAR/ZN)/153.6
      PBMI=((QS+R)*GBAR/ZN)/153.6
      TPMA=0.
      TPMI=0.
      TLENG=1.0/ZN
      TMEAS=TLENG
      IOT=1
```

```
      7 IN=NP
      4 TAU=TAU+DELTA
        ZBAR=VBAR*TAU
        IF(RANGE-TAU) 10,10,300
C
C     ***** PRINT MAXIMUM VALUES AND DEFORMED SHAPE *****
     10 PRINT 21
        PRINT 20,(DPAMX(I),I=K,J)
        PRINT 20,(TMAX(I),I=K,J)
        PRINT 278,RK,TERC,TBETA,TGAMMA,TLAMDA,TKBAR
        PRINT 20,(SOF(I),I=K,J)
        PRINT 20,(EF(I),I=K,J)
        DO 279  I=K,J
    279 SOF(I)=0.5*(SOF(I)+EF(I))
        PRINT 20,(SOF(I),I=K,J)
     20 FORMAT(1H0,9F10.5)
     21 FORMAT(1H0,10X,31H END. MAX. DISPLACEMT. AND TIME)
        DO 270 I=2,N
        THPL(I)=ANGLA(I)-BMA(I)/STFA
    270 THPL(I)=THPL(I)/3.14592654**2
        PRINT 271,(THPL(I),I=2,11)
        PRINT 20,(THPL(I),I=12,N)
    271 FORMAT(1H0,10F10.5)
        PRINT 97,PBMA
        PRINT 97,TPMA
        PRINT 97,PBMI
        PRINT 97,TPMI
        NP=7*NP/12
        CER=TCER*ZN
        IF(TMED-VBAR)1002,1001,1001
   1002 STOP
C
C       LOCATION OF MOVING MASS
    300 IF(TKN-ZBAR)296,298,299
    299 GAM=ZBAR+0.01*DELTA*VBAR
        IF(TKN-GAM) 298,298,302
    302 ZBAR=ZBAR-TNLE
        ASSIGN 290 TO LIL
        GO TO 5
    298 ZBAR=TKN-TNLE
    297 ASSIGN 291 TO LIL
        GO TO 5
    296 ZET=ZBAR-0.01*DELTA*VBAR
        IF(TKN-ZET) 301,298,298
    301 TKN=TKN+1.0
```

```
      TNLE=TNLE+1.0
      KT=KT+1
      GO TO 302
C
C     ***** INTEGRATE BY BETA METHOD *****
    5 DO 102 I=2,M
      ACB(I)=ACD(I)
      X=0.5*ACB(I)+0.5*ACA(I)
      VEB(I)=VEA(I)+X
      X=0.5*ACA(I)-BETA*ACA(I)
      DDP(I)=VEA(I)+X+BETA*ACB(I)
  102 DPB(I)=DPA(I)+DDP(I)
      DPB(N+2)=DPB(N)
      ASB=ASI
      VSB=VSA+0.5*(ASB+ASI)
      SYB=SYA+VSA+0.5*ASI+BETA*(ASB-ASI)
C
C     ***** COMPUTE ANGLE OF ROTATION *****
      DO 18 I=2,M
      ANGLB(I)=-DPB(I-1)+2.0*DPB(I)-DPB(I+1)
   18 DA(I)=ANGLB(I)-ANGLA(I)
C
CC    ***** COMPUTE BENDING MOMENT *****
      DO 79 I=2,M
      IF(DA(I)) 50,50,65
   50 IF(TMNA(I)+STFA*DA(I)) 51,52,55
   51 C=RK
      GO TO 53
   52 C=0.0
   53 TMNB(I)=0.0
      X=STFA*DA(I)+TMNA(I)
      BMB(I)=BMA(I)-TMNA(I)+C*X
      GO TO 56
   55 TMNB(I)=TMNA(I)+STFA*DA(I)
      BMB(I)=BMA(I)+STFA*DA(I)
   56 TMPB(I)=2.0-TMNB(I)
      GO TO 79
   65 IF(TMPA(I)-STFA*DA(I)) 70,71,75
   70 C=RK
      GO TO 73
   71 C=0.0
   73 TMPB(I)=0.0
      X=STFA*DA(I)-TMPA(I)
      BMB(I)=BMA(I)+TMPA(I)+C*X
      GO TO 76
```

```
   75 TMPB(I)=TMPA(I)-STFA*DA(I)
      BMB(I)=BMA(I)+STFA*DA(I)
   76 TMNB(I)=2.0-TMPB(I)
   79 CONTINUE
C
C       *****  AUXILIARY  ROUTINE  *****
       DO 23 I=2,N
       X=ZN**2*(BMB(I-1)-2.0*BMB(I)+BMB(I+1))
   23 ACD(I)=DELTA*38.4*DELTA*X
       IF(N-KT)310,322,322
  322 IF(KT-1) 304,304,305
  304 X=1.0/(1.0+R*ZBAR**2)
       YM1=ZBAR*DPB(KT+1)
       VM=VBAR*DPB(KT+1)*DELTA+ZBAR*VEB(KT+1)
       CH=X*DELTA*(SK*(SYB-YM1)*ZBAR*DELTA+DC*(VSB-VM)*ZBAR)
       ACD(KT+1)=X*DELTA*(38.4*ZN*(ZN*(BMB(KT)-2.0*BMB(KT+1)+BMB(KT+2))+
     18.0*FBAR*ZBAR)*DELTA-2.0*R*VBAR*ZBAR*VEB(KT+1))+CH
       GO TO 310
  305 IF(KT-N) 306,307,308
  308 PRINT 309
  309 FORMAT(1H2,10X,12HKT=TOO LARGE)
  307 REMD=1.0-ZBAR
       X=1.0/(1.0+R*REMD**2)
       Y=BMB(KT-1)-2.0*BMB(KT)+BMB(KT+1)
       YM1=REMD*DPB(KT)
       VM=REMD*VEB(KT)-VBAR*DPB(KT)*DELTA
       CH=X*DELTA*(SK*(SYB-YM1)*REMD*DELTA+DC*(VSB-VM)*REMD)
       ACD(KT)=X*DELTA*(38.4*ZN*DELTA*(ZN*Y+8.0*FBAR*REMD)-2.0*R*VBAR*
     1REMD*(VEB(KT+1)-VEB(KT)))+CH
       GO TO 310
  306 REMD=1.0-ZBAR
       S=1.0/R+REMD-ZBAR*REMD
       T=R*(ZBAR*REMD)**2
       U=R*ZBAR**2
       V=1.0/(1.0-T/S+U)
       W=BMB(KT-1)-2.0*BMB(KT)+BMB(KT+1)
       X=ZN**2*ZBAR*REMD*W
       Y=ZN*ZBAR*REMD**2*FBAR
       Z=BMB(KT)-2.0*BMB(KT+1)+BMB(KT+2)
       YE=2.0*R*VBAR*ZBAR*(REMD**2/S-1.0)*(VEB(KT+1)-VEB(KT))
       YM1=DPB(KT)+ZBAR*(DPB(KT+1)-DPB(KT))
       VM=VEB(KT)+VBAR*DELTA*(DPB(KT+1)-DPB(KT))+ZBAR*(VEB(KT+1)-VEB(KT))
       XIX=1.-(REMD**2)/S
       CH=DELTA*(SK*(SYB-YM1)*ZBAR*DELTA+DC*(VSB-VM)*ZBAR)
       ACD(KT+1)=V*DELTA*(38.4*ZN**2*Z+8.0*38.4*ZN*FBAR*ZBAR-38.4*X/S-8.0
```

```
     1*38.4*Y/S)*DELTA+V*DELTA*YE+V*XIX*CH
      TIM=1.0/(1.0+R*REMD-R*ZBAR*REMD)
      CH=DELTA*(SK*(SYB-YM1)*REMD*DELTA+DC*(VSB-VM)*REMD)
      ACD(KT)=TIM*(DELTA*(38.4*ZN**2*W+8.0*38.4*ZN*FBAR*REMD)*DELTA
     1-R*ZBAR*REMD*ACD(KT+1)-2.0*DELTA*R*VBAR*REMD*(VEB(KT+1)-VEB(KT)))
     2+TIM*CH
  310 DO 35 I=2,N
      X=0.5*(ACD(I)+ACA(I))
   35 VEB(I)=VEA(I)+X
      VSB=VSA+0.5*(ASD+ASI)
      GO TO LIL
  290 ADAC=0.
      AUT=0.
      YOJ=0.
      GO TO 289
  291 AUT=-DELTA*R*VBAR*(DPB(KT+2)-2.*DPB(KT+1)+DPB(KT))/(1.+R)
      ADAC=-2.*R*VBAR*(VEB(KT+2)-2.*VEB(KT+1)+VEB(KT)-AUT)*DELTA/(1.+R)
      YOJ=(2.*VBAR)/(1.+R)*(VEB(KT+2)-2.*VEB(KT+1)+VEB(KT)-AUT)*DELTA
      IF(N-KT)425,426,426
  425 GO TO 289
  426 ZIB=0.
  289 LOT=KT+1
      IF(N-LOT) 288,287,287
  287 ACD(KT+1)=ACD(KT+1)+ADAC
      VEB(KT+1)=VEB(KT+1)+AUT
C
C
  288 IF(N-KT)40,254,254
  254 AMM=ACD(KT)/DELTA**2+2.*VBAR*(VEB(KT+1)-AUT-VEB(KT))/DELTA
     1+(ZBAR/DELTA)*(ACD(KT+1)-ADAC-ACD(KT))/DELTA
      TYOJ=YOJ/DELTA**2
      AMM=AMM+TYOJ
      PBAR=(R*(((QS+R)/R)*GBAR-AMM+SK*(SYB-YM1)/R)/ZN)/153.6
   40 ASD=-DELTA*(SK*(SYB-YM1)*DELTA+DC*(VSB-VM))/QS
C
C    ***** PREPARE FOR NEXT STEP OF INTEGRATION *****
      DO 45 I=2,N
      BMA(I)=BMB(I)
      TMPA(I)=TMPB(I)
      TMNA(I)=TMNB(I)
      ACA(I)=ACD(I)
      VEA(I)=VEB(I)
      DPA(I)=DPB(I)
      ANGLA(I)=ANGLB(I)
   45 CONTINUE
```

```
      ASI=ASD
      VSA=VSB
      SYA=SYB
C
C    *****  COMPUTE  MAXIMUM  RESPONSE  *****
      J=N
      K=2
      SIK=ZN/VBAR+3.
      IF(TAU-SIK) 1101,285,285
 1101 DO 109 I=K,J
      DPS(I)=1.25*DPA(I)/3.141592654**2
      SOF(I)=DPS(I)
      EF(I)=DPS(I)
      IF(DPS(I)-DPAMX(I)) 109,109,112
  112 DPAMX(I)=DPS(I)
      TMAX(I)=TAU*VBAR/ZN
  109 CONTINUE
      IF(PBMA-PBAR)261,262,262
  261 PBMA=PBAR
      TPMA=TAU*VBAR/ZN
  262 IF(PBMI-PBAR)264,264,263
  263 PBMI=PBAR
      TPMI=TAU*VBAR/ZN
  264 GO TO 48
  285 DO 280 I=K,J
      DPS(I)=1.25*DPA(I)/3.141592654**2
      IF(SOF(I)-DPS(I)) 283,282,282
  283 SOF(I)=DPS(I)
  282 IF(EF(I)-DPS(I)) 280,280,281
  281 EF(I)=DPS(I)
  280 CONTINUE
C
C     *****  TEST  TIME  TO  PRINT  *****
   48 IF(IN-1)  115,115,16
   16 IN=IN-1
      GO TO 4
  115 TTAU=TAU*VBAR/ZN
      PRINT 97,TTAU
   97 FORMAT(1H0,F12.7)
      PRINT 98,(DPS(I),I=K,J)
   98 FORMAT(1H0,9F10.5)
      IF(TAU-ZN/VBAR)266,266,267
  266 SHO=1.25*AMM/3.141592654**2
      COV=(SK*(SYB-YM1)/ZN)/153.6
```

```
      PRINT 260,PBAR,SHO,COV
  260 FORMAT(1H0,5HPBAR=F10.6,2X,F10.6,2X,F10.6)
  267 ZIB=0.
C
C     ***** STATIC DEFLECTION *****
      IF(N-KT) 324,323,323
  323 ABAR=(ZBAR+TNLE)/ZN
      IF(1.0-ABAR) 398,399,399
  398 PRINT 397
  397 FORMAT(1H2,20HABAR=LARGER THAN ONE)
  399 IF(TMEAS-ABAR) 400,401,401
  400 TMEAS=TMEAS+TLENG
      IOT=IOT+1
      GO TO 401
  401 BBAR=1.0-ABAR
      DIST=0.
      REMD=0.
      DO 802 I=2,IOT
      DIST=DIST+TLENG
  802 DIF(I)=12.8*BBAR*DIST*(ABAR*(BBAR+1.0)-DIST**2)
      TIT=IOT
      DIST=TIT*TLENG-TLENG
      JJ=IOT+1
      DO 803 I=JJ,N
      DIST=DIST+TLENG
      REMD=1.0-DIST
  803 DIF(I)=12.8*ABAR*REMD*(BBAR*(ABAR+1.0)-REMD**2)
      DO 804 I=2,N
  804 STDE(I)=1.25*FBAR*DIF(I)
      PRINT 98,(STDE(I),I=K,J)
      DO 570 I=2,N
      THPL(I)=ANGLA(I)-BMA(I)/STFA
  570 THPL(I)=THPL(I)/3.141592654**2
      PRINT 98,(THPL(I),I=2,N)
  324 GO TO 7
      END
      END
```